Multi-*omics* analysis of human brain tissue and an animal model of Parkinson's Disease

Dissertation

for the award of the degree

"Doctor rerum naturalium"

of the Georg-August-Universität Göttingen

within the doctoral program

"International Max Planck Research School for Neurosciences"

of the Georg-August University School of Science (GAUSS)

submitted by

Lucas A. Caldi Gomes

Born in Londrina, Paraná, Brasil

Göttingen, September, 2019

Thesis Committee

Prof. Dr. Paul Lingor (Rechts der Isar Hospital of the Technical University Munich, Dept. of Neurology – Translational Neurodegeneration Laboratory)

Prof. Dr. André Fischer (University Medical Center Göttingen, Dept. Epigenetics and Systems Medicine in Neurodegenerative Diseases, DZNE Göttingen)

Prof. Dr. Silvio Rizzoli (University Medical Center Göttingen, Dept. of Neuro- and Sensory Physiology)

Members of the Examination Board

1st Referee: **Prof. Dr. Paul Lingor** (Rechts der Isar Hospital of the Technical University Munich, Dept. of Neurology – Translational Neurodegeneration Laboratory)

2nd Referee: **Prof. Dr. André Fischer** (University Medical Center Göttingen, Dept. Epigenetics and Systems Medicine in Neurodegenerative Diseases, DZNE Göttingen)

Further members of the Examination Board

Prof. Dr. Silvio Rizzoli

(University Medical Center Göttingen, Department of Neuro- and Sensory Physiology)

Dr. Camin Dean

(European Neuroscience Institute Göttingen, Trans-synaptic Signaling Laboratory)

Dr. Jens Gruber

(German Primate Center, Medical RNA Biology Laboratory)

Dr. Sebastian Kügler

(University Medical Center Göttingen, Dept. of Neurology – Viral vectors Laboratory)

Date of oral examination: 11.10.2019

“I am driven by two main philosophies: know more today about the world than I knew yesterday and lessen the suffering of others. You'd be surprised how far that gets you.”

— Neil deGrasse Tyson

Table of Contents

1. Introduction

1.1. Neurodegenerative diseases in modern society

With the advances in medicine, public health and economic development, the life expectancy of the population has increased steadily over the last two centuries. Alongside the increase in average lifespan and a continuously aging society, a much higher incidence of neurodegenerative diseases takes place. Between the years of 1990 and 2015, the number of deaths decurrent from neurological disorders increased in dramatic 36.7% (Feigin et al., 2017). Several studies have shown that neurodegenerative diseases configure an important cause of disability, mortality, and lead to an important social and economic burden worldwide (Feigin et al., 2017; Oeppen and Vaupel, 2002; Riley, 2001; Tuljapurkar et al., 2000).

Neurodegenerative diseases are a product of neuronal dysfunction and neuronal cell death in the central and/or peripheral nervous system, usually associated to protein misfolding, aggregation and, in many cases, inflammation and immune cell activation. That results in a progressive neurological pathology in affected patients (Bredesen et al., 2006; Glass et al., 2010; Ross and Poirier, 2004; Skovronsky et al., 2006). Among the most common neurodegenerative diseases, Parkinson's Disease (PD) is the second most prevalent and fastest-growing neurological disorder. The number of affected individuals is expected to double in the next 20 years (Dorsey and Bloem, 2018; Feigin et al., 2017). Therefore, efforts into understanding the key pathogenetic mechanisms and the development of disease-modifying therapies are of fundamental importance and have been object of intense research recently.

1.2. Parkinson's Disease

1.2.1. Parkinson's Disease – history, epidemiology and etiology

The first scientific record on PD dates from 1817. In James Parkinson's "Essay on the Shaking Palsy", the cardinal motor features of PD were described in a group of patients. The main symptoms related to the disease - which include resting tremors, rigidity, postural instability and bradykinesia/hypokinesia - remain the clinical hallmarks used in PD diagnosis to this date (Agid, 1991; Lees, 2007). Later on, it was shown that the motor dysfunctions presented by patients result from a progressive neurodegeneration of dopaminergic cells

in the nigrostriatal pathway (Agid, 1987, 1991; Hornykiewicz, 1966). Besides the extrapyramidal motor dysfunction, patients present a number of non-motor symptoms that range from sensory abnormalities to autonomic dysfunctions, as well as sleep alterations, mood disorders, depression and cognitive decline (Agid, 1991; Dauer and Przedborski, 2003a; Lim et al., 2009).

PD is the second most prevalent neurodegenerative disease worldwide, only after Alzheimer's disease (AD). It is an age-related disorder, affecting up to 2% of individuals aged over 60 years. For the age group between 85 and 89 years of age, PD is prevalent in up to 3,4% of individuals in Europe (De Lau and Breteler, 2013; de Rijk et al., 2000). From 1990 to 2015, the prevalence of PD more than doubled worldwide (Feigin et al., 2017). The majority of the cases is composed of the sporadic form of the disease, and around 5% of the cases comprise familial/autosomal cases. Several autosomal mutations linked to the development of the familial form of PD were identified in the last decades. Classical PD-related mutations affect genes that include, for example, SNCA, LRRK2, PINK1, DJ-1, and parkin. Although familial cases present different pathogenetic mechanisms and a wider age span in their occurrence, there are several common mechanisms between those cases and idiopathic forms of PD. Those include oxidative stress, excitotoxic mechanisms, mitochondrial dysfunction and defects in protein handling, for example (De Lau and Breteler, 2013; Dexter and Jenner, 2013a; Johnson et al., 2019).

The presence of proteinaceous inclusions called Lewy bodies (LB) in the brains of PD patients is one of the pathological hallmarks of the disease. LBs are intracytoplasmic inclusions majorly composed of the protein alpha-synuclein (αSyn), but also contain ubiquitin and neurofilaments (Spillantini et al., 1997). As previously mentioned, mutations in the αSyn coding gene (SNCA) are broadly linked to familial forms of PD. However, LBs are present in both sporadic and familial PD cases (Bendor et al., 2013; Polymeropoulos, 1997; Singleton, 2003). Moreover, these aggregates are not constrained to the affected dopaminergic neurons but found spread throughout affected brains (Braak et al., 2003; Spillantini et al., 1997). The pathological role of LB formation is not completely understood. While some studies suggest they might be a direct cause of death to the affected nerve cells, others hypothesize that these inclusions might be a reactive mechanism aiming to protect the cell from the toxicity of misfolded proteins (Braak et al., 2003; Dexter and

Jenner, 2013a; Lu et al., 2005; Olanow et al., 2004). Nevertheless, the formation of protein aggregates in both familial and sporadic forms of PD suggests that a defective protein handling machinery is a mechanism directly related to the pathogenesis of PD (Bendor et al., 2013).

Neuroinflammatory mechanisms have also been broadly linked to neurodegenerative diseases, including PD. The presence of activated microglial cells in the substantia nigra of PD-affected brains was one of the first findings correlating neuroinflammation to PD (McGeer et al., 1988a). The main neuroinflammatory mechanisms in PD pathology include microglial activation, lymphocytic infiltration and astrogliosis (Hirsch and Hunot, 2009). A series of studies showed that a chronic inflammatory state contributes to the neurodegenerative processes in PD. The release of neurotoxic cytokines by glial cells likely extends the neuronal cell damage even further (Joers et al., 2017; Liddelow et al., 2017; Macchi et al., 2015). Markers of inflammation are reported to be present not only in the brain of PD patients but also in the periphery (Macchi et al., 2015). Furthermore, there is evidence for the contribution of inflammatory mediators to αSyn misfolding and aggregation (Gao et al., 2008). Currently, neuroinflammation is not only referred as a consequence of the neurodegeneration in PD but also as one of the possible primary causes to the progression of PD.

Several environmental and genetic risk factors may predispose to the occurrence of PD (Dexter and Jenner, 2013a; Schapira and Jenner, 2011). Nonetheless, there is no canonical mechanism or pathway that would describe the exact pathogenesis of PD to date. Despite the several known mechanisms contributing to different aspects of PD pathology, recent studies in the field point to a multitude of primary causes that might differ between affected patients, suggesting that PD might not be configured as a single disease, but rather be a multifactorial syndrome with multiple pathogenic subgroups (Dexter and Jenner, 2013a; Johnson et al., 2019).

1.2.2. Pathophysiology and progression of PD

PD patients present a chronic and progressive phenotype of motor dysfunction intimately related to the degeneration of dopaminergic neurons taking place in the

midbrain. The loss of pigmentation in one of the nuclei of the midbrain, the substantia nigra, was one of the earliest histological findings linked to PD (Trétiakoff, 1919), which was, later on, proved to be resultant from the degeneration of the neuromelanin-positive dopaminergic cells in that region (Marsden, 1983). A very prominent dopaminergic cell loss occurs in the nigrostriatal system, more specifically in the *substantia nigra pars compacta* (SNpc) (Figure 1A). Studies have shown that by the start of the clinical signs of PD, there is a dramatic reduction on dopamine levels in the striatum of the patients (up to 80% reduction), while only 30-50% of the dopaminergic cell bodies seem to be degenerated at that phase. Those findings suggest that a retrograde dopaminergic degeneration occurs in the nigrostriatal pathway, starting from the striatal pre-synaptic terminals of axonal projections, progressing to the cell bodies located in the substantia nigra. The severe deficits in motor control and initiation of voluntary movements observed in PD patients are intrinsically related to the degeneration of nigral dopaminergic neurons and the consequent dopamine depletion in the nigrostriatal system. (Braak et al., 2003; Burke and O'Malley, 2014; Dauer and Przedborski, 2003a; Schmidt and Kretschmer, 1997).

The basal ganglia comprise a collection of subcortical nuclei that include the striatum (formed by the putamen and the caudate nucleus), the globus pallidus (internal and external parts), the subthalamic nucleus (STN) and the substantia nigra. These nuclei present extensive connectivity between each other and several other brain regions, forming complex neuronal networks that regulate motor functions in different levels. The anatomical organization of the motor circuit is illustrated in Figure 1B. In more detail, glutamatergic excitatory projections from the motor cortex reach the striatum (at the postero-lateral putamen), communicating with GABAergic neurons. These inhibitory neurons are involved in two distinct projection pathways - the so-called "direct" and the "indirect" basal ganglia signaling pathways. They encompass the connection of the striatum to other two basal ganglia nuclei: the internal globus pallidus (GPi) and the substantia nigra pars reticulata (SNpr). In the direct pathway, GABAergic striatal neurons make direct connections to the GPi and the SNpr, exerting inhibitory input to the neurons present in those nuclei. Upon activation, the direct pathway leads to inhibition of the neurons in the GPi/SNpr and subsequent excitation of the thalamus and the motor cortex, a loop that facilitates the initiation of voluntary movements. On the other hand, in the indirect

pathway, the putamen is primarily connected with the external globus pallidus (GPe) and the STN, which finally send projections to the GPi/SNpr regions. The GPe contains GABAergic inhibitory neurons, while STN neurons are glutamatergic. Upon stimulation, the striatal neurons belonging to the indirect pathway promote inhibition of the GPe and subsequent disinhibition of the STN, which finally leads to excitation of the GPi/SNpr nuclei, inhibiting thalamic/cortical regions and, consequently, suppressing motor activity. The antagonistic effects of these two pathways influence the output activity of the basal ganglia, regulating voluntary movement initiation and motor control (Forno, 1996; Obeso et al., 2000).The dopaminergic neurons present in the SNpc exert a key regulatory input to the motor circuit by innervating the spiny striatal neurons present in the putamen. Striatal neurons belonging to each pathway express a different type of dopamine receptor. Neurons that are part of the direct pathway express excitatory D_1 receptors, while the indirect pathway contains neurons bearing inhibitory D_2 receptors. Thus, the dopamine signaling in the nigrostriatal circuit produces dual effects on the motor circuit, promoting either the enhancement of the direct pathway or the suppression of the indirect pathway. In the parkinsonian state, the dopamine deficiency caused by the nigral neurodegeneration results in an impairment in both direct and indirect pathways, which ultimately leads to increased activity in the GPi and the SNpr. With that, excessive inhibition of the thalamus and the motor cortex takes place, progressively affecting motor control in PD patients (Forno, 1996; Obeso et al., 2000; Schmidt and Kretschmer, 1997).

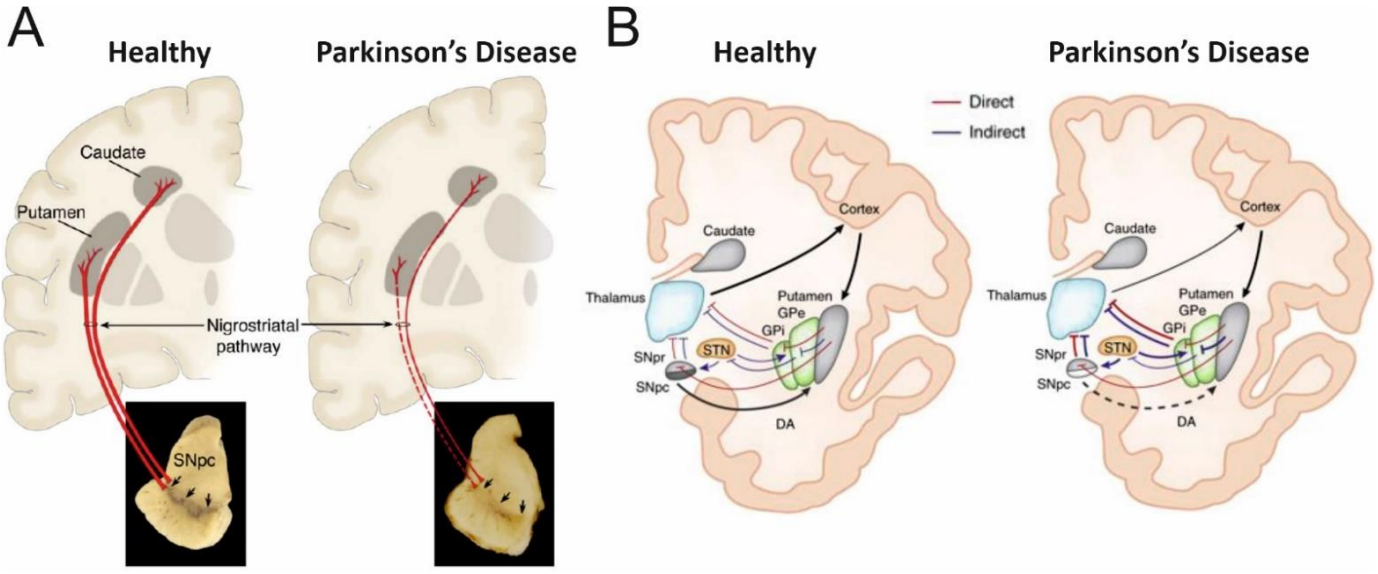

Figure 1. (A) Nigrostriatal projections - schematic representation. In a midbrain section of a healthy subject (left side), the substantia nigra pars compacta (SNpc) presents normal pigmentation

by the presence of neuromelanin expressing dopaminergic neurons. Preserved striatal projections represented in red (thick lines); in the parkinsonians state (right side), a marked depigmentation is observed in the SNpc due to the degeneration of the dopaminergic neurons. A consequent disruption of the striatal projections is represented in red (thin/dotted lines). (Dauer and Przedborski, 2003a), adapted. **(B) Representation of coronal brain sections depicting the basal ganglia circuits (both in healthy and Parkinson's Disease states).** Thickness of lines indicates the strength of the connections. In the parkinsonian state, nigral degeneration leads to increased thalamic inhibition. DA: dopamine; GPe: globus pallidus externus; GPi: globus pallidus internus; SNpc: substantia nigra pars compacta; SNpr: substantia nigra pars reticulata; STN: subthalamic nucleus. (Calabresi et al., 2014; Dauer and Przedborski, 2003a), adapted.

Furthermore, the basal ganglia present connections to a number of other brain regions. These include for instance the limbic system, prefrontal cortex, medulla oblongata and the pons. Hence, the PD pathology produces a series of nonmotor neuropsychiatric symptoms that are present in a majority of all PD cases (Braak et al., 2003; Dexter and Jenner, 2013a; Witjas et al., 2002).

1.2.3. PD diagnosis and therapeutic alternatives

The diagnosis of PD strongly relies on the clinical manifestation of the motor phenotype. Generally, the criteria considered for the diagnosis of PD are the presence of bradykinesia together with other cardinal features, such as muscular rigidity, resting tremor or postural instability and the absence of exclusion criteria (Postuma et al., 2015). Recently, neuroimaging techniques and biochemical tests with cerebrospinal and peripheral body fluids have been employed as additional evidence for differential diagnosis. However, PD misdiagnosis is still a major problem (Tolosa et al., 2006). Particularly, there is a strong need for better diagnosis at early stages, since PD patients start to display the first motor symptoms only when the dopaminergic neurodegeneration is already at an advanced stage (Kalia and Lang, 2015).

Despite extensive studies on the mechanisms contributing to the neurodegeneration and disease progression in PD, the exact pathogenetic events – possibly occurring decades before the symptoms start to emerge – are not completely

understood. Allied to the late diagnosis, the limited regenerative capability of neurons in the central nervous system substantially hinder the development of causative treatment options. Although there are multiple and effective therapeutic options for PD, all currently available therapies for PD are symptomatic. The most common of them relies on the pharmacological replenishment of dopamine by oral or enteric administration of the prodrug L-3,4-dihydroxyphenylalanine, also known as levodopa (L-DOPA). L-DOPA administration is usually combined with drugs that prevent its peripheral metabolism, enhancing the bioavailability of this dopamine precursor before it crosses the blood-brain barrier. In spite of attenuating the symptoms, the treatment with L-DOPA presents a number of limitations and possible side effects. The majority of the patients on a long-term L-DOPA therapy experience loss of efficacy, drug-induced dyskinesia, fluctuations or toxicity by the drug. Other common adverse effects are progressive cognitive defects, depression and other neuropsychiatric dysfunctions (Connolly and Lang, 2014; Marsden, 1994; Nutt et al., 1994)

Due to the lack of effective therapeutic strategies for PD, effort into understanding the pathogenic mechanisms in more detail and finding possible biomarkers for the disease would be of extreme importance, facilitating the early diagnosis and allowing the development of novel curative treatments for PD.

1.3. Gene expression regulation and miRNA biology

Recently, a number of studies showed that dysfunctions in the regulation of gene expression are critical to the development of brain diseases. Several studies have shown that non-coding RNAs (ncRNAs) are necessary for the development and survival of neurons. They are involved in a myriad of cellular mechanisms and of major importance for the homeostatic maintenance of cells. In addition, they have been shown to play a very important role in the pathogenesis of neurodegenerative diseases (Eacker et al., 2009; Galasso et al., 2010; Hebert and De Strooper, 2007; Roser et al., 2018a).

Among the ncRNAs classes, miRNAs are by far the most studied species, and research has drawn substantial attention to the role of miRNAs in brain diseases in the last years (De Guire et al., 2013; Hebert and De Strooper, 2007; Rao et al., 2013). miRNAs

provide a widespread machinery of post-transcriptional regulation of gene expression by mechanisms similar to RNA interference, targeting multiple genes and a variety of pathways in health and disease (He and Hannon, 2004).

1.3.1. Overview on epigenetics and miRNAs

The number of studies concerning the epigenetic regulation of gene expression has increased dramatically in the last decades. The term “epigenetics” was initially introduced by Conrad Waddington in 1942, even before the first studies on structural and functional properties of genes were published. Waddington referred to an “epigenetic landscape” while postulating on the ways genetic information act systemically in order to produce a phenotype (Waddington, 1942, 2012). A modern definition for epigenetics was proposed by Riggs and colleagues, stating that epigenetics comprise “the study of mitotically and/or meiotically heritable changes in gene function that cannot be explained by changes in the DNA sequence” (Allen, 2015; Holliday, 2006; Riggs, 1996). To date, known epigenetic mechanisms include histone modifications, DNA methylation and ncRNAs. The latter class has been extensively studied in the context of CNS diseases (Bird, 2007; Fischer, 2014).

NcRNA species are usually classified according to their nucleotide length: small ncRNAs present up to 200 base pairs, while species with over 200 base pairs are referred as long ncRNAs. Small ncRNAs are further subdivided into Piwi-interacting RNAs (piRNAs), small nucleolar RNAs (snoRNAs) and micro RNAs (miRNAs). miRNAs are processed from the transcripts of endogenous genes and comprise the most-studied class of ncRNAs. They exert a post-transcriptional regulation of gene expression, targeting mRNAs by base-pair complementarity. Upon binding to the 3’ untranslated regions (UTR) of transcripts, miRNAs are able to silence genes via translational repression or mRNA destabilization/degradation. Furthermore, miRNAs are involved in a number of important cellular and biological processes, including differentiation and development, cellular proliferation, homeostatic maintenance, hematopoiesis and inflammation. Disbalance in miRNA networks are linked to the development of a series of diseases, from cancer to metabolic and neurologic disorders (Bartel, 2004; Berezikov et al., 2006; Fabian et al., 2010; Friedman and Jones, 2009; Friedman et al., 2008; He and Hannon, 2004; Hebert and De Strooper, 2007).

The coding sequences for miRNA species are located in both coding and intergenic regions, and they are processed either from introns or from exons after splicing. Mature miRNAs are encoded from genomic stem-loop precursors, presenting very short nucleotide length (between 17-24 nucleotides) (Bartel, 2004; Berezikov et al., 2006; He and Hannon, 2004). A recent review refers to over 2,000 miRNA species already identified in humans, which are responsible for collective targeting and regulation of more than 60% of the genes from the human genome (Friedman et al., 2008; Hammond, 2015). A remarkable feature from miRNAs is that each mature sequence may target hundreds of targets mRNAs. Furthermore, individual genes can be targeted by several different miRNA species, creating a very complex regulatory network of gene expression that potentially affects thousands of genes (Friedman and Jones, 2009; Friedman et al., 2008). Those findings were confirmed in a number of important studies that employed transcriptomic and proteomic profiling approaches, indicating that translational repression by miRNAs encompasses an important mechanism of fine-tuning for protein expression at the cellular level (Baek et al., 2008; Elkan-Miller et al., 2011; Gillardon et al., 2008; Lim et al., 2005; Moraes et al., 2017).

1.3.2. miRNA biogenesis and gene silencing

The biogenesis of miRNAs takes place in the nucleus, and most of the described miRNAs are derived from the canonical biogenesis pathway (illustrated in Figure 2). Primary miRNA genes are transcribed by RNA Polymerase II enzymes into long precursor transcripts, the pri-miRNAs. Those long transcripts are then processed by the RNAse III enzyme known as *Drosha,* giving rise to long hairpin-looped miRNA precursors (pre-miRNAs). The cleavage by *Drosha* is dependent on the interaction with the DGCR8 class of proteins for the active binding to double-stranded RNA molecules (Han, 2004; Lee et al., 2003, 2004). The newly formed hairpin-shaped pre-miRNAs are then carried to the cytoplasm by the Exportin-5 transporter (a process dependent on RAN-GTP binding proteins), to be further cleaved by another kind of RNAse III called *Dicer.* These interactions take place in the so-called processing (p-) bodies in the cytoplasm. The resulting oligonucleotides duplexes present already short length, typical from miRNAs. One of the strands is then converted into the mature form of the given miRNA, while the exceeding strand is usually degraded. *Dicer* also recruits the so-called *Argonaute* (AGO) proteins – a process dependent on TRBP mediating

proteins - and this interaction is fundamental to the silencing activity of miRNAs. More specifically, the AGO2 subtype of these proteins is exclusively present in active miRNA silencing complexes in humans. Upon assembly, miRNA-AGO2 complexes finally turn into the active *RNA-induced silencing complex* (RISC) and are able to target mRNAs by nucleotide complementarity (Bartel, 2004; Chendrimada et al., 2005; Gregory et al., 2005; Haase et al., 2005; Kim et al., 2009; Kulkarni et al., 2010).

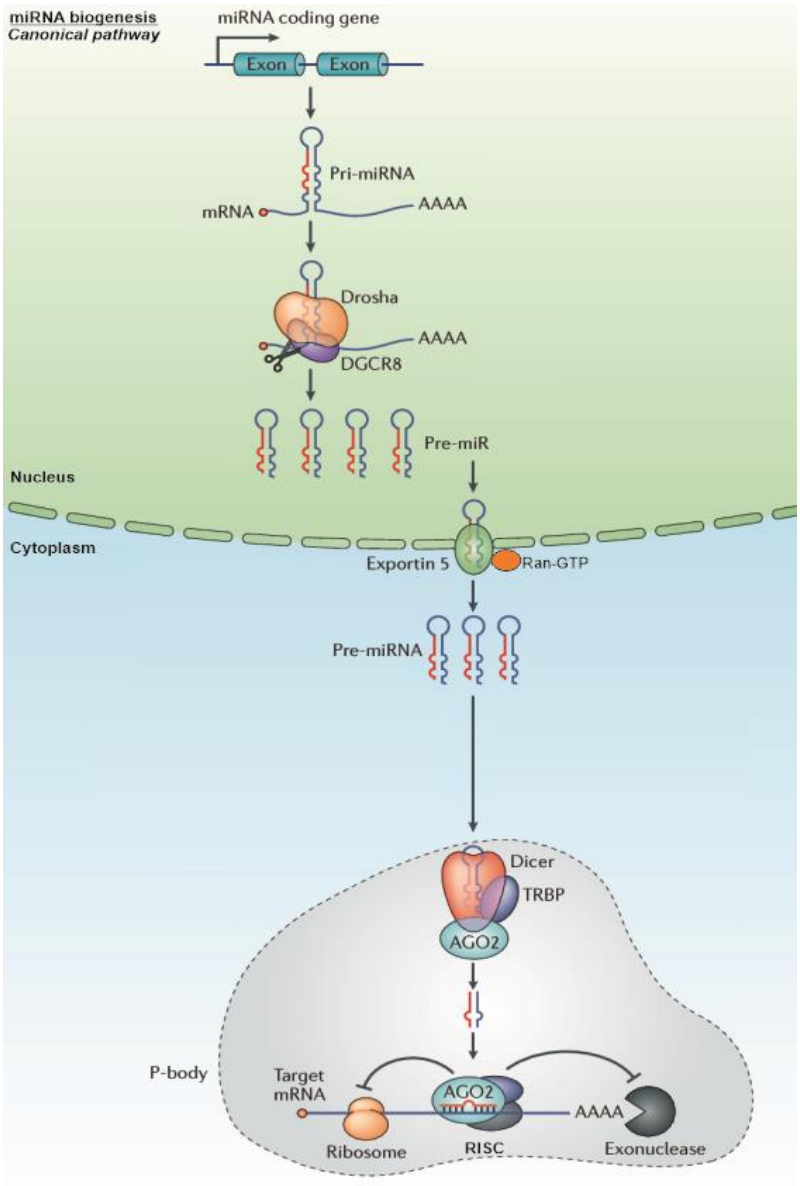

Figure 2. Canonical miRNA biogenesis pathway - schematic representation. Inside the nucleus, miRNA coding genes are transcribed into pri-miRNA transcripts, which are further processed by an RNase type III (Drosha) associated with DGCR8. The resulting looped Pre-miRNAs are exported to the cytoplasm by RAN-GTP dependent exportin-5 and cleaved by *Dicer*, resulting in a duplex miRNA molecule. Upon assembly with AGO2 proteins, the RNA-induced silencing factor (RISC) is formed and miRNAs are able to target mRNAs for gene expression regulation. (Li and Rana, 2014), adapted.

1.3.3. The role of miRNAs in neurodegeneration and PD

miRNAs are widely expressed over all the different types of human tissue, but astonishing 70% of all miRNAs are expressed in the human central and peripheral nervous system (Nowak and Michlewski, 2013). Numerous studies have shown that miRNAs contribute to a variety of biological processes in nervous tissue, including neurogenesis and differentiation, neuronal development, maintenance, morphogenesis and regulation of programmed cell death (Chen and Qin, 2015; Kapsimali et al., 2007; Narayan et al., 2015; Schratt et al., 2006). For their absolute importance in maintenance and function of neuronal cells, defects in miRNAs networks might lead to a series of pathogenic processes in the brain.

Alterations in miRNA expression have been linked to a number of neurodevelopmental and neurodegenerative diseases (Sun and Shi, 2015). For example, the expression levels of several miRNAs were found altered in the brains of AD and Huntington's disease (HD) patients (Quinlan et al., 2017; Shioya et al., 2010; Zovoilis et al., 2011). Similarly, several described alterations in miRNA expression are also reported in PD, both in nervous tissue and in peripheral fluids of affected patients (Mouradian, 2012; Roser et al., 2018b). A couple of studies found deficient levels of miR-133b in the midbrain of both PD patients and from mouse models of PD (Hebert and De Strooper, 2007; Kim et al., 2007). Another important study found alterations in the levels of miR-34b/c in several regions of PD-affected brains. By manipulation of the levels of these miRNAs in vitro, researchers were able to mimic impairments in mitochondrial functions and oxidative stress, pathomechanisms believed to be crucial for the development of PD (Miñones-Moyano et al., 2011). Furthermore, studies identified two specific miRNAs regulating the expression of αSyn (namely, miR-7 and miR-153) *in vitro*. Interestingly, the former has been found altered in the striatum and substantia nigra of PD patients, as well as in murine models of PD (Doxakis, 2010; Farh, 2005; Junn et al., 2009). In addition, target prediction and enrichment analyses identified several miRNAs that might regulate PD-associated genes, in regard to autophagy and lysosomal related pathway. Those miRNAs species include miR-98, miR-124, miR-142, miR-130, and miR-204 (Jegga et al., 2011; Junn et al., 2009).

Another important aspect of miRNA regulation in PD is the fact that they are fundamental for the development and function of dopaminergic neurons. A prominent

study in the field showed that the deletion of the enzyme *Dicer* – pivotal for the biogenesis of miRNAs – led to reduced neurogenesis and a strong dopaminergic degeneration *in vitro*. Similarly, when analyzing a murine model presenting a conditional *Dicer* knockout, a marked and progressive dopaminergic neurodegeneration is observed in the midbrain of the animals, reaching up to 90% of dopaminergic cell loss in up to 6 weeks of age. Remarkably, the phenotype is significantly rescued when transfecting *Dicer*-deleted cultured neurons with midbrain-derived small RNAs (<200bp), but not with large RNAs (>200bp) of same origin, indicating that the miRNA machinery as a whole is of vital importance for the development and maintenance of dopaminergic neurons (Kim et al., 2007). All in all, the aforementioned findings suggest that disruption in the miRNA machinery might be intrinsically related to the pathogenesis and progression of PD.

The studies presented above here indicate that miRNAs comprise a very promising tool for the discovery of novel pathological aspects of PD and, consequently, for the improvement of diagnosis and therapeutic options for this disease. Moreover, the possibility of studying not only miRNA expression profiles but also the ones of their direct mRNA interactors (by transcriptomic profiling) and the final protein products (by proteomics experiments) represents a powerful strategy into the field of neurodegenerative diseases.

1.4. Objectives of this doctoral thesis

With the advance of biotechnology, large scale high-throughput *omics* studies permit the generation of very detailed datasets with high efficiency and relative low costs. That represents a huge advantage to the study of molecular mechanisms and pathways involved in the development of complex diseases. Analytical approaches for the visualization and integration of multi-*omics* data allow a deeper look into underlying pathophysiological mechanisms, and might permit the exploitation of the finding into novel therapeutic strategies. These approaches are especially important in the context of neurodegenerative diseases, including PD. Exploring the exact molecular mechanisms taking place in the midbrains of PD-affected patients is fundamental for better understanding the pathogenesis and progression of the disease.

Thus, the central aim of this doctoral thesis was to analyze postmortem midbrain tissue samples from a cohort of PD patients and controls through a set of multi-*omics* approaches, in order to profile miRNA expression patterns, their target transcripts, the final protein products and possible genomic alterations underlying the pathologic phenotypes. The main techniques employed here were the following:

- **Gene panel sequencing and Multiplex ligation-dependent probe amplification:**
  To verify the presence of classic mutations and other genetic alterations linked to PD in a selected set of genes;

- **Small RNA sequencing;**
  To profile the miRNA expression patterns in the present midbrain samples;

- **RNA sequencing;**
  To obtain the transcriptomic profiles from the present midbrain samples;

- **Mass spectrometry;**
  To evaluate the quantifiable proteome in the present midbrain samples;

Each generated dataset might contain a large number of potential underlying mechanisms from PD pathology per se and was analyzed in depth individually. In addition, we have been especially interested in analyzing the generated datasets in an integrative

fashion, aiming to depict pathways of deregulation across the *omics* data that might permit the exploration of novel miRNA-based regulatory mechanisms. Overall, our findings are likely to reveal molecular networks involved in PD pathogenesis as well as drugable targets for the development of novel therapeutic alternatives.

Finally, to complement our studies in the human tissue, another objective was to validate the small RNA / RNA sequencing results from human midbrains in an established animal model of PD (the αSyn.A53T transgenic mouse line). By comparing the validation results from both sources, our main goal was to verify whether the expression patterns observed in PD-affected human brains correlate with the ones found in the animal tissue, assessing the validity of the model in terms of miRNA / mRNA expression.

2. Material and Methods

2.1. Materials

2.1.1. Human samples

Case ID	Age	Sex	Duration (y)	PMI (h)	Neuropathological diagnosis
PD					
PD029	76	M	7	15	LBDBS
PD039	82	F	15	12	LBDBS
PD050	82	F	14	18	LBDBS
PD074	85	M	9	17	LBDBS
PD125	74	M	25	20	LBDN
PD134	74	M	10	21	LBDBS
PD153	76	F	7	12	LBDN
PD180	85	F	15	15	LBDN
PD182	75	M	10	3	LBDN
PD184	71	M	7	24	LBDE
PD187	72	M	8	11	LBDN
PD201	87	M	11	19	LBDN
PD203	84	F	18	19	LBDN
PD207	81	M	10	11	LBDN
PD229	85	F	18	7	LBDN
PD268	72	M	20	8	LBDN
PD334	87	M	9	21	LBDN
PD458	73	M	19	10	LBDBS
PD666	93	F	15	24	LBDBS
Controls					
C028	60	F		13	Diffuse hypoxic damage
C046	65	M		24	Ischemic infarct caudate and capsule
CO54	66	M		16	n.a.
C064	63	F		21	n.a.
CO74	84	F		22	n.a.

C075	88	M	8.5	n.a.
C077	84	F	12	n.a.
PDC023	78	F	23	n.a.
PDC034	90	M	12	n.a.
PDC035	89	F	13	Diffuse hypoxic damage
PDC040	61	F	15	n.a.
PDC078	91	M	18	n.a.
PDC087	92	F	24	n.a.
PDC088	96	F	24	n.a.
PD549	76	M	25	Age associated changes - normal control

Table 1: Characterization of the human tissue samples analyzed in this thesis. PMI: post-mortem intervals; LBD-BS: Lewy body disease, brain stem predominant. LBD-N: Lewy body disease, neocortical (according to Lewy-body pathology classification (Alafuzoff et al., 2009)).

2.1.2. Reagents

Reagent	Producer
1-Bromo-3-Chloropropane	Sigma Aldrich (Germany)
2-Propanol	AppliChem (Germany)
Ethanol absolute	AppliChem (Germany)
GlycoBlue Coprecipitant	ThermoFisher Scientific (USA)
Phosphate buffered saline (PBS)	AppliChem (Germany)
DNase I (2U/µL)	Life Technologies (USA)
RNase OUT	Life Technologies (USA)
Nuclease free water	Sigma Aldrich (Germany)
10X DNAse I Incubation buffer	Life Technologies (USA)

Reagent	Producer
Trizol (TRI Reagent)	Sigma Aldrich (Germany)

Table 2: List of Reagents

2.1.3. Primers and Kits

Kit / Primer	Producer
RNA Clean & Concentrator-5 KIT	Zymo Research (USA)
QIAamp DNA Mini Kit	Qiagen (Germany)
miScript II RT Kit	Qiagen (Germany)
miScript SYBR Green PCR Kit	Qiagen (Germany)
Quantitect RT Kit	Qiagen (Germany)
QuantiTect SYBR Green PCR Kit	Qiagen (Germany)
SALSA P051 Parkinson MLPA kit	MRC Holland (The Netherlands)
SALSA P052 Parkinson MLPA kit	MRC Holland (The Netherlands)
TruSeq Small RNA Library Prep Kit	Illumina (USA)
CleanTag Library Preparation for Next-Generation Sequencing Kit	TriLink (USA)
dsDNA 905 Kit	Agilent (USA)
dsDNA 905 Reagent Kit	Agilent (USA)
TruSeq Stranded Total RNA	Illumina (USA)
RiboMinus	Thermo Fisher Scientific (USA)
Bradford Roti-Nanoquant protein quantification kit	Carl Roth (Germany)

Pierce High pH Reversed-Phase Peptide Fractionation Kit	Thermo Fisher Scientific (USA)
Hs_RNU6-2_11 miScript Primer Assay	Qiagen (Germany)
Hs_GAPDH_1_SG Quantitect Primer Assay	Qiagen (Germany)
Hs_RIMS1_1_SG Quantitect Primer Assay	Qiagen (Germany)
Hs_DHX57_1_SG QuantiTect Primer Assay	Qiagen (Germany)
Hs_RNF170_1_SG QuantiTect Primer Assay	Qiagen (Germany)
Hs_TMEM178B_1_SG QuantiTect Primer Assay	Qiagen (Germany)
Hs_C7orf73_1_SG QuantiTect Primer Assay	Qiagen (Germany)
Hs_STEAP3_1_SG QuantiTect Primer Assay	Qiagen (Germany)
Hs_MIER2_1_SG QuantiTect Primer Assay	Qiagen (Germany)
Hs_FOXF1_1_SG QuantiTect Primer Assay	Qiagen (Germany)
Hs_SOCS4_1_SG QuantiTect Primer Assay	Qiagen (Germany)
Hs_BRWD1_1_SG QuantiTect Primer Assay	Qiagen (Germany)
Hs_PPTC7_1_SG QuantiTect Primer Assay	Qiagen (Germany)
Hs_ENTPD5_1_SG QuantiTect Primer Assay	Qiagen (Germany)
Mm_Socs4_1_SG QuantiTect Primer Assay	Qiagen (Germany)
Mm_Steap3_1_SG QuantiTect Primer Assay	Qiagen (Germany)
Mm_Mier2_1_SG QuantiTect Primer Assay	Qiagen (Germany)
Mm_Foxf1_1_SG QuantiTect Primer Assay	Qiagen (Germany)
Mm_Pink1_1_SG QuantiTect Primer Assay	Qiagen (Germany)
Mm_Polg_1_SG QuantiTect Primer Assay	Qiagen (Germany)

Mm_Nfkb2_1_SG QuantiTect Primer Assay	Qiagen (Germany)
Mm_Hspa1a_2_SG QuantiTect Primer	Qiagen (Germany)
Mm_Sqstm1_1_SG QuantiTect Primer Assay	Qiagen (Germany)
Mm_Dyrk1a_1_SG QuantiTect Primer Assay	Qiagen (Germany)
Mm_Rims1_1_SG QuantiTect Primer Assay	Qiagen (Germany)
Mm_Galc_1_SG QuantiTect Primer Assay	Qiagen (Germany)
Mm_Nod2_1_SG QuantiTect Primer Assay	Qiagen (Germany)
Mm_Gapdh_3_SG QuantiTect Primer Assay	Qiagen (Germany)
Mm_miR-143_1 miScript Primer Assay	Qiagen (Germany)
Mm_miR-122a_1 miScript Primer Assay	Qiagen (Germany)
Mm_miR-10a_2 miScript Primer Assay	Qiagen (Germany)
Hs_let-7i_1 miScript Primer Assay	Qiagen (Germany)
Hs_miR-26a_2 miScript Primer Assay	Qiagen (Germany)
Hs_miR-218_1 miScript Primer Assay	Qiagen (Germany)
Hs_miR-424_1 miScript Primer Assay	Qiagen (Germany)
Hs_miR-29c_1 miScript Primer Assay	Qiagen (Germany)
Hs_let-7g_2 miScript Primer Assay	Qiagen (Germany)
Hs_miR-20a_1 miScript Primer Assay	Qiagen (Germany)
Hs_miR-145_1 miScript Primer Assay	Qiagen (Germany)
Hs_miR-98_1 miScript Primer Assay	Qiagen (Germany)

Table 3: List of Kits and Primer Assays

2.1.4. Buffers

Component	Amount
7M Urea (Sigma)	10.51 g
2M Thiourea (Sigma)	3.8 g
4% Chaps (Applichem)	1 g
ASB14 2% (Sigma)	0.5 g
cOmplete™, Mini, EDTA-free Protease Inhibitor (Roche)	1:25 (v/v %)
Phos Stop Phosphatase Inhibitor (Roche)	1:20 (v/v %)
Deionized water	q.s. 25 ml

Table 4. Composition of lysis buffer for Proteomics experiments

2.1.5. Equipment

Equipment	Producer
96 well micro test plates	Sarstedt (Germany)
MicroAmp Optical 96-Well Reaction Plates	Applied Biosystems (USA)
Tecan Spark 10M Plate reader	Tecan (Switzerland)
Mastercylcer nexus X2	Eppendorf (Germany
Micro-centrifuge 5415R	Eppendorf (Germany)
NanoDrop One	Thermo Fisher Scientific (USA)
Agilent 2100 Bioanalyzer	Agilent (USA)
Fragment Analyzer	Agilent (USA)
Quant Studio 3 q-RT-PCR system	Thermo Fisher Scientific (USA)
QuantiFluor dsDNA System	Promega (USA)
ABI 3130XL or 3500XL capillary seq	Applied Biosystems (USA)
HiSeq 4000 sequencing platform	Illumina (USA)
RNAse-Exitus Plus	AppliChem (Germany)
Eksigent nanoLC425 nanoflow chromatography system	AB Sciex (USA)
Hybrid triple quadrupole-TOF mass spectrometer (TripleTOF 5600+)	AB Sciex (USA)
Chrommatography Pre-column (0.18 mm ID x 20 mm; symmetry C18, 5 µm)	Waters (USA)
Chrommatography RP-C18 column	Waters (USA)
Perfusion syringe	Becton Dickinson
NuPAGE Novex Bis-Tris Minigels	Invitrogen (USA)
Thermomixer Comfort	Eppendorf (Germany)
1.5ml Biosphere Safeseal tubes	Sarstedt (Germany)

Table 5. List of equipment

2.1.6. Software

Software	Producer
CorelDraw Graphics Suite	Corel Corporation (Canada)
GraphPad Prism software version 8.1.2	GraphPad software (USA)
R software (version 3.5.1)	R Core Team, 2017
Python v.2.7.1	Python Software Foundation
limma (version 3.36.5)	(Ritchie et al., 2015)
Rank-Rank Hypergeometric Overlap (RRHO)	(Plaisier et al., 2010)
FastQC version 0.11.5	(Andrews et al., 2010)
QuantStudio Design and Analysis Software v1.5.1	Thermo Fisher Scientific (USA)
BaseCaller software	Thermo Fisher Scientific (USA)
Analyst TF 1.7.1 software build 1163	AB Sciex (USA)
Cutadapt	(Martin, 2011)
RNA-STAR version STAR_2.5.2b	(Dobin et al., 2013)
htseq-count script (HTSeq package version 0.9.1)	(Anders et al., 2015)
Bowtie version 1.1.2	(Langmead et al., 2009)
Coffalyser	MRC Holland (The Netherlands)
ProteinPilot Software version 5.0	AB Sciex (USA)
PeakView Software version 2.1	AB Sciex (USA)
SWATH quantitation microApp version 2.0	AB Sciex (USA)
Perseus 1.5.6.0	Computational Systems Biochemistry, Max Planck Institute, Martinsried Germany (Tyanova et al. 2016)

Table 6. List of software used for experiments, data analysis and figure design

2.1.7. Genes selected for MLPA and gene panel sequencing experiments

Gene	Technique
SNCA	MLPA
PARK2	MLPA
UCHL1	MLPA
PINK1	MLPA
PARK7	MLPA
ATP13A2	MLPA
LRRK2	MLPA
GCH1	MLPA
A30P (point mutation)	MLPA
G2019S (point mutation)	MLPA
Parkin	Gene panel sequencing
PINK1	Gene panel sequencing
DJ-1	Gene panel sequencing
SNCA	Gene panel sequencing
LRRK2	Gene panel sequencing
GBA	Gene panel sequencing
VPS35	Gene panel sequencing
PLA2G6	Gene panel sequencing
RAB39B	Gene panel sequencing

VPS13C	Gene panel sequencing
TOR1A	Gene panel sequencing
THAP1	Gene panel sequencing
GCH1	Gene panel sequencing
GNAL	Gene panel sequencing
SGCE	Gene panel sequencing
KMT2B	Gene panel sequencing
ANO3	Gene panel sequencing
PRKRA	Gene panel sequencing
RAB12	Gene panel sequencing
TAF1 (4 variants)	Gene panel sequencing
ADCY5	Gene panel sequencing
COX20	Gene panel sequencing
MCOLN1	Gene panel sequencing
PDGFB	Gene panel sequencing
PDGFRB	Gene panel sequencing
SLC20A2	Gene panel sequencing
XPR1	Gene panel sequencing
POLG	Gene panel sequencing
VAC14	Gene panel sequencing

Table 7. List of genes analyzed in MLPA and gene panel sequencing experiments

2.2. Methods

2.2.1. Human samples

2.2.1.1. Human midbrain sample source and ethics statement

All human midbrain samples were provided by the Parkinson's UK Brain Bank (Imperial College London, London, England). Midbrain tissue blocks (snap frozen) were transported and stored under controlled temperature conditions (-80°C). The samples were conceded to the Lingor Lab (Department of Neurology of the University Medical Center Göttingen, Göttingen, Germany). Ethical approval was given by the Multicenter Research Ethics Committee (07/MRE09/72). Table 1 encloses all information about the human samples.

2.2.1.2. Midbrain tissue sampling

For the sake of having the midbrain blocks under controlled temperature conditions, the samples were transferred to a cryostat chamber and kept at -20°C for 20 minutes for temperature balancing. Each frozen tissue block was punched with a 20-G Quincke Spinal Needle (Becton Dickinson, Madrid, Spain), and around 20 mg of were collected into RNAse/DNAse free tubes for each sample. Tissue punches were kept at -80°C until further use.

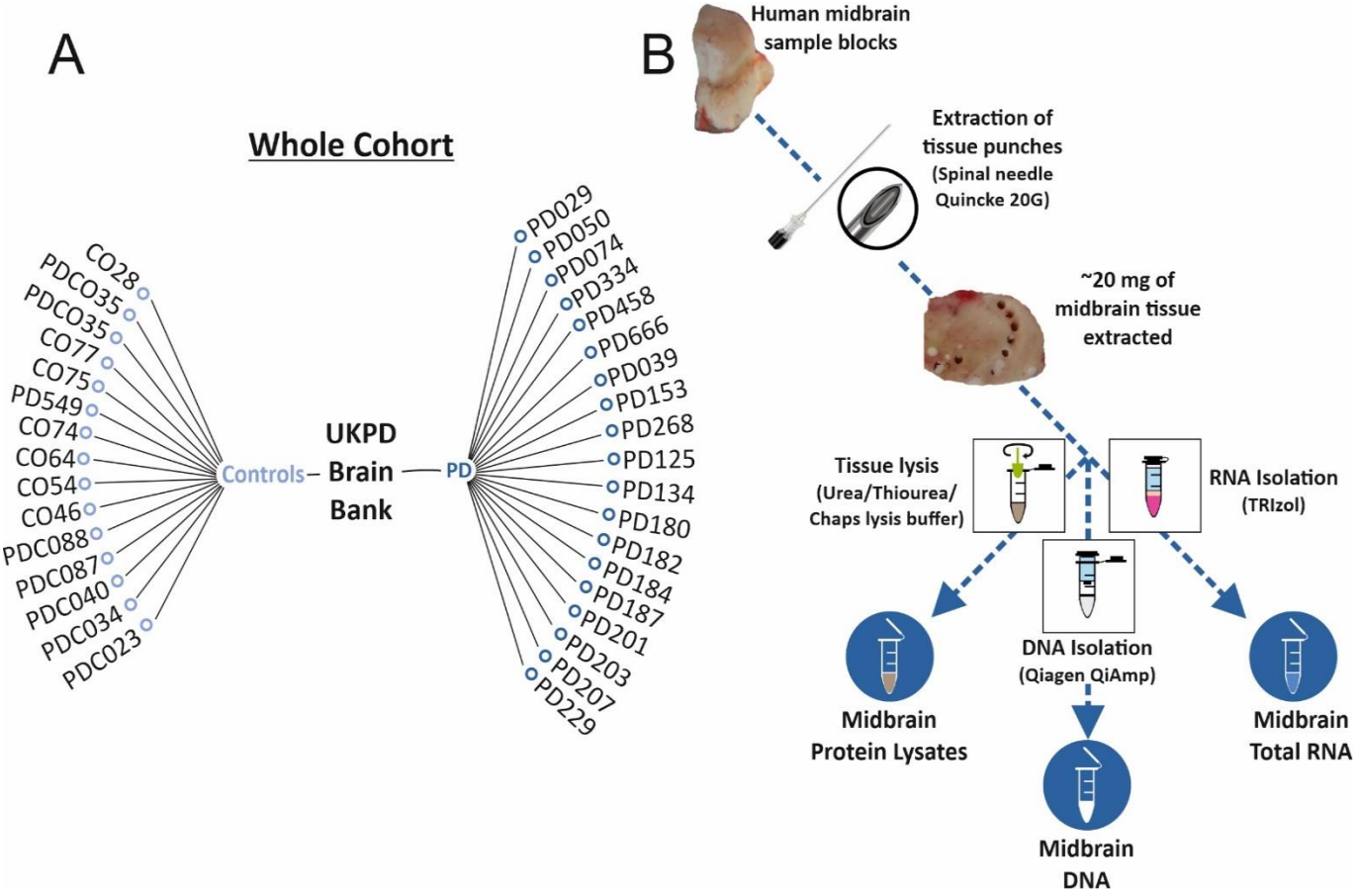

Figure 3. Information on human midbrain Samples and tissue processing. **(A)** Human midbrain sample IDs; sample source: UKPD brain bank. **(B)** Experimental design for RNA isolation and protein lysate preparation experiments; extraction of tissue punches was performed with a spinal needle. RNA isolation done by the TRIzol method. Protein lysates prepared with Urea/Thiourea/Chaps lysis buffer.

2.2.2. Animal samples

2.2.2.1. αSyn.A53T mice selection and cohort designing

Transgenic Prnp-SNCA*A53T mice were provided by the central animal facility (ZTE) of the University Medical Center Göttingen. Wild-type / homozygous animals were selected upon 10-12 weeks of life and kept in ventilated cages (multiple housing; groups of maximum 6 individuals per cage), under a 12-hour dark-light cycle and fed *ad libitum*. Six different cohorts (n = 5 animals/group) were designed according to genotype and age for sacrification. Animals in the 'early-stage' cohorts were kept until 100 days of age before sacrification. For the 'intermediate-stage' and 'late-stage' cohorts, animals were kept for

250 and 400 days of age before scarification, respectively. Animals showing any signals of paralysis or weight loss were immediately sacrificed. All experiments were performed in accordance with the national German animal protection law under the project 17/2470, grant no. 13/1118 approved by the local authorities.

2.2.2.2. Animal euthanasia and tissue processing

2.2.2.2.1. Cervical dislocation

Cervical dislocation was employed for mouse euthanasia and performed by a trained individual. The animals were restrained by the base of the tail on the wire-bar grid of a housing cage. After the animals gripped on the grid, the body was carefully stretched, so the base of the skull was completely accessible. Closed scissors were placed on the back of the neck/base of the skull and the cervical dislocation was performed with a firm horizontal push of the scissors whilst pulling the tail base to the opposite direction. Cervical dislocation effectiveness was assessed by palpation of the cervical tissues, and the death of the animals was confirmed by checking toe pain reflexes and respiratory arrest.

2.2.2.2.2. Transcranial perfusion

In order to obtain RNA of good quality for further experiments, fresh, nonfixed mouse brain tissue was required. For that sake, after euthanasia, the animals were quickly moved to a perfusion table and the abdominal skin was cut open longitudinally. The rib cage was cut open in order to expose the heart and a perfusion cannula was inserted into the left ventricle. A perfusion syringe (Becton Dickinson, Heidelberg, Germany) filled with 50 ml of ice-cold PBS was connected to the cannula and the animals were perfused with that volume for 3 minutes. After perfusion, the cranium was cut open, the brain was removed and placed on an ice pad for microdissection.

2.2.2.2.3. Preparation of midbrain regions from fresh mouse brain

The mouse brains were microdissected in order to isolate the midbrain region from both hemispheres. For that, brains were cut sagittally with a scalpel. After removing the olfactory bulb and the cerebellum (by cutting at the cerebellar peduncle), the cortex was flipped over until unraveling of the hippocampal structure and both were excised. The remaining structures containing the basal ganglia and the pons were further dissected to isolate the midbrain region. Freshly prepared midbrains were collected into Nuclease-free tubes, snap-frozen with liquid nitrogen and kept at -80°C until RNA isolation experiments.

2.2.3. Molecular biology techniques

2.2.3.1. RNA isolation, DNAse treatment of RNA samples, RNA cleaning and concentration

Total RNA was isolated from human and animal midbrain samples using TRI Reagent (Sigma Aldrich, Taufkirchen, Germany). All RNA-related experiments were performed under an RNA-workstation fume hood. Shortly, 1 ml of TRI Reagent was added to each midbrain sample and incubated for 5 minutes, followed by addition of 100µl of 1-Bromo-3-Chlor-Propane (Sigma Aldrich, Taufkirchen, Germany). The reaction tubes were mixed by inversion for 10 - 15 seconds and incubated at room temperature for 3 minutes. The lysates were centrifuged at 12.000 x g for 15 minutes / 4°C, leading to separation of organic and aqueous phases. The RNA-containing aqueous phase was transferred to a fresh Nuclease-free tube. RNA precipitation was performed by adding 500 µl of 2-propanol (AppliChem, Darmstadt, Germany) and 2 µl GlycoBlue Co-precipitant (15 mg/ml) (ThermoFisher, Waltham, MA, USA), followed by overnight incubation at -20°C. Next, the samples were centrifuged at 12.000 x g for 30 minutes / 4°C, the supernatant was discarded and the RNA pellets washed three times with 75% ice-cold ethanol (AppliChem, Darmstadt, Germany). The pellets were dried for 5 minutes under the fume hood, reconstituted with 15-20 µl of Nuclease-free water (Sigma Aldrich, Taufkirchen, Germany) and RNA samples incubated at 55°C for 2 minutes in a thermoshaker in order to completely dissolve the RNA.

After the RNA isolation, a DNAse treatment was performed in order to remove any remaining DNA from the samples. For that, 5µl of 10X DNAse I Incubation buffer (Life Technologies, Carlsbad, CA, United States) were added to each sample, followed by the addition of 5µl DNase I (2U/µL) and 0.5µl - RNase OUT (40U/µl). Samples were made up to a volume of 50 µl by the addition of Nuclease-free water, followed by incubation at 37°C for 20 minutes. Finally, the RNA samples were cleaned and concentrated with the RNA Clean & Concentrator-5 KIT (Zymo Research, Irvine, CA, USA), following the manufacturer's instructions.

2.2.3.2. DNA isolation and sample processing

DNA isolation from human midbrain samples was performed with the QIAamp DNA Mini Kit following the manufacturer's instructions. Midbrain DNA samples were freshly prepared and directly shipped to the Laboratory of Translational Neurogenetics (Institute of Neurogenetics, University of Lübeck) for MLPA and gene panel sequencing experiments.

2.2.3.3. Determination of nucleic acid concentration and purity

Directly after RNA / DNA isolation, nucleic acid concentration and purity were measured in the NanoDrop One spectrophotometer (ThermoFisher, Waltham, MA, USA). Spectrophotometric quantification in the NanoDrop system required 1 µl of each sample. For RNA samples used in RNA sequencing experiments, RNA integrity was assessed with the Agilent 6000 Nano Chip in the Agilent 2100 Bioanalyzer (Agilent, Santa Clara, CA, USA).

2.2.3.4. Reverse transcription

For quantitative real-time PCR experiments (q-RT-PCR), complementary DNA (cDNA) synthesis was performed. For miRNA q-RT-PCR validation experiments, 500 ng of RNA from each sample were reverse transcribed using the miScript II RT Kit (Qiagen, Hilden, Germany) with the *HiSpec* buffer (designed for the reverse transcription of mature miRNAs). For transcriptomics validation experiments, 1 µg RNA / sample was reversed

transcribed using the QuantiTect Reverse Transcription Kit (Qiagen, Hilden, Germany). All steps were performed on ice. A master-mix was prepared for each RT reaction, as follows:

Component	Volume/reaction
5x miScript HiSpec Buffer	2 µl
10x miScript Nucleics Mix	1 µl
miScript Reverse Transcriptase Mix	1 µl
Template RNA (volume for 500ng)	variable
RNase-free water (quantum sufficit)	variable
Total Volume	**10 µl**

Table 8. Components for Reverse Transcript reactions

Following the addition of the master mix to the samples, the reaction tubes were incubated for 60 minutes at 37 °C in the Mastercycler nexus X2 PCR thermocycler (Eppendorf, Hamburg, Germany), followed by incubation at 95°C for 5 minutes to inactivate the reverse transcriptase. cDNA samples were diluted 1:3 in nuclease-free water and stored at -20 °C until q-RT-PCR experiments.

2.2.3.5. Quantitative Real-Time Polymerase Chain Reaction (q-RT-PCR)

To determine expression levels of selected miRNAs and mRNAs in human and animal midbrain samples, q-RT-PCR reactions were conducted in the QuantStudio 3 system (ThermoFisher, Waltham, MA, USA). For miRNA q-RT-PCR experiments, the miScript SYBR Green PCR Kit (Qiagen, Hilden, Germany) was used, and miRNA expression was normalized to the endogenous control RNU 6. For the validation of transcriptomics experiments, the QuantiTect SYBR Green PCR Kit (Qiagen, Hilden, Germany) was employed, using GAPDH as a housekeeping control. MicroAmp Optical 96-Well Reaction Plates (Applied Biosystems, Foster City, CA, USA) were prepared at room temperature and the reaction plates were tightly sealed with a heat-sealing adhesive film before placement inside the cycler. Reaction volumes were calculated as described in the tables below.

Component	Volume/reaction
2x QuantiTect SYBR Green PCR Master Mix	10 µl
10x miScript Universal Primer	2 µl
10x miScript Primer Assay	2 µl
RNase-free water	4 µl
cDNA template	2 µl
Total volume	**20 µl**

Table 9. miScript q-RT-PCR Reactions Master mix (for miRNA validation experiments)

Component	Volume/reaction
2x QuantiTect SYBR Green PCR Master Mix	12,5 µl
10x miScript Primer Assay	2,5 µl
RNase-free water	9 µl
cDNA template	1 µl
Total volume	**25 µl**

Table 10. QuantiTect q-RT-PCR Reactions Master mix (for mRNA validation experiments)

The cycling conditions are described in the table below. A melt curve analysis was set for every q-RT-PCR run.

Step	Time	Temperature
PCR initial activation step	15 min	95 °C
3-step cycling:		
Denaturation	15 s	94 °C
Annealing	30 s	55 °C
Extension	30 s	70 °C
Cycle number	40 cycles	

Table 11. qPCR cycling settings

The relative expression levels of miRNA and mRNA species were calculated by the ΔΔCt method (delta-delta-Ct). Ct values for each sample were compared to the average of ΔCt of the respective control group.

2.2.3.6. Multiplex Ligation-dependent Probe Amplification (MLPA)

MLPA experiments were performed in order to detect abnormalities in copy numbers (e.g. deletions, duplications, triplications) of specific PD-related genes. For the MLPA analyses, *SALSA P051 and P052 Parkinson MLPA* kits (MRC Holland, Amsterdam, The Netherlands) - a set of standard commercial probes - were employed. These kits cover exons that include Parkin, PINK1, and DJ-1 and selected mutations in LRRK2 and SNCA genes. Further analyzed exons are listed in table 7. DNA samples were prepared (as described in 2.2.3.2) and shipped to the lab of Prof. Christine Klein / Dr. Katja Lohmann (Universität zu Lübeck), were the experiments were perfomed. MLPA experiments were conducted according to the manufacturer's protocol. PCR amplification products were visualized on capillary sequencing machines (either ABI 3130XL or 3500XL) (Applied Biosystems, Foster City, CA, USA) using the coffalyser software (MRC Holland, Amsterdam, The Netherlands).

2.2.3.7. Gene Panel sequencing

For Gene Panel analysis, similar to the MLPA experiments, DNA samples were prepared (as described in section 2.2.3.2) and shipped to the lab of Prof. Christine Klein / Dr. Katja Lohmann (Universität zu Lübeck) for the DNA sequencing. After preparation of the panels, the samples were sequenced on a next-generation sequencing platform with a collaboration partner (Centogene AG, Rostock, Germany). 29 genes previously linked to PD or dystonia (DYT) phenotypes were analyzed. The mean sequencing depth was 600x. Variants were filtered according to quality scores (cut-offs: quality score >200; coverage >10, allele fraction >20%), further filtered for the number of times that they appeared in public databases (cut-off: <0.01 in public databases and the in-house database) and finally for protein-changing variants in PD genes. Candidate variants were confirmed by Sanger sequencing. All genes included in the gene panel are disclosed in table 7.

2.2.3.8. RNA sequencing experiments

2.2.3.8.1. Small RNA sequencing library preparation

Small RNA sequencing experiments were performed in the Transcriptome and Genome Analysis Laboratory (TAL) of the University Medical Center Göttingen. Small RNA libraries were prepared using the *TruSeq Small RNA Library Prep Kit* (Illumina, San Diego, CA, USA) with minor modifications. 600 ng total RNA were used as starting material for library preparation. In order to prevent the formation of adapter dimers (by 5′ and 3′ self-ligation) and consequent amplification of these dimers, the *CleanTag Library Preparation for Next-Generation Sequencing Kit* (TriLink, San Diego, CA, USA) was employed.

2.2.3.8.2. Small RNA sequencing library quality assessment

Small RNA libraries quality and integrity were assessed in the *Fragment Analyzer* platform (Agilent, Santa Clara, CA, USA). Therefore, the standard sensitivity RNA Analysis Kit was used. All samples selected for sequencing exhibited a comparable RNA integrity number (7-8). For accurate quantitation of small RNA libraries, a library pool was quantified with the *QuantiFluor dsDNA* System (Promega, Madison, WI, USA). Finally, the size of the small RNA libraries was determined using the *dsDNA 905 Reagent Kit* (Agilent, Santa Clara, CA, USA). Small RNA sequencing was performed on the Illumina HiSeq 4000 platform (Illumina, San Diego, CA, USA), generating 50 bp single-end reads (10-20 Million reads/ sample).

2.2.3.8.3. RNA sequencing library preparation

Likewise small RNA sequencing experiments, transcriptomics were performed in the Transcriptome and Genome Analysis Laboratory (TAL) of the University Medical Center Göttingen. The same RNA source was used for both small RNA and RNA sequencing experiments. RNA libraries were prepared using a modified version of the *TruSeq Stranded Total RNA* protocol (Illumina, San Diego, CA, USA), a strand-specific, massive-parallel cDNA sequencing protocol. 200 ng of total RNA were used as a start material. A ribosomal RNA (rRNA) depletion protocol (RiboMinus™, ThermoFisher, Waltham, MA, USA) was

performed in order to maintain rRNA content under 5% in the samples. Shortly, this technology utilizes specific locked nucleic acid (LNA) bind rRNA and subsequently to streptavidin-coated magnetic beads to remove those species from the samples. Next, an adaptor ligation step is performed, followed by PCR amplification of the reads. A reduced number of PCR cycles was employed in order to avoid PCR duplication artifacts, as well as primer dimers in the final libraries.

2.2.3.8.4. RNA sequencing library quality assessment

A Fragment Analyzer (Agilent, Santa Clara, CA, USA) was used for assessment of RNA quality and integrity. RNA integrity numbers from all samples selected for sequencing ranged from 7-8. For accurate quantitation of the libraries, the *QuantiFluor dsDNA* System (Promega, Madison, WI, USA) was employed. cDNA library sizes were determined with the *dsDNA 905 Kit* (Agilent, Santa Clara, CA, USA). Finally, the libraries were pooled and sequenced on an Illumina HiSeq 4000 (Illumina, San Diego, CA, USA) generating 50 bp single-end reads (30-40 Million reads/sample).

2.2.3.8.5. Raw sequencing reads and sequencing quality check

After RNA sequencing runs, sequence images were transformed to BCL files with the *BaseCaller* software. Thereafter, the files were demultiplexed to fastq files with *bcl2fastq* v2.17.1.14. Both software were provided by Illumina (Illumina, San Diego, CA, USA). Quality check of the reads fastq files was done with FastQC version 0.11.5 (Andrews et al., 2010)

2.2.3.9 Proteomics experiments

2.2.3.9.1 Lysate preparation

For proteomics experiments, human midbrain tissue lysis was performed in freshly prepared Urea/Thiourea/Chaps lysis buffer. The detailed composition of the lysis buffer is depicted in table 4. Samples were homogenized with plastic stabs and lysates were spinned-down in order to remove bubbles produced by the manual homogenization. For a

fine homogenization of the lysates, the samples were sonicated twice for 15-second intervals at an amplitude of 40%. Sonication was performed on ice. A new centrifugation step was performed to remove the produced bubbles.

2.2.3.9.2 Protein quantification and sampling

Protein quantification was performed with the modified-Bradford Roti-Nanoquant protein quantification kit (Carl-Roth, Karlsruhe, Germany), following the manufacturer's instructions. The prepared colorimetric reactions were read in the TECAN Spark 10M Plate reader. A final amount of 50 µg protein was aliquoted for further proteomics experiments.

2.2.3.9.3 Mass spectrometry runs

For mass spectrometry (MS) experiments, previously prepared protein aliquots (50µg protein/sample) were loaded into a 4-12% NuPAGE Novex Bis-Tris Minigels (Invitrogen, Carlsbad, CA, USA). Samples were run for 1.5 cm by electrophoresis and stained with Coomassie Brilliant Blue. The bands were cut out, diced and undergo reduction with the use of dithiothreitol, alkylation with iodoacetamide. Next, proteins were digested with trypsin overnight. Tryptic peptides were extracted from the gel and the solution was dried in a Speedvac (Atanassov and Urlaub, 2013). For the generation of peptide libraries, equal aliquots from each sample were pooled to a total of 80 µg and further separated into eight fractions using a reversed-phase spin column (Pierce High pH Reversed-Phase Peptide Fractionation Kit) (ThermoFisher, Waltham, MA, USA). Spike-ins from a synthetic peptide standard were added to the samples and used for retention time alignment (iRT Standard, Schlieren, Switzerland). Protein digests were analyzed on the Eksigent nanoLC425 nanoflow chromatography system (AB Sciex, Framingham, MA, USA), hyphenated to a hybrid triple quadrupole-TOF mass spectrometer (TripleTOF 5600+) equipped with a Nanospray III ion source (Ionspray Voltage 2400 V, Interface Heater Temperature 150°C, Sheath Gas Setting 12) and controlled by Analyst TF 1.7.1 software build 1163 (AB Sciex, Framingham, MA, USA). Briefly, peptides were dissolved in a loading buffer (composed of 2% acetonitrile and 0.1% formic acid in water) to a concentration of 0.3 µg/µl. For each analysis, 1.5 µg of digested protein was enriched on a pre-column of dimensions 0.18 mm ID x 20 mm and

symmetry C18, 5 µm (Waters, Milford, MA, USA). Next, separation was performed on an analytical RP-C18 column of dimensions 0.075 mm ID x 250 mm, HSS T3, 1.8 µm (Waters, Milford, MA, USA) using a 90 min linear gradient of 5-35 % acetonitrile / 0.1% formic acid (v:v) at 300 nl min^{-1}.

2.2.3.9.4 Mass spectrometry analysis

Qualitative liquid chromatography/tandem mass spectrometry (LC-MS/MS) analysis was performed using a Top25 data-dependent acquisition method. For that, an MS survey scan of m/z 350–1250 accumulated for 350 ms at a resolution of 30,000 full width at half maximum (FWHM) was performed. MS/MS scans of m/z 180–1600 were accumulated for 100 ms at a resolution of 17,500 FWHM and a precursor isolation width of 0.7 FWHM, resulting in a total cycle time of 2.9 s. Precursors above a threshold of 125 cps for MS intensity and with charge states of 2+ / 3+ / 4+ were selected for MS/MS. Dynamic exclusion time was set to 30 s. An MS/MS activation was achieved by CID using nitrogen as a collision gas. The manufacturer's default rolling collision energy settings were employed. Three technical replicates per reversed-phase fraction were analyzed to construct a spectral library. For quantitative sequential window acquisition of all theoretical fragment ion spectra (SWATH) analysis, MS/MS data were acquired using 65 variable size windows across the 400-1,050 m/z range. Fragments were produced using rolling collision energy settings for charge state 2+, and fragments acquired over an m/z range of 350–1400 for 40 ms per segment. With the inclusion of a 100 ms survey scan, the overall cycle time was of 2.75s. Either two or three replicate injections were acquired for each biological sample (Gillet et al., 2012; Losensky et al., 2017; Zhang et al., 2015).

2.2.3.10 Bioinformatics analyses

MLPA and gene panel sequencing data processing was done in collaboration with the lab of Prof. Christine Klein / Dr. Katja Lohmann (Universität zu Lübeck). RNA sequencing quality control and data processing were performed with the assistance of Dr. Gaurav Jain (Lab of Prof. André Fischer, DZNE Göttingen) using in-house developed pipelines. Processing of Proteomics data was performed in collaboration with the lab of Prof. Henning

Urlaub / Dr. Christof Lenz (UMG Göttingen). Proteomics differential expression (DE) analyses were done with the assistance of the Department of Medical Statistics (UMG Göttingen).

2.2.3.10.1 Small RNA sequencing data processing and mapping

After small RNA sequencing, the data was processed with a customized in-house pipeline (Jain, 2018). After fastq file quality control check with FastQC, the 3' adapters were trimmed and reads with the minimum length of 16 nucleotides were filtered out with the Cutadapt pipeline (Martin, 2011). The reads are then mapped to the reference genome for miRNAs and piRNAs known sequences, followed to the reference genome made from other small noncoding RNAs. The remaining unmapped reads were mapped to the human genome. Bowtie version 1.1.2 (Langmead et al., 2009) was employed for all mapping steps, and no mismatches were allowed for reads ≤ 32 b. For reads between 33 b and 50 b, one mismatch was tolerated.

2.2.3.10.2 RNA sequencing analyses data processing and mapping

Likewise, the small RNA sequencing data processing, the RNA sequencing data were processed with a customized in-house pipeline (Jain, 2018). Adapter trimming and demultiplexing were performed alongside base calling. Quality control of raw sequencing reads was performed using FastQC. RNA reads were mapped to the human transcriptome using RNA-STAR version STAR_2.5.2b (Dobin et al., 2013) for all mapping steps. The reads were mapped in the non-splice-junction-aware mode and no mismatches for the reads <19 b were allowed. For reads between 20 b and 39 b, one mismatch was allowed, and for reads between 40 b and 59 b, two mismatches were tolerated. Besides the parameters depicted here, all other parameters were default in RNA-STAR. Aligned reads overlapping exons (for each gene) was counted with the *intersection-non-empty* mode of the htseq-count script (HTSeq package version 0.9.1) (Anders et al., 2015).

2.2.3.10.3 Mass spectrometry data processing and mapping

Protein identification was achieved using ProteinPilot Software version 5.0 build 4769 (AB Sciex, Framingham, MA, USA) at *thorough* settings. A total of 407,752 MS/MS spectra from the combined qualitative analyses were searched against the UniProtKB human reference proteome (revision 04/2018, 93.609 entries) augmented with a set of 52 known common laboratory contaminants. Spectral library generation and SWATH peak extraction were achieved in PeakView Software version 2.1 build 11041 (AB Sciex, Framingham, MA, USA) using the SWATH quantitation microApp (version 2.0 build 2003). Following retention time correction by the iRT standard, peak areas were extracted using information from the MS/MS library at a False Discovery Rate (FDR) of 1% (Lambert et al., 2013). Finally, the resulting peak areas were summed to peptide area values and next to protein area values.

2.2.3.10.4 Differential expression and sample correlation analyses for small RNA sequencing/transcriptomics

In order to identify the differentially expressed (DE) small RNAs and genes (from both small RNA sequencing and transcriptomics experiments), linear shifts associated with different batches of shipped samples were removed using the removeBatchEffect function from the limma package (Ritchie et al., 2015). Thereafter, unwanted sources of variation (RUVs) were identified and corrected by the RUVSeq script (v. 1.8.0) (Risso et al., 2014). Finally, the DESeq2 pipeline (v. 1.14.1) using a variance-stabilizing transformation was employed to perform the DE analysis for small RNA / transcriptomics datasets (Anders and Huber, 2010; Love et al., 2014). Heatmaps and volcano plots were generated either with a custom python script (python v.2.7.1 and Matplotlib 1.5.1) or with the web-enabled Heatmapper tool (Babicki et al., 2016). For the for small RNA sequencing dataset, the cut-offs for significantly DE small RNAs were basemean ≥ 20, log2foldchange <> 0.20 and FDR ≤ 0.1 were adopted for further analyses. Because of the substantially greater number of mapped reads for the transcriptomics dataset, more stringent cut-offs were adopted for further analyses, as follows: basemean ≥ 20, log2foldchange <> 0.20 and FDR ≤ 0.05. Pairwise sample correlation analyses for small RNA sequencing results were performed using Bayesian Hierarchical Clustering (Heller and Ghahramani, 2005; Savage et al., 2019)

2.2.3.10.5 Differential expression analyses for proteomics

For the proteomics data, DE analyses were conducted in the R software (version 3.5.1) (R Core Team, 2017) using the limma (version 3.36.5) (Ritchie et al., 2015) accounting for technical replication (Smyth et al., 2005). Normalized protein quantitation data have been log2 transformed prior to the analyses. Heatmaps and volcano plots were generated with R-based Ggplot2 (Wickham, 2009) and the web-enabled Heatmapper tool (Babicki et al., 2016).

2.2.3.10.6 Putative signature for miRNA data

Using the miRNA expression data, a putative signature iteration was performed in order to identify potential informative features for differentiation between PD and Control groups in the dataset. Briefly, Measure of Relevance (MoR) was performed in the first iteration. With the MoR analysis, the features were evaluated according to parameters that include biological difference, distribution overlap and dispersion parameters of the samples. Thereafter, a machine learning variable ranking was performed in order to filter out low ranking miRNAs from the previous iteration. MoR values are then assigned to the features and filtered (as described in Yassouridis et al., 2012). A reliability investigation iteration (RiA) (Denk et al., 2015) was performed to test the output features in randomized stratified samplings of the dataset (n = 500), and class weights were adopted in order to minimize false negatives. The final features were selected from the overlapping outputs from both analyses.

2.2.3.10.7 Stepwise candidate selection from integrative results (within datasets)

Figure 4 illustrates the exact steps performed for the multi-omics integration, from the complete datasets (DE results from each technique) to the selection and validation of overlapping candidates across the datasets. Further details on each method are depicted below.

2.2.3.10.7.1 Rank-Rank Hypergeometric Overlap

The integration of the datasets was performed stepwise, first from the small RNA to the transcriptomics datasets, and then from the transcriptomics to the proteomics dataset. For the integration of the first two datasets, the available pipeline entitled *Rank-Rank Hypergeometric Overlap* (RRHO) was applied (Plaisier et al., 2010). Briefly, this bioinformatical pipeline assigns an enrichment score to the components of two different datasets based on DE data (p-value / log2FoldChange values and directionality). Then, the method overlaps the two ranked lists using features that include rank-based gene set enrichment analysis and hypergeometric statistics. For the miRNAs / transcripts integration, only the discordant overlap was considered (i.e. down-regulated miRNAs from small RNA sequencing dataset paired with the respective up-regulated target (mRNA) from the transcriptomics dataset, and vice-versa). In contrast, for mRNAs / proteins integration, only concordant overlaps were considered (i.e. only up-regulated transcripts from the transcriptomics dataset paired with the respective up-regulated protein product from the proteomics dataset - and vice-versa). The full datasets were used as an input for the pipeline and the output results were generated in the form of excel sheets.

2.2.3.10.7.2 Cross-checking lists

After the stepwise integration using the RRHO pipeline, the output lists were extracted and filtered in terms of significance. For that, the specific cut-offs defined for each dataset during DE analyses. A manual stepwise cross-check of DE lists was performed. Similar to the RRHO pipeline integration, only valid interactions were considered (i.e. discordant expression between miRNA and mRNAs, concordant expression between mRNAs and proteins), narrowing down the RRHO output results to a final list of candidates from the stepwise dataset integration. These final lists were considered for the selection of validation candidates both in human and animal q-RT-PCR validation experiments.

2.2.3.10.7.3 Selection of validation targets from RNA sequencing experiments

After obtaining the final list of miRNA and mRNA candidates from the RRHO and list cross-check methods, the probability of interaction between miRNA-mRNA pairs was assessed in the TargetScan 7.2 database (Agarwal et al., 2015). Among its functionalities, this database allows the ranking of the targeting predictions by their probability of conserved targeting (Pct scores) (Friedman et al., 2008). For the selection of miRNA / mRNA candidates for q-RT-PCR validation experiments, only interactions with Pct values ≥ 0.7 were considered (aiming for pairs with the highest probability of interaction among the ones identified in the integrative approaches).

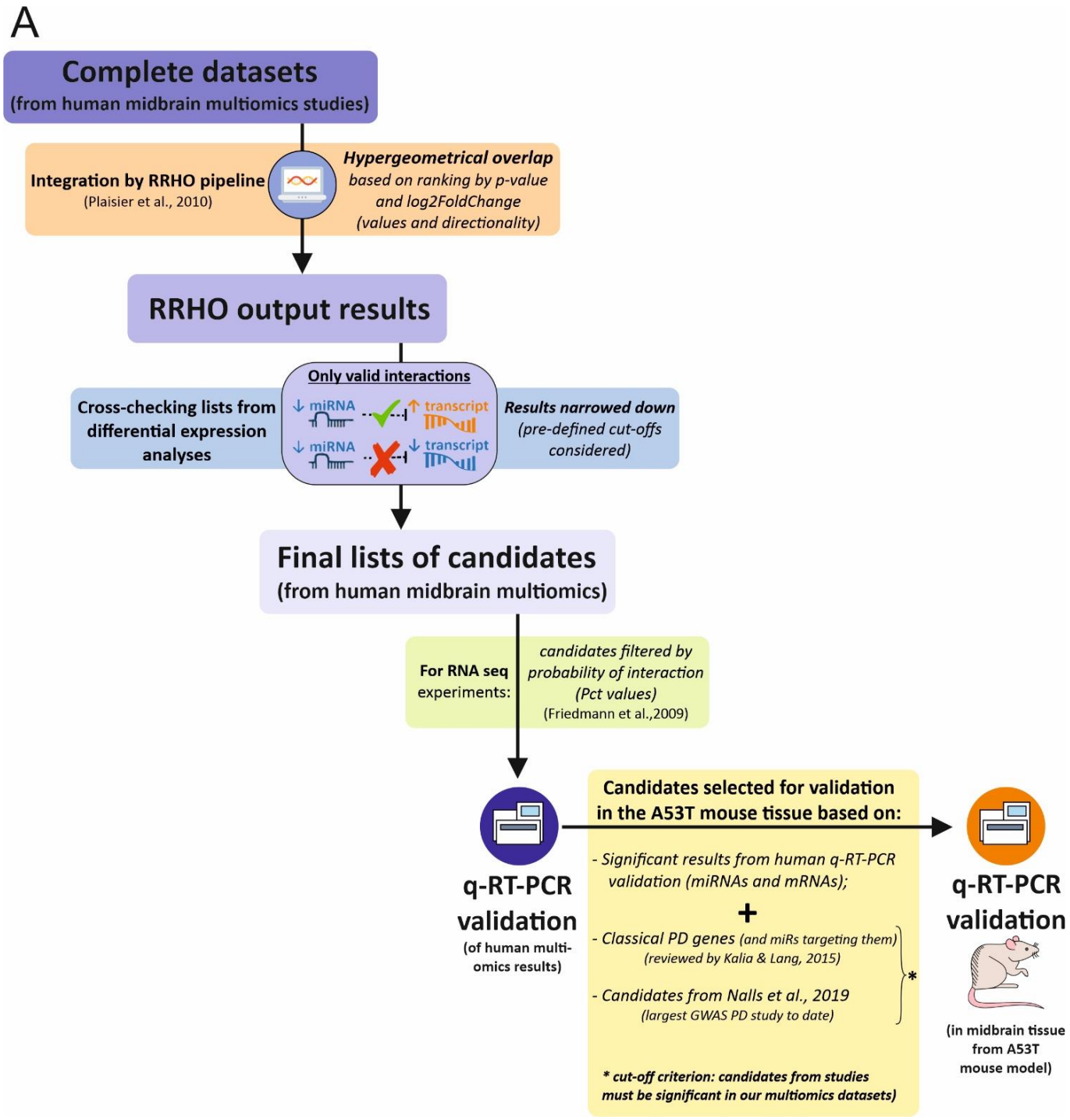

Figure 4. (A) Stepwise integration of the human multi-omics datasets and candidate selection for q-RT-PCR validations (both for miRNA and transcriptomics in human and mouse midbrain tissue). DE results from each technique considered as the starting input for integrative approaches.

2.2.3.10.8 Functional annotation and target prediction tools

As described in the previous section, target prediction of miRNA species was done with the TargetScanHuman 7.2 database (Agarwal et al., 2015). This database predicts miRNA targeting according to nucleotide sequence and miRNA seed region. Experimentally validated targets were retrieved from the miRTarBase database (Chou et al., 2018). Functional annotation of transcripts / miRNA predicted targets, as well as enrichment analyses (Gene Ontology and KEGG Pathway analyses), were performed both with the DAVID 6.8 platform (Huang et al., 2009a, 2009b) and WEBGESTALT (Liao et al., 2019). Data mining for experimentally validated miRNA target lists was performed with the miRWalk 3.0 database (Sticht et al., 2018).

2.2.3.10.9 Statistical analyses

Besides the aforementioned bioinformatical pipelines for DE analyses, statistical analyses were conducted with the GraphPad Prism software version 8.1.2 (GraphPad, San Diego, CA, USA). q-RT-PCR relative expression data were tested for normality with both D'Agostino & Pearson omnibus normality test and Shapiro-Wilk tests. For the human relative expression values, group comparisons were tested with the non-parametric Mann-Whitney-U test. For the animal validation experiments, group comparisons were performed with mixed-effects ANOVA followed by the Bonferroni post-hoc test. Statistical tests and cohort numbers are always indicated in the respective figure legends. Data are given as mean ± standard error of the mean (SEM). Differences were considered significant when $p < 0.05$ (* $p < 0.05$ / ** $p < 0.01$ / *** $p < 0.001$ / $p < 0.0001$).

3 Results

3.1 Assessment of genetic alterations in PD patients by MLPA and gene panel sequencing

In order to explore the genetic background of PD patients selected for this study, genomic DNA from midbrains of the PD patient cohort was extracted and both *Multiplex Ligation-dependent Probe Amplification* (MLPA) and gene panel sequencing were performed (Figure 5A). The presence of classic mutations and further genetic alterations previously linked to PD pathophysiology were assessed for selected genes.

First, deletions, duplications and triplications in specific PD-related genes were verified using MLPA runs. This is a multiplex PCR-based method that allows the detection of abnormal copy numbers for given genes. PD-specific MLPA probemix kits – the SALSA P051 and P052 – were applied. The screening revealed no changes in copy numbers of the examined genes. MLPA results revealed no alterations in copy numbers of genes that included Parkin, PINK1, DJ-1, LRRK2 and SNCA genes (Figure 5B).

A gene panel comprising 29 genes previously linked to PD or DYT phenotypes was applied for targeted next-generation sequencing analysis of the PD patient cohort. No major alterations were found in the patients by gene panel sequencing. One patient (PD666) presented a variation of uncertain significance (VUS) for the POLG gene (single nucleotide variant, NM_001126131.1:c.2542G>A). Studies linked the presence of this variant to alteration in PD predisposition and progression in the carriers (Gui et al., 2015b; Luoma et al., 2007). None of the other patients presented mutations in the analyzed genes according to the gene panel sequencing (Figure 5C). The findings indicate that the cohort is composed of idiopathic PD cases, excluding a major genetic influence to the PD cases analyzed in this work. In spite of phenotypic overlaps between familial and idiopathic cases for PD, the different pathogenic/cellular events underlying autosomal forms of PD have not been focused in the course of this study (Cookson et al., 2005; Papapetropoulos et al., 2007; Vibha et al., 2010).

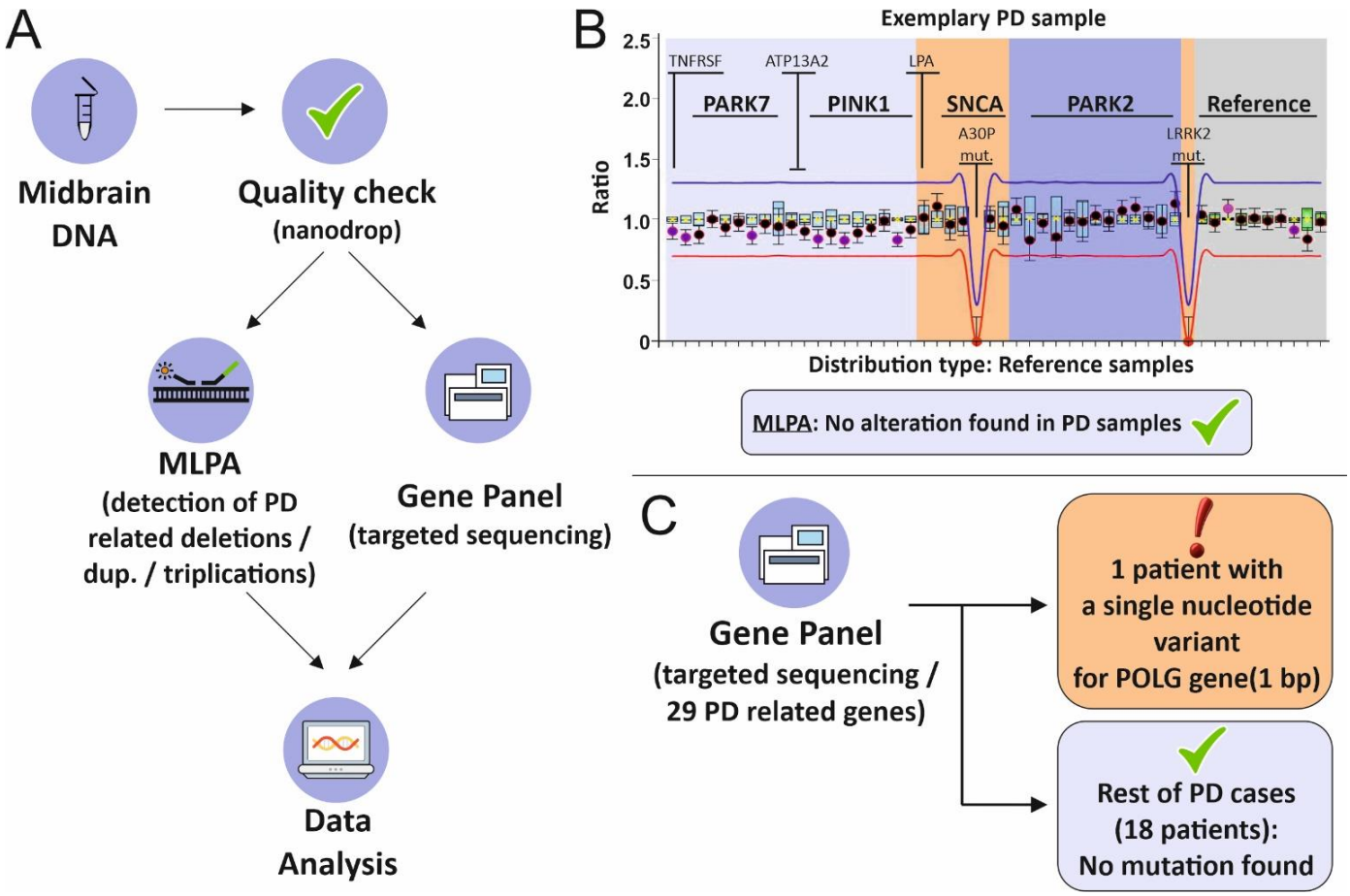

Figure 5. Gene panel and MLPA experiments overview. (A) Experimental design; after quality check, DNA samples were processed in MLPA / Gene panel sequencing experiments **(B)** Exemplary MLPA results for a PD patient showing no alteration (deletion, duplications or triplications) for the explored genes. Likewise, no alterations were found in the PD patient cohort. **(C)** Gene panel experiments reveal a single nucleotide variant (length: 1 bp) for the POLG gene in one of the PD patients (PD666). No mutations found for the rest of the cohort.

3.2 Small RNA sequencing overview and small RNA profiles in PD / control midbrains

In order to evaluate the small RNA content and profile the miRNA expression patterns in the present cohorts, total RNA was isolated from the midbrain of controls and PD patients. Subsequently, RNA quality control and small RNA sequencing was performed on the Illumina HiSeq 4000 platform (Figure 6A). To this, small RNA libraries were prepared from total RNA from each midbrain sample. Libraries from all patients had a satisfactory number of uniquely mapped reads (>50.000 reads/library) and were further used for downstream analyses of sequencing results (Figure 6B).

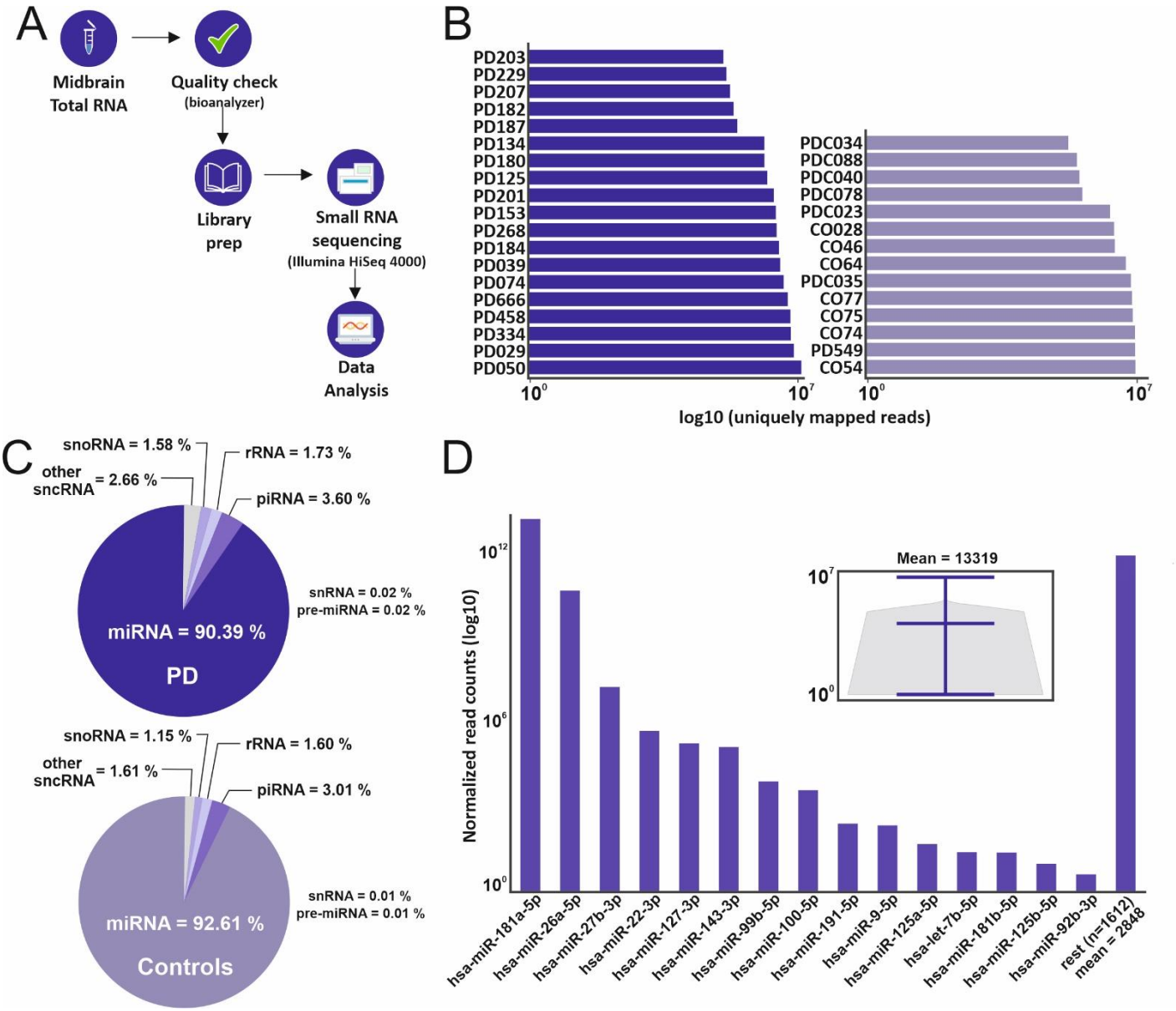

Figure 6. Small RNA sequencing overview. (A) Experimental design; after quality check, small RNA libraries were prepared from total RNA from each midbrain sample. Sequencing performed in the Illumina HiSeq 400 platform was followed by bioinformatical analysis. **(B)** Barplots representing

small RNA library size for samples from individual subjects (dark purple: PD patients; light purple: controls). Values correspond to uniquely mapped reads. **(C)** Pie charts showing average ratios of the different small RNA species detected in the small RNA libraries as a readout for quality of the sequencing technique; miRNAs represent the vast majority of mapped small non-coding RNAs in both conditions (dark purple: PD patients; light purple: controls). **(D)** Top 15 expressed miRNAs in all samples; bar at the far right represents the sum of remaining miRNAs found in the samples. The central plot represents the distribution of all miRNA species detected in the sequencing.

All bioinformatical analyses were performed in collaboration with the Lab of Prof. André Fischer using in-house modified pipelines. The vast majority of mapped small RNA sequencing counts were composed by miRNAs in both PD and control conditions (90.39 % and 92.61 % of all mapped counts for different small RNA species, respectively) (Figure 6C). Amongst the top 15 miRNA with the highest average expression in all subjects, at least 4 miRNAs (miR-181a-5p, miR-127-3p, miR-99b-5p, miR-9-5p) have been previously reported to be brain / CNS specific (Figure 6D) (Hinske et al., 2014). The normalized expression for miRNA species was considered for the following downstream and DE analyses.

3.3 Differential expression analyses of small RNA sequencing results reveal regulated and potential signature miRNAs for PD

DE analyses conducted with small RNA sequencing results showed regulation in the expression of a number of miRNAs in PD patient samples in comparison to controls (Figure 7A). A custom cut-off for a minimum number of reads was defined in order to exclude very lowly expressed miRNAs (min. number of reads per condition = 20). Under the default DESeq2 pipeline conditions for DE analyses ($\log2FC \pm 1$; $FDR < 0.05$), 21 miRNAs were found regulated. For exploratory handling of the miRNA expression data, less stringent cut-offs were applied for the fold-change in expression and FDR corrections ($\log2FC \pm 0.1$; $FDR < 0.1$) and considered for subsequent pathway enrichment analyses with miRNA targets. Under those parameters, significant differences in the expression of 27 miRNAs were observed. The majority of these miRNAs (74 % of them) were found up-regulated in PD patients.

In order to have an overview about the expression levels of regulated small RNA species in different disease states (PD / controls), a heatmap was created using the full output of the DESeq2 differential analyses (Figure 7C). The heatmap shows variable expression patterns for the different species within conditions with a rather high inter-individual variability in both PD and control groups.

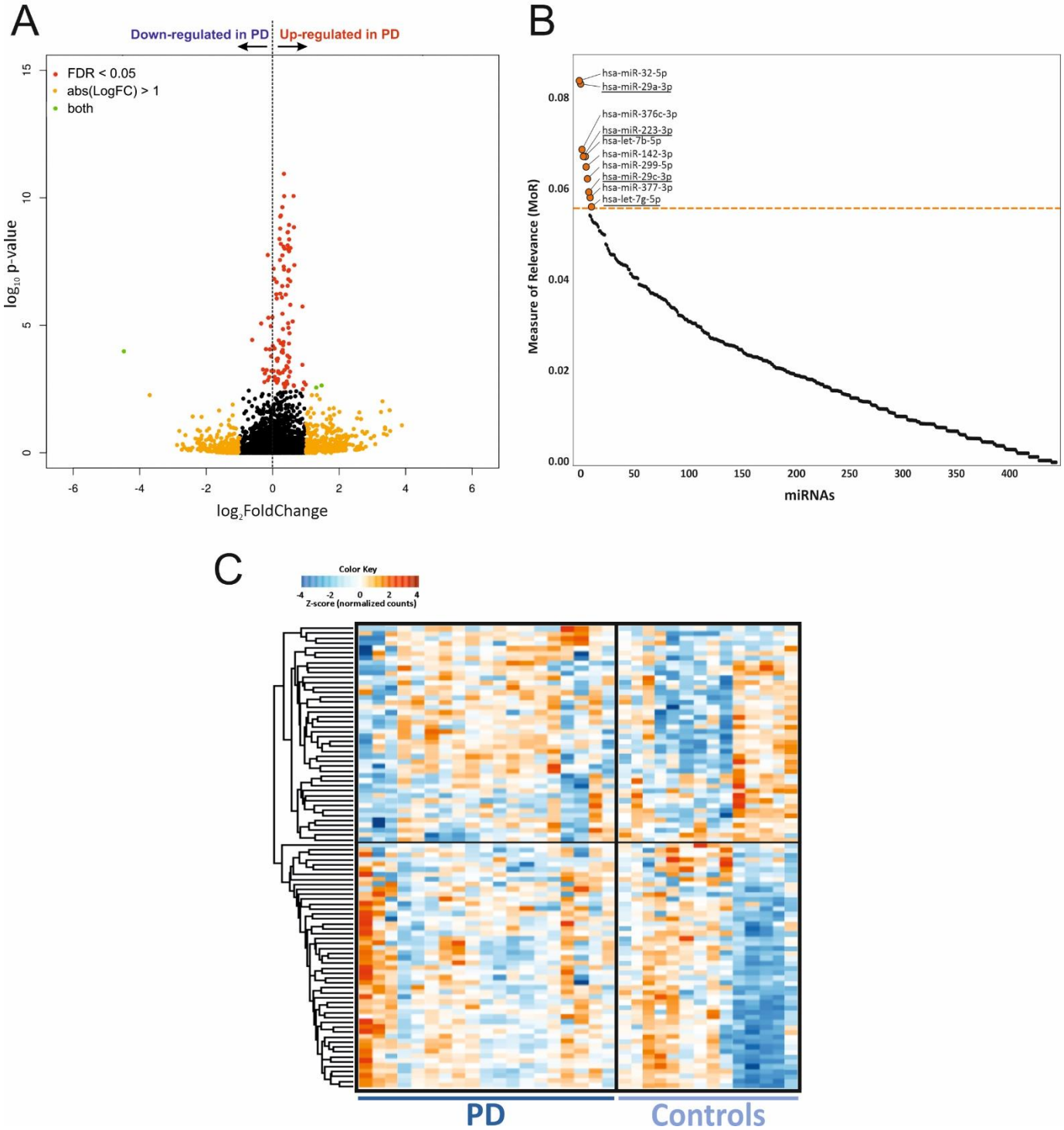

Figure 7. **Differential expression results for small RNA sequencing experiments. (A)** Volcano plot showing DE miRNAs in midbrain samples from the different cohorts. Plot correlates significance to

the log2FoldChange in the expression of transcripts. The volcano plot was generated under default DESeq2 pipeline cut-offs (Significant species indicated in colors; red = FDR < 0.05; green = FDR < 0.05 and log2FC ± 1). A custom cut-off for a minimum number of reads was defined (min. nr. Reads per condition = 20), and a less stringent cut-off for the log2FC and FDR correction was employed for subsequent exploratory pathway analyses(log2FC ± 0.1; FDR < 0.1). With that, 27 miRNAs were found DE and were considered for further analyses. **(B)** Plot showing the Measure of Relevance (MoR) used for the identification of miRNA putative signatures for the discrimination of disease state in the analyzed cohorts. The dotted orange line represents the MoR value cut-off. miRNAs above the cut-off are considered informative. **(C)** Heatmap for DE transcripts; comparison between PD and control samples. The color key indicates expression levels of DE small RNAs per patient. The dendrogram on the left indicates hierarchical clustering based on expression level.

Parallel to the DE analyses, the small RNA sequencing dataset was used for the development of an iterative feature analysis based on miRNA expression. Aiming to identify candidates for the discrimination between PD and control samples, Measure of Relevance (MoR) analysis was performed, followed by a machine learning variable ranking for the selection of the informative features. All the mapped miRNA reads were used as an input to the MoR pipeline. Additionally, a reliability analysis (RiA) was performed with the discovered candidates (as depicted in section 2.1.3.10.6). With these analyses, a set of 10 miRNAs were identified as potential putative signatures for the discrimination of disease states with the analyzed samples (Figure 7B). Four of those were also significant in the aforementioned DE analyses and are marked with stars in the putative signature plots (namely, miR-29a-3p, miR-223-3p, miR-29c-3p, let-7g-5p).

3.4 Sample correlation analyses

In order to check the overall inter-individual differences in small RNA expression of PD patients, a Bayesian Hierarchical Clustering was performed. These analyses required normalized mapped counts without any transformation as an input. Therefore, the batch correction algorithms used to treat the data prior to DE analyses were not applied here. In order to exclude a bias related to the different sequencing runs, the expression data from PD patients from the largest batch (13 patients) were considered in the hierarchical

clustering (Figure 8). The results show that the PD patients show high heterogeneity in regard to small RNA expression, concordant to what was observed in the Heatmap for DE analyses. Different clusters and sub-clusters for patients with similar small RNA expression are revealed with hierarchical clustering analyses. Relevant clinical data are also depicted for each analyzed patient. Parameters that include age, gender, disease duration and post-mortem intervals (PMI) are shown in color codes and indicate also a big variability in the distribution of clinical features. Although, there is no obvious correlation from those with the different clusters for small RNA expression.

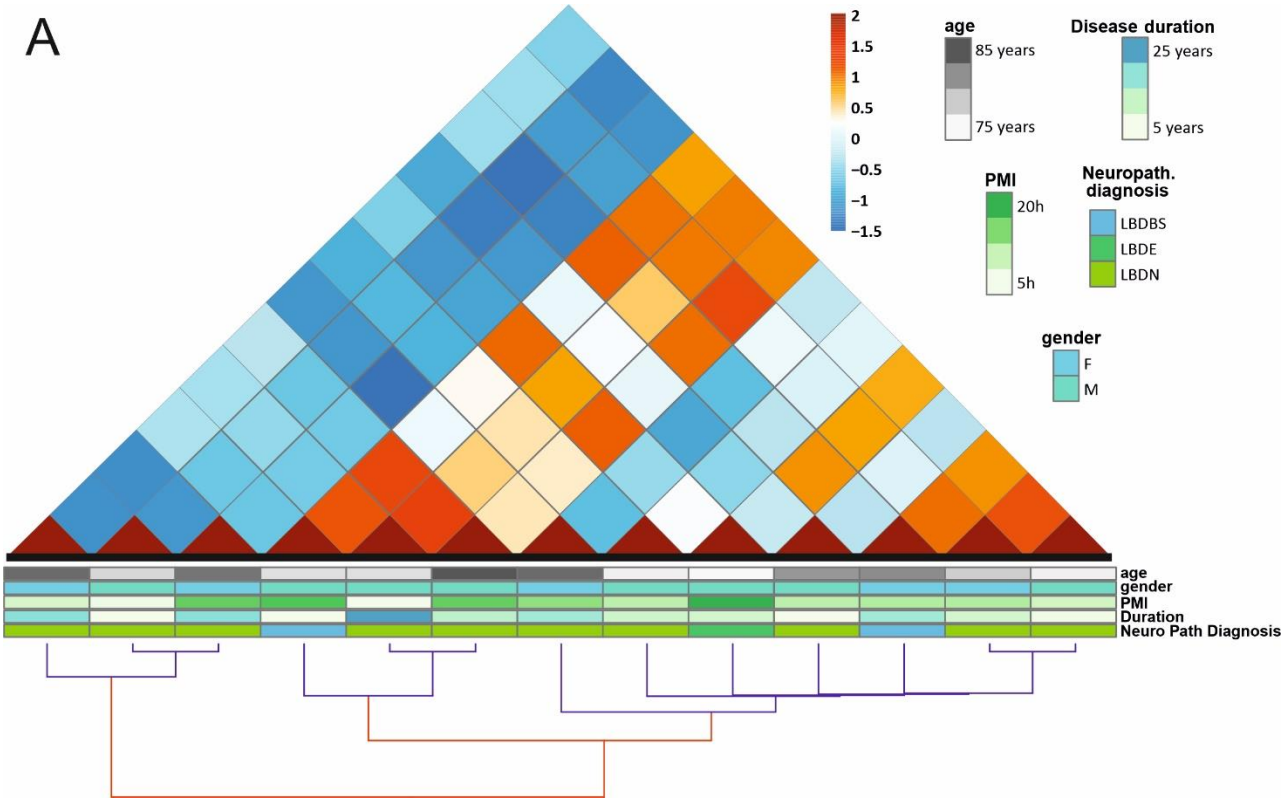

Figure 8. Bayesian Hierarchical Clustering analysis of PD patients for small RNA sequencing data. **(A)** Triangular heatmap showing unbiased clustering analysis. Samples with similar expression are located next to each other in clusters (dendrogram links in blue and red). PD patients of a single batch from sequencing runs considered for the analyses (n = 13). Clinical parameters corresponding to each PD patient showed in rectangles at the bottom of the triangular heatmap. PMI: Post-mortem intervals; LBDBS: Lewy body disease (alpha-synucleinopathy), brain-stem predominant; LBDE: LBDE: Lewy body disease, early-neocortical; LBDN: LBDN Lewy body disease, neocortical. (according to Lewy-body pathology classification (Alafuzoff et al., 2009)).

3.5 Literature screening links differentially expressed miRNAs to important biological processes both in health and disease

A thorough literature search was performed using the miRNAs found significantly deregulated in the present study. The PubMed database (NCBI-NIH) was screened for publications that included the regulated miRNAs until the year 2019. The various key-terms employed in the literature mining were related to important biological and cellular processes that included, for example, neuronal development, function, plasticity and survival, as well as neurodegenerative processes and disorders, inflammatory and immune response, among others. The key-terms were sub-categorized as shown in Figure 9.

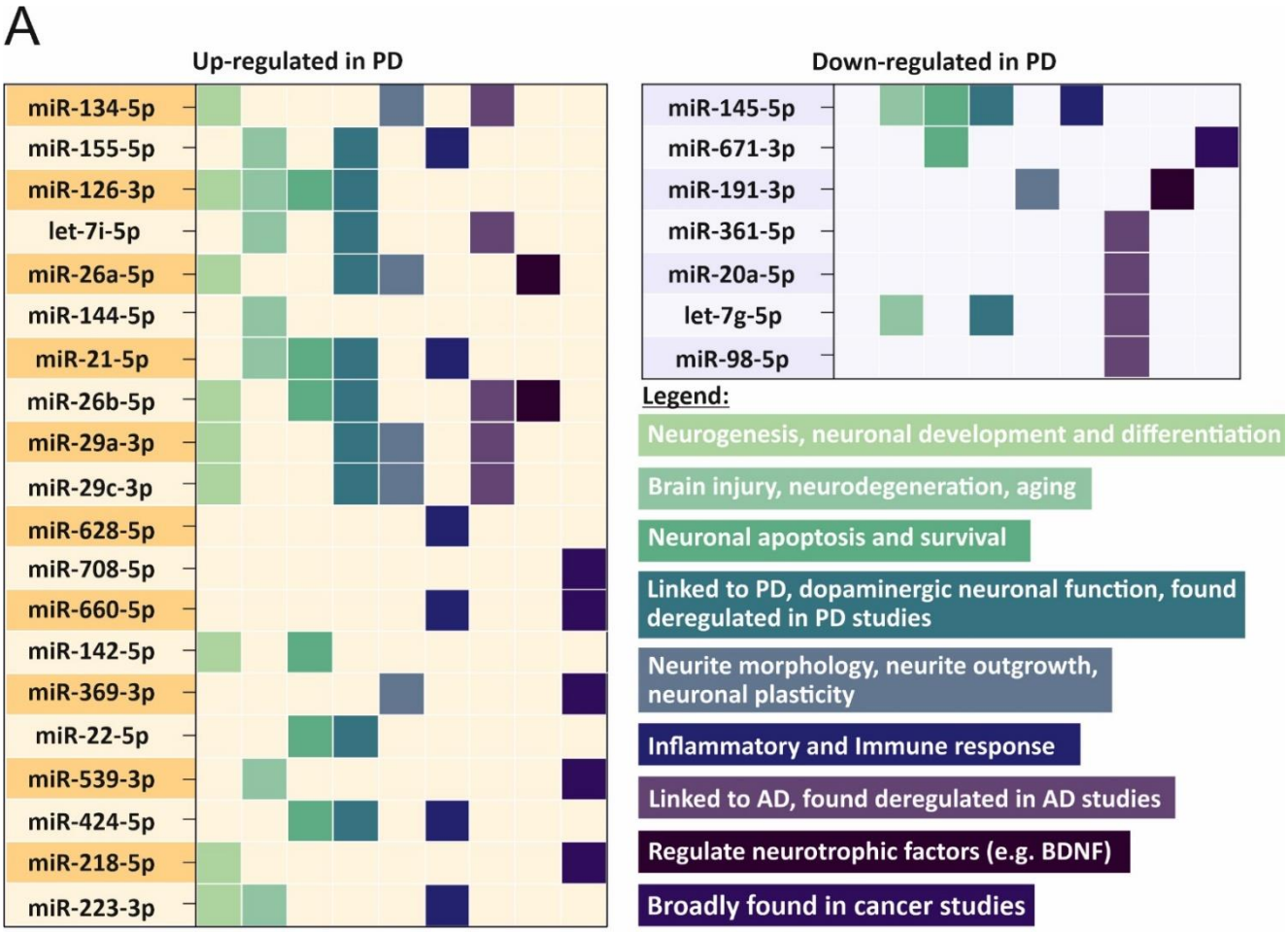

Figure 9. Literature compilation; key terms related to the differentially expressed miRNAs found in the small RNA sequencing experiments. (A) Up-regulated miRNAs in PD on the left-hand side (list in orange), Down-regulated miRNAs in the right-hand side (list in blue). Color key indicates the involvement of a given miRNA to the respective key-term according to the literature screening.

The diagram shows that the candidates have been already linked to several neuron-related processes (both in health and disease), as well as in cancer studies. The screening revealed that almost half of the DE miRNAs found here were previously linked to PD or dopaminergic neuronal function, the category with the highest number of matches. Several of them were also linked to processes that include neuronal differentiation and development, aging and neurodegeneration, as well as neuronal apoptosis and survival. Several of the up-regulated miRNAs were also linked to inflammatory and immune response, processes which have been broadly associated to neurodegenerative diseases, including PD (Barcia et al., 2003; Hunot and Hirsch, 2003; Tiwari and Pal, 2017).

3.6 Functional annotation with targets of differentially expressed miRNAs identify important enriched pathways in the context of PD

In order to further explore the functional role of the DE miRNAs in the context of PD, a computational miRNA-target prediction was performed, followed by functional enrichment analysis in the Web-based gene set analysis toolkit (WebGestalt). Gene ontology (GO) for biological processes (BP) and cellular components were annotated using the targets of up- and down-regulated miRNAs separately (Figure 10). Moreover, only experimentally validated targets were retrieved for the functional annotation, aiming to have the highest level of evidence enriched in the gene ontology terms. For targets of up-regulated miRNAs, results show that almost one-third of the enriched gene ontology terms are related to neuronal function, follow by a high ratio of processes related to nucleus/chromosome and cell division. Cytoskeleton related terms account to one-fifth of the enriched gene ontology terms. Figure 10B show the 15 most significant gene ontology terms for biological processes for targets of miRNAs found up-regulated in PD patients. Enriched terms include cell development and proliferation-related processes, as well as processes related to the biosynthesis of macromolecules and regulation of cell death.

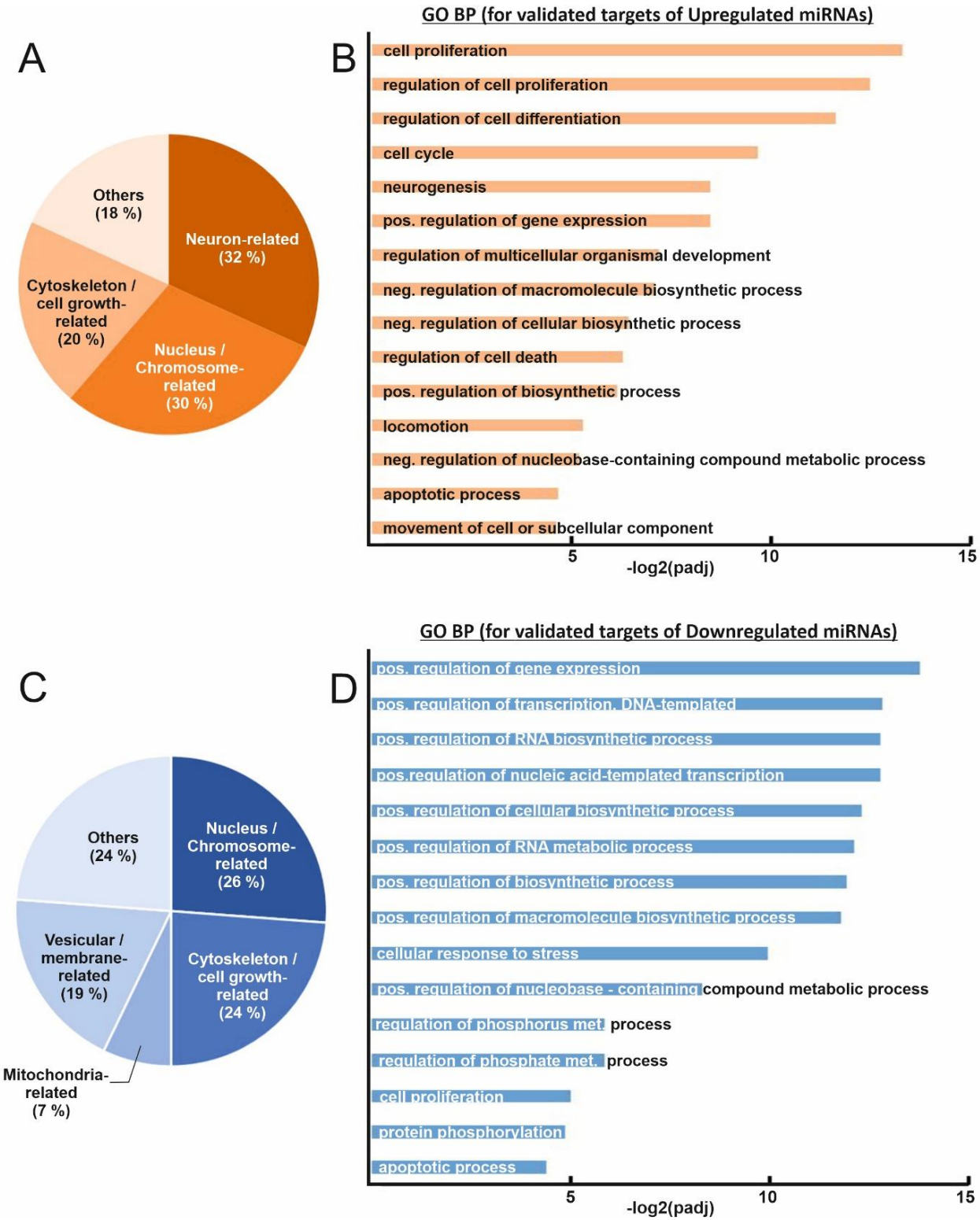

Figure 10. Functional enrichment analysis for targets of differentially expressed miRNAs. (A and C) Proportion of enriched gene ontology processes to different cellular component merged categories. **(B)** Gene ontology term enrichment for targets of significantly up-regulated miRNAs. **(D)** Gene ontology term enrichment for targets of significantly down-regulated miRNAs. X-axes represent -log2 of FDR corrected values for the functional enrichment. Experimentally validated targets considered for the analyses. GO-BP: gene ontology for biological processes.

On the other hand, validated targets for miRNAs found down-regulated in PD showed no enrichment for neuronal-related processes. Nucleus/chromosome- and cell division- related terms followed by cytoskeleton- and cell growth-related terms account to 50 % off all enriched gene ontology terms (26 % and 24 %, respectively) (Figure 10C). Vesicular- and membrane-related terms account to 19 % of the GO results, while mitochondria-related terms comprise 7% of the enrichment. In more detail, several of the most highly ranked significant GO terms are related to gene expression, transcription and other RNA-related processes. Furthermore, gene ontology terms related to response to stress, apoptosis and protein phosphorylation, as well as regulation of phosphorus and phosphate metabolic processes are among the top 15 most significant enriched GO-BP terms (Figure 10D). Functional enrichment analyses for regulated miRNA targets indicate that these candidates might be involved in important biological processes that range from cell proliferation and maintenance to gene expression, stress and apoptotic related processes. The previous evidence for the involvement of those miRNAs in PD pathophysiological events is further explored in the integration of the various datasets object of this work.

3.7 RNA sequencing overview and transcriptomic raw data processing

RNA sequencing experiments were performed in order to assess the transcriptomic profiles of the present midbrain cohorts. For that, RNA aliquotes coming from the same sample source used for the small RNA sequencing experiments were used. RNA sequencing experiments were performed on the Illumina HiSeq 400 platform. In a similar way, as previously described for the small RNA sequencing, RNA libraries were prepared directly from the sourced total RNA from each midbrain sample for both PD and control cohorts (Figure 11A). Quality control performed with the sequencing output files (fastQC) denoted satisfactory quality information from the RNA sequencing for all analyzed samples (Figure 11B). Read counts coming from individual patient/control libraries were then mapped and relative expression values for the whole transcriptome were assigned to the sequencing results of each subject. Normalization and removal of unwanted variances (RUV) were performed with the output results (Figure 11C) previous to downstream functional enrichment analyses. Sequencing read counts were mapped and assigned to the reference genome, accounting to a total of 46,500 genes with valid read values before filtering.

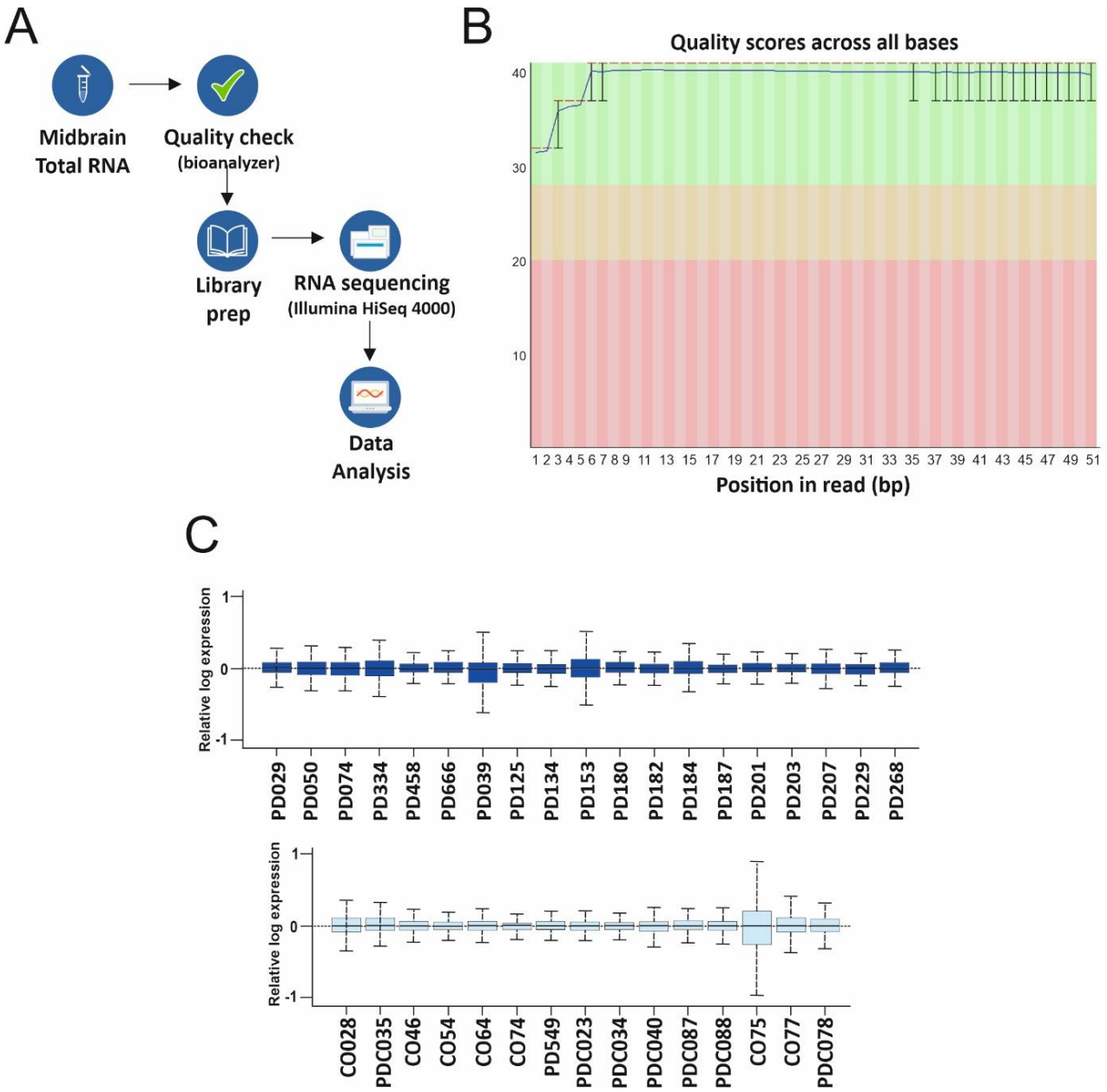

Figure 11. **RNA sequencing overview. (A)** Experimental design; after quality check, RNA libraries were prepared from total RNA from each midbrain sample. Sequencing performed in the Illumina HiSeq 400 platform followed by bioinformatical analysis. **(B)** Exemplary plot showing quality information from the sequencing of an RNA sample. Quality (Phred) score is represented in the Y-axis. Quality scores reflect the Illumina estimate for the probability of a particular base to be identified incorrectly (cite). In the example, all read nucleotides lie on the 'good quality' region of the plot (same for the rest of the samples) **(C)** Relative log expression (RLE) plots showing the expression levels of the whole transcriptome for all samples; plots represent variances after removal of unwanted variances (RUV) bioinformatically (dark blue: PD patients; light blue: controls).

3.8 Transcriptomic differential expression analyses point towards dopaminergic depletion and massive inflammation/immune response in midbrains of PD subjects

DE analysis was performed with the RNA sequencing results in order to explore gene expression in midbrains of PD patients when compared to controls. Following the mapping, the complete output from the RNA sequencing was used for the DESeq2 pipeline. Only protein-coding genes were considered for downstream analyses. A cut-off value for a minimum number of reads was adopted in order to filter out very lowly expressed genes from the differential analysis (min. nr. reads = 50). Furthermore, custom cut-offs values for the fold change in expression and false-discovery rate were applied during data analysis ($log2FC \pm 0.2$; $FDR < 0.05$). Under these conditions, a total of 1452 transcripts were found significantly deregulated in PD in comparison to controls. Similar to what was observed in the small RNA sequencing results, the majority of transcripts – 975 of them - were found up-regulated in PD, whereas 477 transcripts appear down-regulated in that condition.

A volcano plot correlating significance to the log2FoldChange in gene expression is presented in Figure 12A, showing DE transcripts in colors. These plots were generated under DESeq2 default settings for FDR and log2FoldChange and considered the full transcriptomic expression data before the aforementioned filtering. Highlighted transcripts were extracted from pathway enrichment analyses depicted below. A gene expression heatmap was generated for the transcriptomic significant results, in order to have an overview of the overall expression in different subjects and disease states. (Figure 12B). Despite inter-individual variabilities in the expression profiles, the general transcriptomic profile seems to be concordant to the disease state, showing a more obvious pattern in terms of group separation than the small RNA sequencing data.

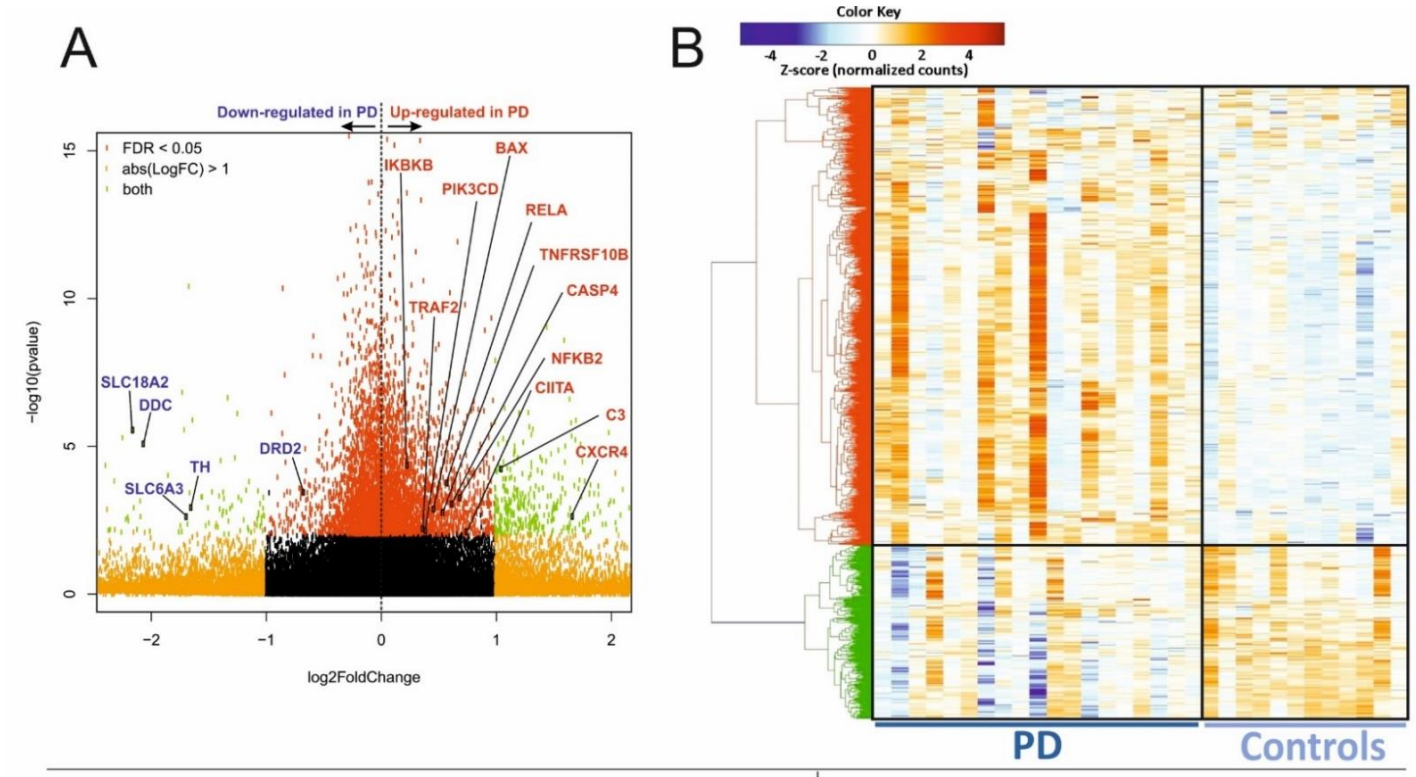
A
Down-regulated in PD
Up-regulated in PD
FDR < 0.05
abs(LogFC) > 1
both
BAX
IKBKB
PIK3CD
RELA
TNFRSF10B
CASP4
TRAF2
NFKB2
CIITA
C3
CXCR4
SLC18A2
DDC
DRD2
TH
SLC6A3
−log10(pvalue)
log2FoldChange
B
Color Key
Z-score (normalized counts)
PD
Controls

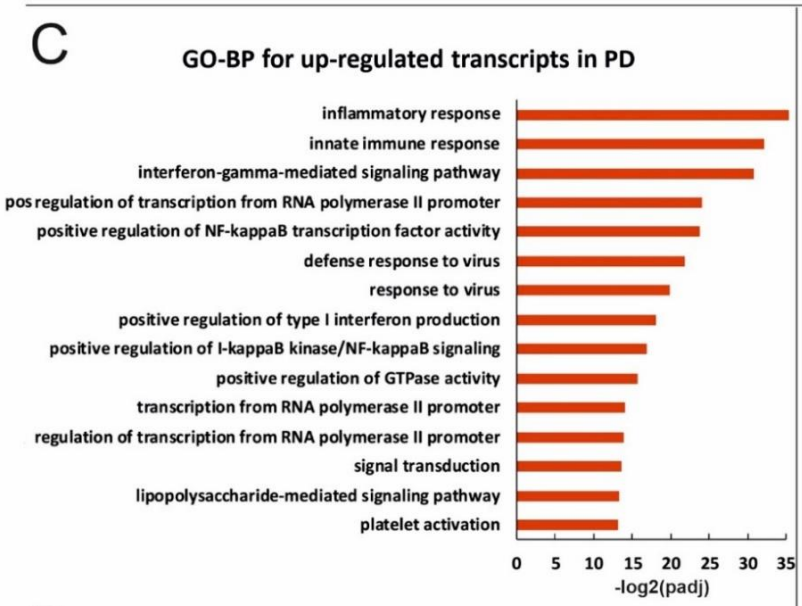
C
GO-BP for up-regulated transcripts in PD
inflammatory response
innate immune response
interferon-gamma-mediated signaling pathway
pos regulation of transcription from RNA polymerase II promoter
positive regulation of NF-kappaB transcription factor activity
defense response to virus
response to virus
positive regulation of type I interferon production
positive regulation of I-kappaB kinase/NF-kappaB signaling
positive regulation of GTPase activity
transcription from RNA polymerase II promoter
regulation of transcription from RNA polymerase II promoter
signal transduction
lipopolysaccharide-mediated signaling pathway
platelet activation
-log2(padj)

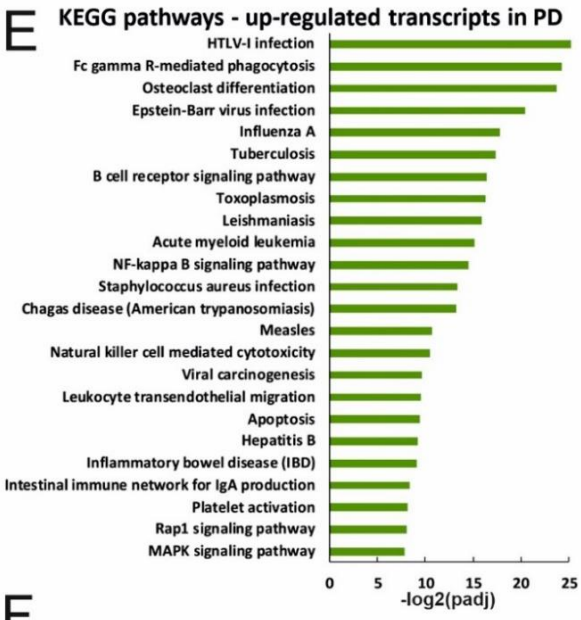
E
KEGG pathways - up-regulated transcripts in PD
HTLV-I infection
Fc gamma R-mediated phagocytosis
Osteoclast differentiation
Epstein-Barr virus infection
Influenza A
Tuberculosis
B cell receptor signaling pathway
Toxoplasmosis
Leishmaniasis
Acute myeloid leukemia
NF-kappa B signaling pathway
Staphylococcus aureus infection
Chagas disease (American trypanosomiasis)
Measles
Natural killer cell mediated cytotoxicity
Viral carcinogenesis
Leukocyte transendothelial migration
Apoptosis
Hepatitis B
Inflammatory bowel disease (IBD)
Intestinal immune network for IgA production
Platelet activation
Rap1 signaling pathway
MAPK signaling pathway
-log2(padj)

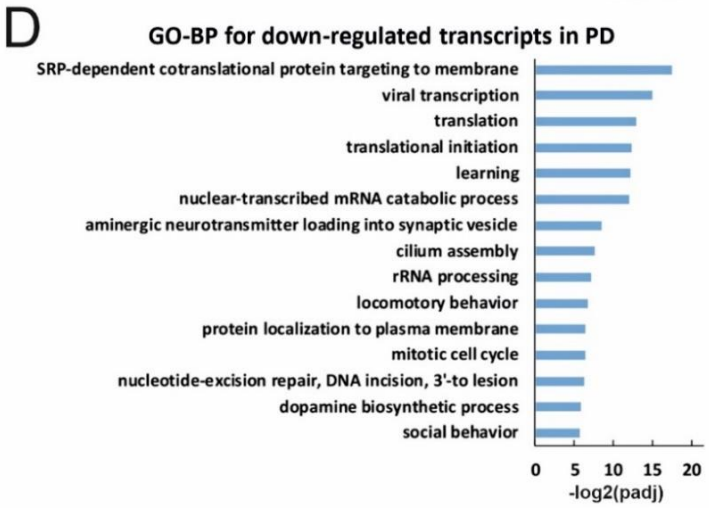
D
GO-BP for down-regulated transcripts in PD
SRP-dependent cotranslational protein targeting to membrane
viral transcription
translation
translational initiation
learning
nuclear-transcribed mRNA catabolic process
aminergic neurotransmitter loading into synaptic vesicle
cilium assembly
rRNA processing
locomotory behavior
protein localization to plasma membrane
mitotic cell cycle
nucleotide-excision repair, DNA incision, 3'-to lesion
dopamine biosynthetic process
social behavior
-log2(padj)

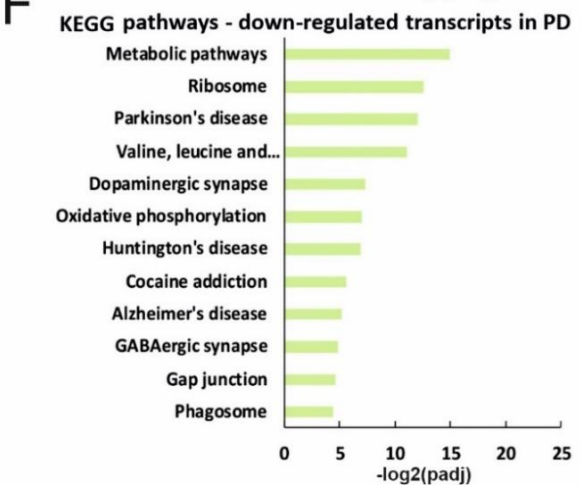
F
KEGG pathways - down-regulated transcripts in PD
Metabolic pathways
Ribosome
Parkinson's disease
Valine, leucine and...
Dopaminergic synapse
Oxidative phosphorylation
Huntington's disease
Cocaine addiction
Alzheimer's disease
GABAergic synapse
Gap junction
Phagosome
-log2(padj)

Figure 12. **Differential expression results for RNA sequencing experiments and pathway analyses.** **(A)** Volcano plot showing DE miRNAs in midbrain samples from the different cohorts. Significant species indicated both in colors (volcano plots created under DESeq2 default settings: red = FDR < 0.05; green = FDR < 0.05 and log2FC ± 1). For the sub-sequential pathway and integrative analyses, only coding genes were considered. Custom cut-offs for a minimum of 50 reads per condition and minimum log2FC of ± 0.2 were employed, leading to a final number of DE 1452 transcripts (PD vs. controls comparison). Enrichment analyses (performed with the DAVID Database) revealed altered biological processes related to inflammatory response and several pathways related to the immune response in PD midbrains (highlighted for up-regulated transcripts); down-regulated transcripts show enrichment to terms that include translational machinery and dopamine-related processes. **(B)** Heatmap for DE transcripts; comparison between PD and control samples. Color key indicates expression levels of DE transcripts per patient. **(C)** *Gene Ontology (GO) – Biological Processes* term enrichment status for down-regulated transcripts in PD. **(D)**. *Gene Ontology (GO) – Biological Processes* term enrichment status for up-regulated transcripts in PD. **(E)** *KEGG PATHWAY* enrichment status for down-regulated transcripts in PD. **(F)** *KEGG PATHWAY* enrichment status for up-regulated transcripts in PD. Bars represent p-values (log2 transformed) for the respective terms. Pathway analyses conducted in DAVID Functional Annotation Tool 6.8.

Functional enrichment analyses were conducted aiming to explore pathophysiological events that might underline the results for the transcriptomic profiling of PD and control midbrains. Up- and down-regulated transcripts in PD from the DE analysis were considered separately (Figures 12D/F). The functional annotation with down-regulated transcripts revealed enrichment for several important gene ontology terms, including translational machinery, synaptic transmission and protein localization. Pathways related to dopamine signaling/metabolism and locomotory behavior, hallmark processes in PD pathology (Dauer and Przedborski, 2003b; Langston et al., 1983; Ungerstedt et al., 1974), were among the enriched terms. KEGG pathway analyses retrieved alterations in metabolic pathways, ribosome processes, dopamine-related pathways and neurodegenerative diseases including PD itself (as the third most significant pathway enriched for down-regulated transcripts). The annotated down-regulated transcripts included tyrosine hydroxylase (TH), Dopa decarboxylase (DDC), dopamine transporters (SLC6A3 and SLC18A1) and dopamine receptor D2 (DRD2) (Figure 12A, highlighted in blue).

For up-regulated transcripts, functional enrichment analyses revealed altered gene ontology terms (GO-BP) related to inflammatory response and several pathways related to the immune response in PD midbrains (Figure 12C). Moreover, KEGG pathway analyses with up-regulated genes indicate a massive activation of the immune system and inflammation-related pathways, being the majority of significantly enriched pathways related to those processes. Inflammation and activation of the adaptative immune system have been implicated in the context of PD progression (Fiszer et al., 2009; McGeer et al., 1988b; Ouchi et al., 2005; Tristão et al., 2016). Pathways related to apoptosis, NFKB-, MAPK- and RAB1-signalling were also enriched for transcripts up-regulated in PD (Figure 12E). The presence of different infectious diseases enriched in the analyses might be related to the high number of immune system-related transcripts found up-regulated in PD (as highlighted in the volcano plot in Figure 12A – highlighted transcripts in red selected from the intersection between inflammatory/immune response and apoptosis enriched pathways. Highlighted transcripts, namely, *IKBKB; BAX; RELA; PIK3CD;TRAF2; TNFRSF10B; CASP4; NFKB2; CIITA; C3; CXCR4*).

In summary, findings in this dataset indicate that multiple pathways contribute to PD mechanisms, rendering an integrative analysis for the present multi-omics data very promising for the exploration of novel miRNA-based regulatory mechanisms.

3.9 Differences in protein content in PD and control midbrain are portrayed by proteomics analysis

Mass spectrometry experiments were performed in order to profile the proteomic changes in PD and control midbrains samples. Protein lysates were prepared from midbrain tissue punches directly adjacent to the ones used for small and RNA sequencing experiments. The protein content was run into electrophoresis gels and subsequentially digested for preparation of peptide libraries. The analysis method of *Sequential window acquisition of all theoretical fragment ion spectra* (SWATH) was employed for the mass spectrometry experiments. (Figure 13A). A spectral library was used to extract peptide-specific peak areas. These areas are combined with protein quantitation values, which are then identified and mapped to the human reference proteome (Figure 13B). After normalization of protein quantitation, 2,257 proteins were uniquely identified, all subject

to an FDR of 1%. DE analyses were conducted with the log2 transformed data of protein quantitation and the significance level was set to alpha = 5% for all the differential statistical analyses for the proteomics dataset. DE results revealed 127 significantly regulated proteins in PD in comparison to controls. As seen in the two previous datasets, the majority of the DE proteins were found up-regulated in PD (87 proteins), whereas 40 of them were down-regulated in the same condition. These results are presented in a volcano plot correlating the significance to the log2FoldChange in expression (Figure 13C).

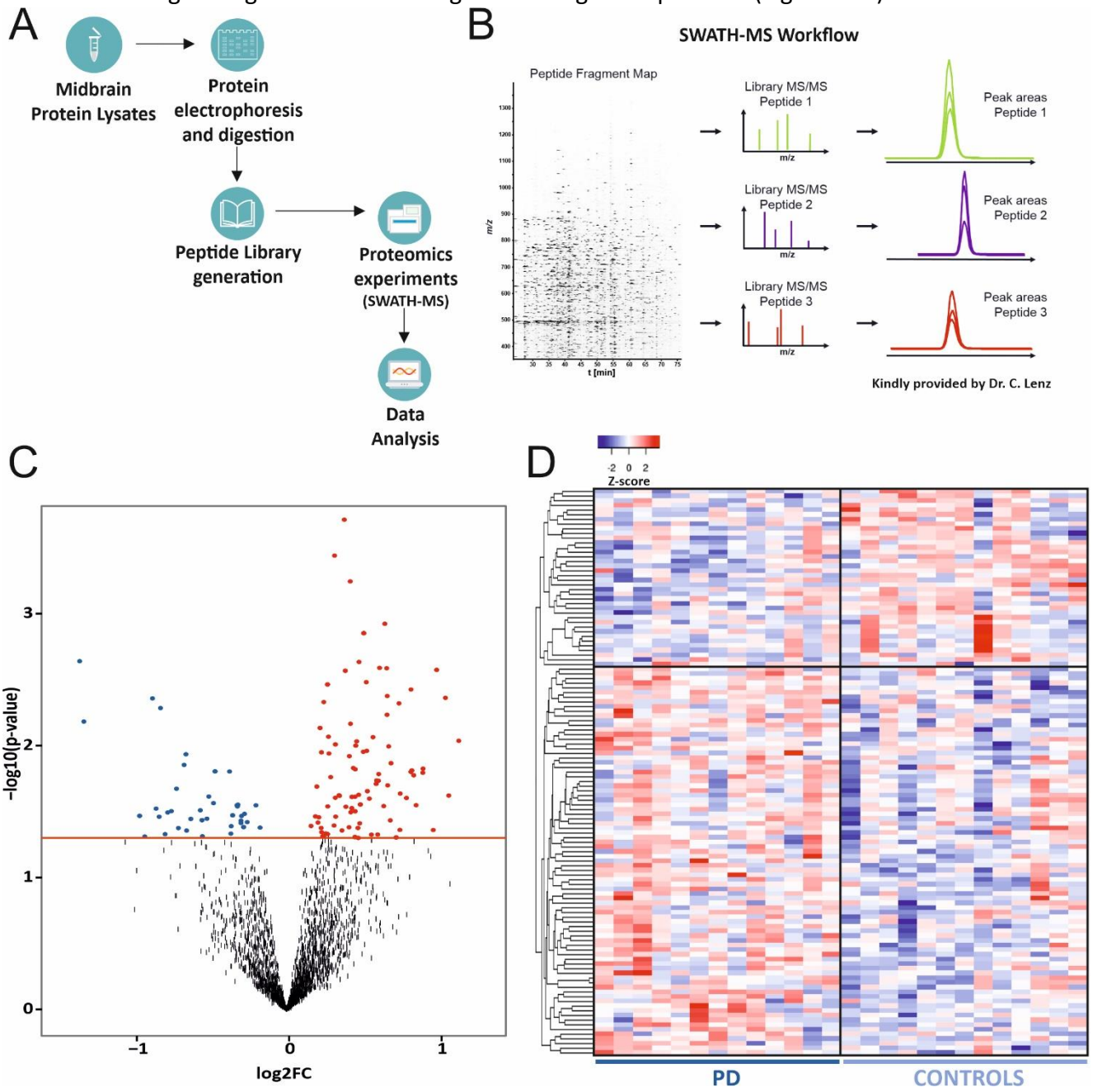

Figure 13. **Proteomics overview and differential expression analyses. (A)** Experimental design; proteins extracted from midbrain tissue undergone electrophoresis and trypsinization, subsequentially. Peptide libraries were generated and proteomics (SWATH-MS) experiments were

performed, followed by data analysis. **(B)** Exemplary workflow for SWATH-MS experiments. The left panel shows the global MS/MS product ion maps of all precursors. A spectral library is used to extract peptide-specific peak areas, which are finally combined for protein quantitation. (Schematic representation of SWATH-MS Workflow kindly provided by Dr. C. Lenz - UMG Göttingen). **(C)** Volcano plot showing DE proteins in midbrain samples. Significant species indicated in colors; down-regulated (in blue) and up-regulated (in red) in PD in comparison to controls (straight line in red: cut-off for $p < 0.05$). 87 proteins were significantly up-regulated in PD, whereas 40 proteins were found down-regulated in that condition. **(D)** Heatmap for DE transcripts; comparison between PD and control samples. Color key indicates expression levels of DE transcripts per patient.

Next, the results from the DE analyses were used for designing a heatmap for the protein expression (Figure 13D). In order to exclude technical biases linked to the SWATH-MS runs, only the biggest sample batch processed in the mass spectrometry experiments was considered for designing the heatmap (similarly to what was done sample correlation analyses for the small RNA expression). For the proteomics experiments, this batch accounted for 13 PD samples and 13 controls. The profiles for protein expression present certain concordance to the disease state. Nevertheless, inter-individual differences appear similar to the other omics datasets presented previously.

3.10 Functional enrichment of proteomics data reveals regulation in PD-related pathways

Similar to what was done for the previous datasets, DE results from the proteomic profiling were analyzed in terms of functional annotation using the Web-based gene set analysis toolkit (WebGestalt). The enrichment results showed gene ontology terms related to the regulation of *protein folding* as the most enriched category. Defects of protein folding have been extensively linked to neurodegenerative diseases, including PD (Dauer and Przedborski, 2003b; Ebrahimi-Fakhari et al., 2013; Ross and Pickart, 2004; Ryu et al., 2002; Selkoe, 2003, 2004). Another important term appearing in the enrichment analyses for the regulated proteins in PD midbrains is the *Oxidation-reduction* processes, a category that is also broadly linked to PD pathophysiology (Fahn and Cohen, 1992; Jenner, 2003; Jenner and Olanow, 1996; Jenner et al., 1992).

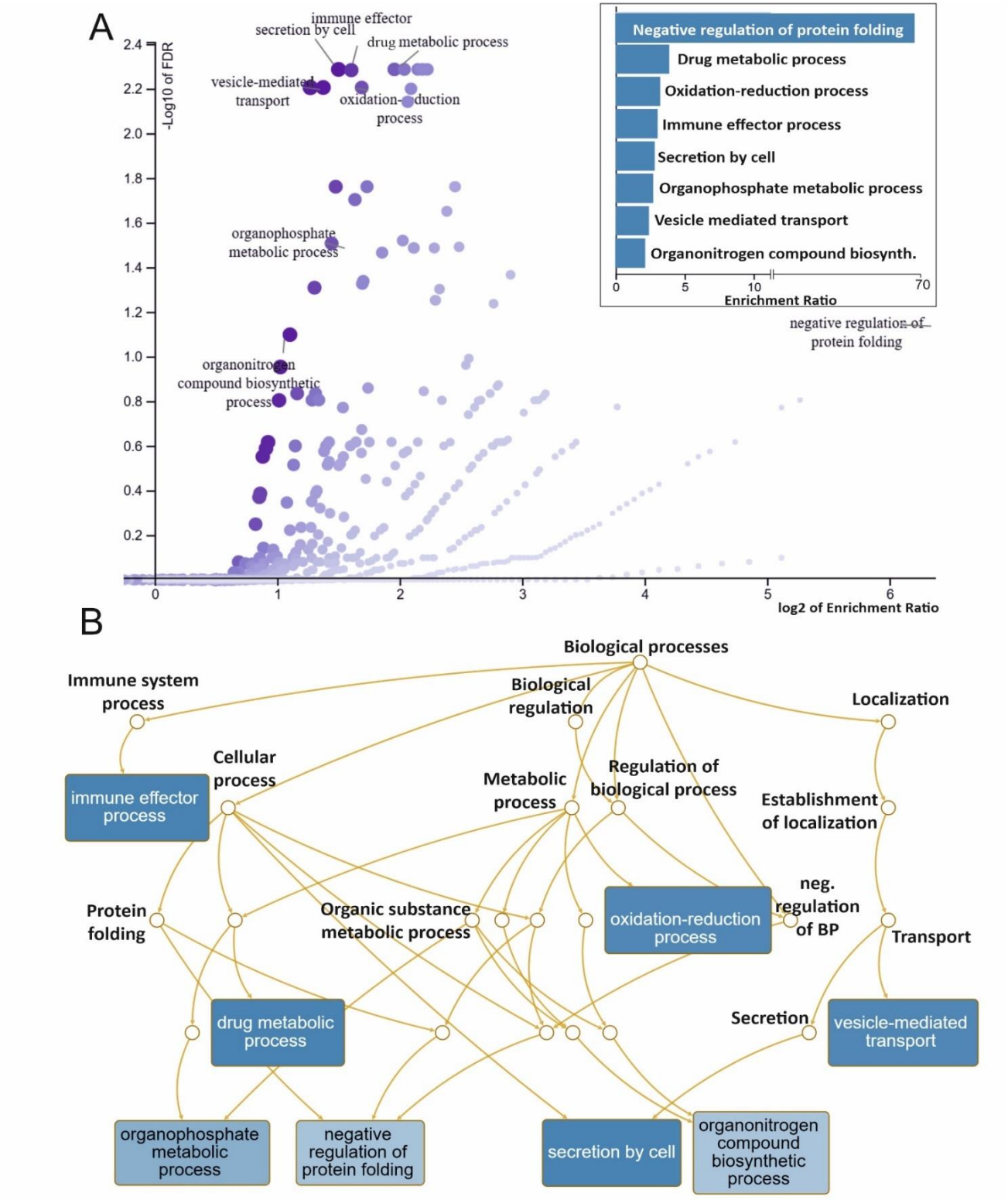

Figure 14. **Functional enrichment results for proteomics expression data. (A)** Enrichment ratio plot correlating the log2 of enrichment values of significant gene ontology terms for biological processes (assigned by the WebGestalt tool); names of the significantly enriched terms are highlighted and also shown in the ranked bar plot on the upper-right corner. **(B)** Directed Acyclic Graph (DAG) visualization Biological processes tree; in blue: enriched terms annotated to the submitted DE protein list.

Enriched GO Terms	Annotated / total nr. of proteins in GO term	Proteins annotated in each GO term set
Negative regulation of protein folding	2 / 5	SNRNP70, ST13
Drug metabolic process	17 / 760	ATP5ME, CBR1, CD47, FAH, GPD1, MAOB, NDUFB3, NDUFB8, NDUFS2, OGDH, PFKFB2, PGM2L1, PRDX1, PRDX6, PRPS2, PSAT1,TH
Oxidation-reduction process	18 / 968	CBR1, CISD1, COX6C, ECHDC1, GPD1, MAOB, MECR, NDUFB3, NDUFB8, NDUFS2, OGDH, DIA4, PGM2L1, PHYHD1, PRDX1, PRDX6, SELENBP1, TH
Immune effector process	20 / 1141	ACTR10, ARPC1A, ATP8A1, C1QC, CAMK4, CD47, CHI3L1, CREG1, CRK, FABP5, HTRA1, KRT1, LAMP2, NCKIPSD, PA2G4, PADI2, PRDX1, PRDX6, RAB18, SERPINA3
Secretion by cell	24 / 1472	ACTR10, ATP8A1, CD200, CD47, CHI3L1, CREG1, ERP29, FABP5, KRT1, LAMP2, LGALS3BP, MAOB, PA2G4, PADI2, PDIA4, PFKFB2, PRDX6, RAB18, RAB8A, SERPINA3, SLC1A3, SLC25A6, SPTBN1, SYP
Organophosphosphate metabolic process	18 / 1148	ATP5ME, CAPN2, CPNE6, ENPP6, FABP5, GPD1, MPI NDUFB3, NDUFB8, NDUFS2, OGDH, PFKFB2, PGM2L1, PLCD3, PRDX6 PRPS2, TKT, VAC14
Vesicle mediated transport	27 / 1942	ACTR10, AP3D1, ARPC1A, ATP8A1, CD47, CHI3L1, CPNE6, CREG1, CRK, CTNNB1, FABP5, KRT1, LAMP2, LGALS3BP, MAP2K2, MSN, NCKIPSD, OSBPL1A, PA2G4, PADI2, PRDX6, RAB18, RAB6B, RAB8A, SERPINA3, SPTBN1, SYP
Organonitrogen compound biosynthetic process	22 / 1776	ATP5ME, CAPN2, CTNNB1, DARS, EIF4A1, FABP5, GPD1, HNRNPR, MPI, MTPN, OGDH, PA2G4, PFKFB2, PGM2L1, PRELP, PRPS2, PSAT1, RPL35, RPLP0, RPN1, SLC1A3, TH

Table 12. List of proteins annotated to each GO category in the functional enrichment

In concordance to the transcriptomics results, the *immune effector process* term was also enriched for the DE proteins in PD. Further enriched processes include *drug metabolic process, secretion by cell, organophosphate metabolic process, vesicle-mediated transport and organonitrogen compound biosynthesis.* These functional enrichment results are presented in a Directed Acyclic Graph (DAG) for a compact biological processes tree (Figure 14B). In summary, the enrichment results for the proteomics results outlined important mechanisms related to PD pathology in the analyzed samples and added another level of evidence further explored in integrative approaches.

3.11 Step-wise integration of multi-*omics* dataset for pathway identification

In order to identify DE pathways across the different omics data sets (miRNA targets or coding products), the multi-omics results were integrated using both a bioinformatical tool (the Rank-Rank Hypergeometric Overlap, RRHO)(Plaisier et al., 2010) and a manual cross-checking method for the differential results lists derived from each technique (see Figure 4 and section 2.1.3.10.7).

3.11.1 Integration of Small RNA and Transcriptomic datasets

A computational target prediction for the DE miRNAs in PD and control midbrains was performed using the TargetScan 7.2 database (Agarwal et al., 2015). This database allows the prediction of miRNA targeting according to nucleotide sequence and miRNA seed region. Furthermore, with TargetScan 7.2 it is also possible to retrieve the probability of conserved targeting scores (Pct scores) for miRNA target prediction (Friedman et al., 2008). For the integration of the present datasets, the list of predicted targets was retrieved for miRNAs found up- and down-regulated in PD midbrains in comparison to controls.

Next, the discordant overlap between the two lists was assessed by RRHO and manual cross-check of differential results for small / total RNA sequencing data (Figure 15A). Significantly regulated candidates from both datasets were considered for these analyses. These methods allowed the extraction of the valid miRNA-mRNA interactions (containing potential pairs that would support hypotheses of a miRNA regulation of gene

expression in the samples - i.e. up-regulated miRNA paired with the respective down-regulated targets mRNA, and vice-versa).

The RRHO algorithm required the full sequencing DE results from both sequencing techniques as an input, retrieving a total of 163 DE transcripts presenting valid interactions with regulated miRNAs. On the other hand, the manual approach used the stricter custom cut-off values applied for the DE and other downstream analyses from each sequencing dataset. With that, miRNAs and transcripts with a very low number of reads and/or very slight fold change in expression were filtered out from start (as described in sections 3.4 and 3.9). Those settings resulted in a much smaller outcome for valid interactions: 23 miRNA targets (DE transcripts) were found cross-checking the differential results.

Remarkably, these two integrative methods showed a great overlap in their outcomes, with 22 out of the 23 DE transcripts found with the manual method being present in the RRHO integrative results. This overlap was considered for further steps, and a final list of 22 transcripts (namely, *DHX57; RNF170; REEP1; TMEM178B; BRWD1; ACADSB; CNTN1; SIAE; NHLRC3; ENTPD5; CGNL1; C7orf73; SOCS4; ZNF202; ATPB3; KCNK6; STEAP3; CYB561D1; MIER2; FOXF1; RIMS1; KLHL6 and PPTC7)* and 9 miRNAs (namely, *let-7i-5p; miR-26a-5p; miR-2018-5p; miR-424-5p; miR-29c-3p; let-7g-5p; miR-20a-5p; miR-145-5p and miR-98-5p*) that potentially regulate those transcripts were extracted (Figure 15B). The exact miRNA-mRNA pairs is depicted in Figure 15C.

In order to narrow down the list of miRNA-mRNA pairs and select candidates for a q-RT-PCR validation of the sequencing results, only interactions with Pct values $\geq$ 0.7 were considered. With that, pairs with the highest probability of interaction among the candidates identified in the integrative approaches were extracted. 12 out of the 22 identified transcripts - and all of the 9 miRNAs potentially regulating them - were selected and further validated by q-RT-PCR (Figure 15C).

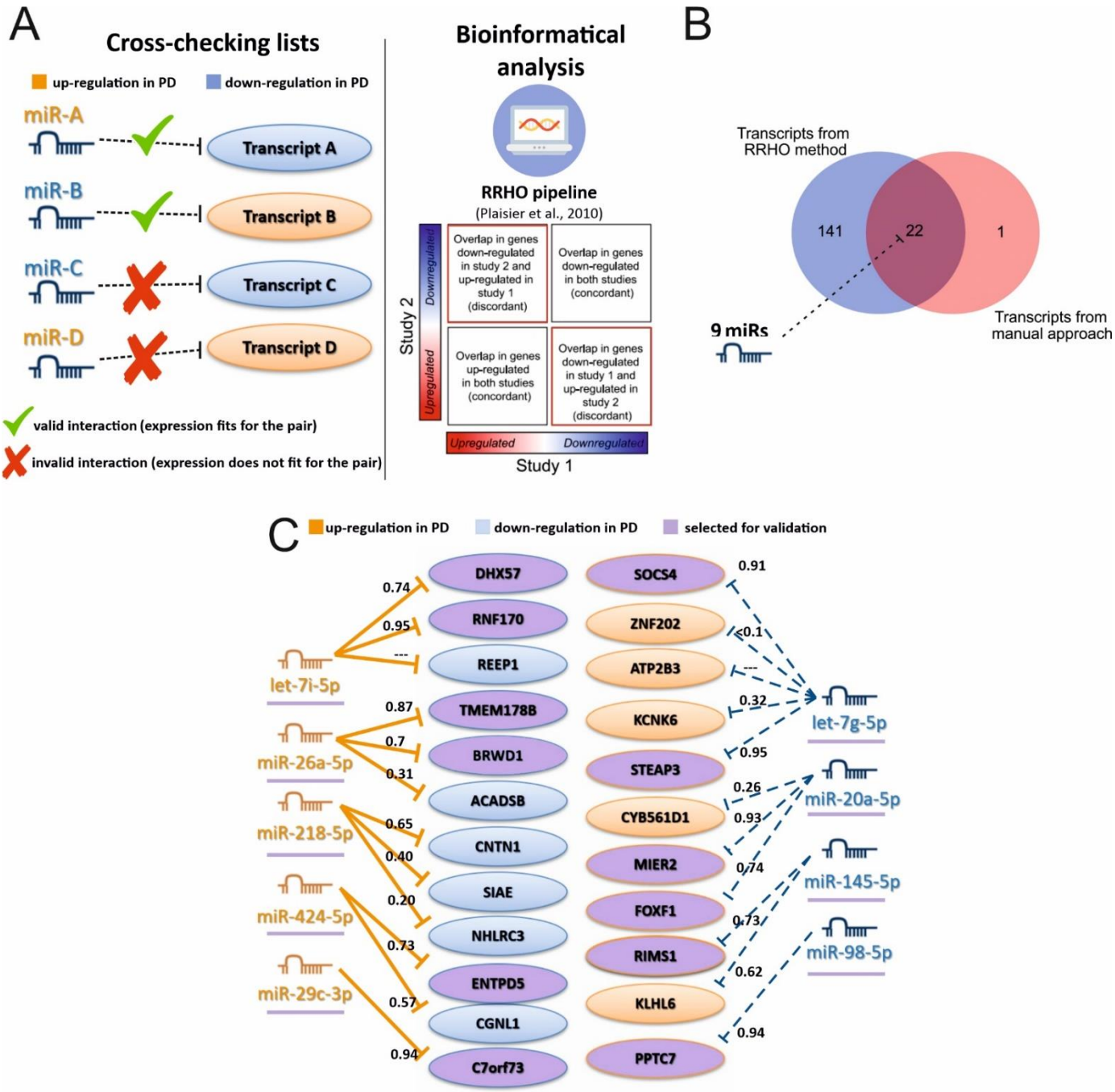

Figure 15. **Integrative approaches for miRNA and mRNA expression data and selection of targets for validation. (A)** Integration was done by two different methods; manual cross-check method between DE lists / RRHO (Rank-Rank Hypergeometrical Overlap) bioinformatical approach (Plaisier et al., 2010). Only valid interaction between miRNA-mRNA pairs were considered. **(B)** Overlap between the two methods shows that 22 mRNA are potentially regulated by 9 miRs. **(C)** Selection of miRNA/mRNA candidates for validation; using a cut-off for Pct values (Pct≥ 0.7) (Friedman, et al., 2009), 9 miRs and 12 mRNAs (circled or underlined in purple) were selected for validation by q-RT-PCR.

3.11.2 Integration of Transcriptomic and Proteomic datasets

Similar to what was done in the previous section, the overlapping results from the transcriptomic and the proteomic datasets were explored. In here, inversely to what was done for the miRNA/transcriptome integration, the concordant overlap between coding transcripts and their respective protein products were of interest (i.e. up-regulated transcript paired with the respective up-regulated protein product). Factors like protein kinetics, synthesis and degradation rates were out of the scope of this study and therefore not considered for these analyses.Here, we applied the manual cross-check method for the integration (Figure 16A), due to the very different nature and coverage of the proteomics results in comparison to the RNA sequencing results. Additionally, the much smaller range of DE proteins (127) was also favorable for such an approach.

The total number of uniquely identified proteins – 2,257 – was more than 20 times smaller than the number of mapped transcripts (46,500). Consequently, several of the transcripts found DE by RNA sequencing did not have their respective protein product identified in the proteomics results, and the opposite was at times also true. The first step for the integration of these two datasets was to look for transcripts and respective protein products which were found differentially regulated in both datasets (Figure 16B). From the 1422 DE transcripts found in RNA sequencing experiments, 30 of them also had the respective protein product significantly deregulated determined by proteomics experiments. When considering only valid mRNA-Protein pairs (concordant expression patterns), the integrative overview of the two datasets delineates a final list of 7 up-regulated candidates (namely, *ATP6V1E1; C9ORF47; CD47; ACOT7; RPL35; SEC23A and RPN1)* and 6 down-regulated candidates (*TH; DBT; CD200; RAB18; NIPSNAP3A and UBE2L3*) (Figure 16C) (regulation given PD vs controls). These candidates are currently being validated by Western Blotting and the results will not figure in the scope of this thesis. The presence of a very important marker for dopamine metabolism (tyrosine hydroxylase [TH]) among the down-regulated candidates in both datasets adds more evidence to the results presented above over the functional enrichment for those results (chapters 3.8 and 3.10).

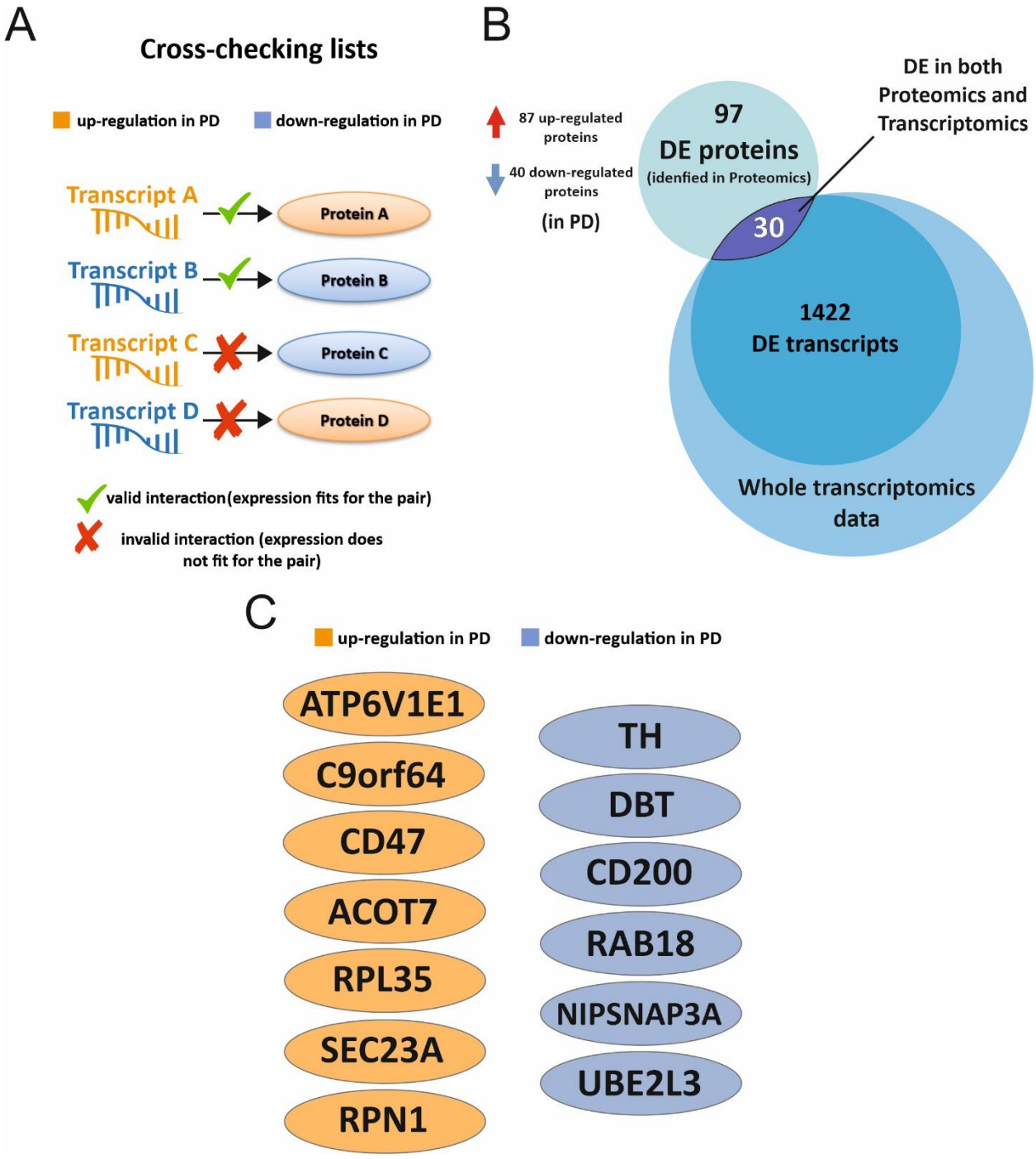

Figure 16. **Integrative approaches for mRNA and protein expression data (A)** Overlap between proteomics and transcriptomics datasets reveal that from 127 significant DE proteins, 30 of them also present the respective DE coding transcript in RNA sequencing experiments. **(B)** Integration was done by two different methods; manual cross-check method between DE lists. Only valid interactions between mRNA-Protein pairs considered. **(C)** Final list of proteins presenting significant DE in both datasets and expressed in the same fashion (in orange: up-regulated transcripts/proteins; in blue: down-regulated transcripts/proteins).

3.12 Validation of small RNA sequencing results in human midbrain tissue by q-RT-PCR

The 9 miRNA candidates selected after the integrative approaches of the small RNA and RNA sequencing results (section 3.11.1) were validated by q-RT-PCR. Since there was a substantial amount of time between the RNA sequencing experiments from the validation of the selected candidates, new tissue punches were collected from frozen midbrain samples from each individual. A fresh RNA isolation was conducted right before the start of the validation experiments, followed by the production of cDNA samples by reverse transcription. q-RT-PCR validation experiments were conducted in the QuantStudio 3 platform (Figure 17A).

For selected miRNAs found down-regulated in PD by RNA sequencing experiments, relative expression levels from q-RT-PCR results show that all tested miRNAs presented significant differences in expression concordant to the small RNA sequencing results (Figure 17B). On the other hand, for selected miRNAs found up-regulated in PD by RNA sequencing experiments, q-RT-PCR results showed a significant difference in expression levels of two miRNAs (let-7i and miR-29c). Interestingly, both miRNAs presented the opposite direction for the regulation.

Overall, four out of the nine selected miRNAs were successfully validated by q-RT-PCR, presenting concordant expression to what was found in DE analyses with the small RNA sequencing data.

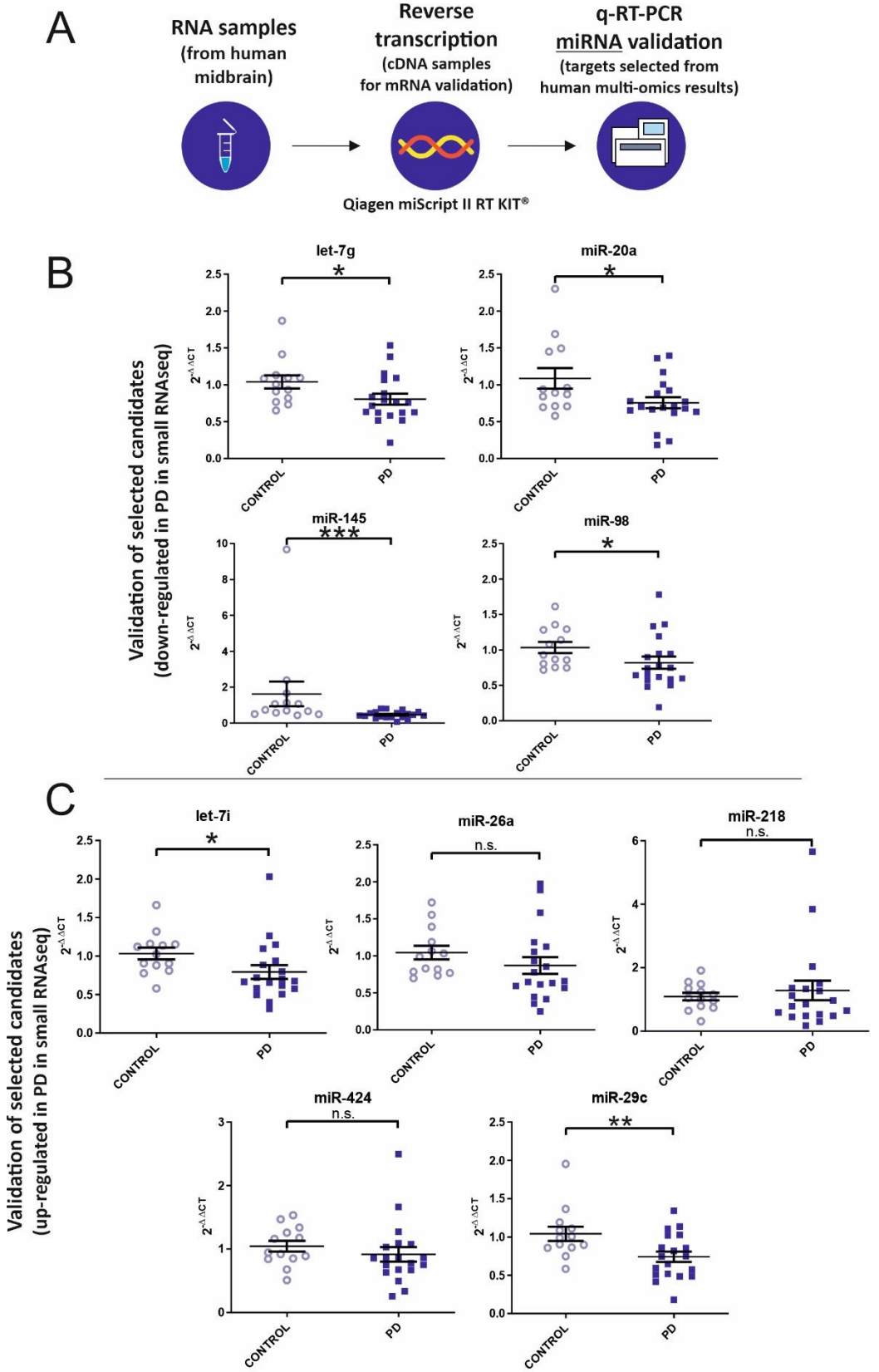

Figure 17. Validation of small RNA sequencing results (selected miRNAs) by q-RT-PCR. (A) Relative expression levels of selected miRNAs found up-regulated in PD patients. **(B)** Relative expression levels of selected miRNAs found down-regulated in PD patients. Error bars show standard error of the mean. Data analyzed by Mann-Whitney-U test. * $p < 0.05$, ** $p < 0.01$, *** $p < 0.001$

3.13 Validation of transcriptomics results in human midbrain tissue by q-RT-PCR

Parallel to the miRNA validation in the midbrain samples, the 12 mRNA transcripts selected in the integrative approaches (section 3.11.1) were also validated by q-RT-PCR. Fresh RNA was aliquoted from the same sample source used for the miRNA q-RT-PCR validation, and cDNA samples were prepared using the Qiagen Quantitect reverse transcription kit. The PCR reactions were conducted in the QuantStudio 3 platform (Figure 16A)

Seven from the selected transcripts presented a significant up-regulation in PD in RNA sequencing experiments. According to the relative expression results, four out of the seven candidates were also found significantly up-regulated in q-RT-PCR experiments, concordant to the findings from the transcriptomics. Another two mRNAs presented apparent up-regulation in PD samples, but relative expression results were not significant (Figure 18B).

Opposite to the aforementioned findings, from the transcripts presenting down-regulation in RNA sequencing results, there were no significant differences in relative expression levels in q-RT-PCR experiments. Despite the non-significant results, all transcripts presented, on average, lower expression levels in comparison to controls. Possibly, the limited cohort size is influencing the statistical power of the experiments presented here (Figure 18C).

In summary, a limited number of candidates found DE in RNA sequencing experiments presented a concordant significant regulation by q-RT-PCR, both for selected miRNAs (4/9 candidates validated) and mRNA transcripts (4/12). Technical and sensitivity differences in the two methods could account for these divergent findings. Nevertheless, the patterns of the relative expression levels determined by q-RT-PCR were similar to the ones found in RNA sequencing experiments for the majority of the selected species.

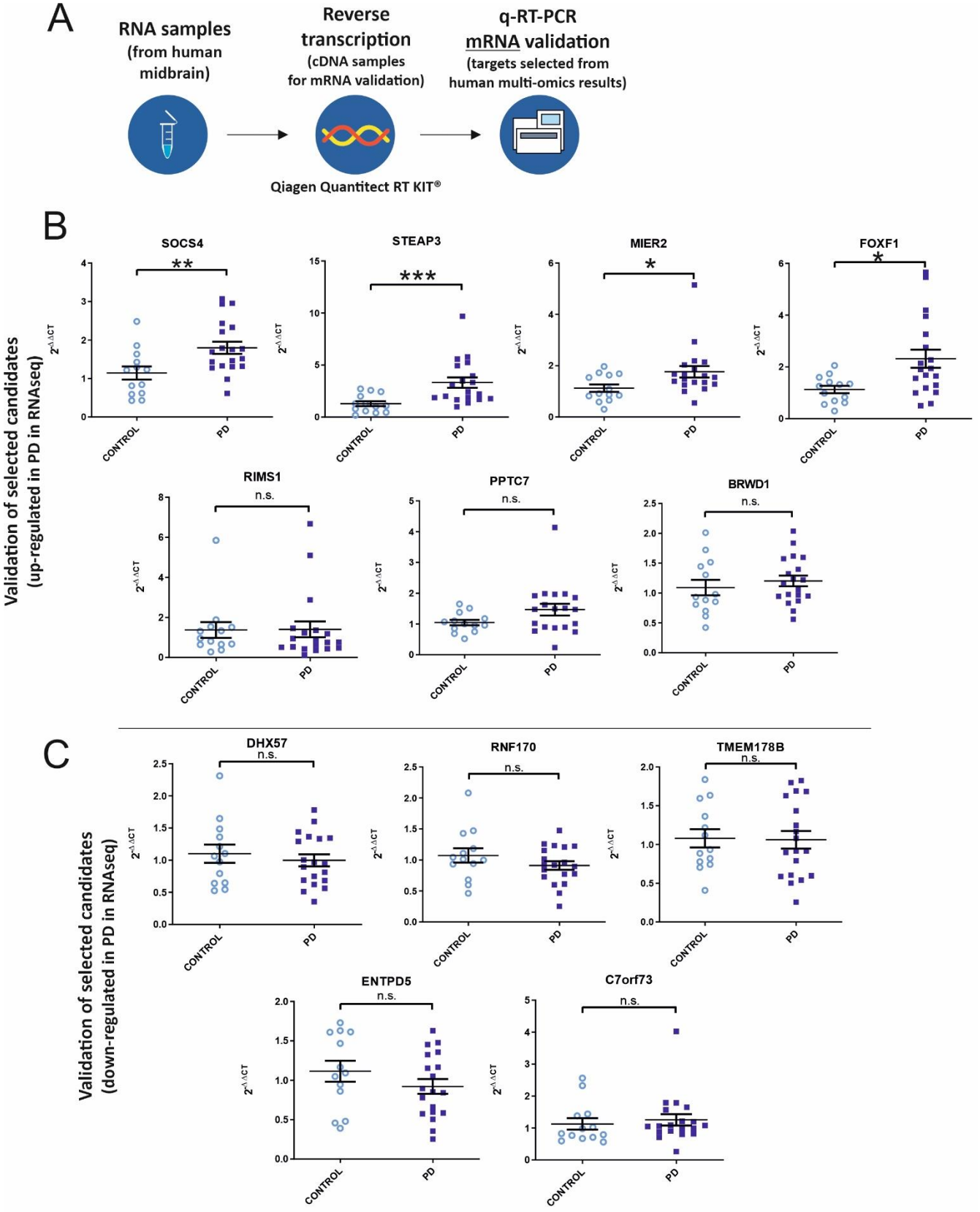

Figure 18. **Validation of RNA sequencing results (selected mRNAs) by q-RT-PCR. (A)** Relative expression levels of selected mRNAs found up-regulated in PD patients. **(B)** Relative expression levels of selected mRNAs found down-regulated in PD patients. Error bars show standard error of the mean. Data analyzed by Mann-Whitney-U test. * $p < 0.05$, ** $p < 0.01$.

3.14 Comparison of human RNA sequencing results with data from a PD mouse model

Another objective of this thesis was to evaluate whether the alterations observed in the human tissue could be reproduced in a common mouse model for PD. Therefore, experiments with the transgenic alpha-synuclein[A53T] mouse model (αSyn.A53T) were designed to explore the findings from the small RNA and RNA sequencing experiments in the midbrain tissue of αSyn.A53T mice. These mice express the human form of the αSyn protein with the A53T point mutation. This mutation can lead to severe and progressive motor phenotypes in the carrier animals, with an average onset at 8 months of age (Giasson et al., 2002) Briefly, transgenic αSyn.A53T mice were bred and both, wild type and homozygous animals, were selected shortly after birth for the experimental cohorts. Six cohorts were designed according to the genotype and the anticipated age at sacrifice (n = 5 animals per group). The animals were kept under controlled conditions. Early-stage animals were sacrificed at 100 days of age, intermediate-stage mice were sacrificed at 250 days of age and late-stage at 400 days of age (or whenever any signs of pathology were shown). After sacrification, animal brains were micro-dissected and snap-frozen. Midbrain tissue from the selected animals was processed in the exact same way as done for human q-RT-PCR validation studies (Figure 19A).

3.14.1 Validation of PD-deregulated miRNAs in αSyn.A53T midbrains

Similar to what was done with the human midbrain tissue, total RNA was isolated from mouse midbrain and cDNA samples were prepared by reverse transcription reactions. The q-RT-PCR validation experiments were conducted in parallel to the ones performed with the human midbrain tissue (Figure 19B). The relative results were tested for significance between mutated and control genotypes within each age group. The miRNAs presenting significant differences in the validations studies in humans were further selected for the validation in mice (Figure 19C). Furthermore, a miRNA target prediction was performed in TargetScan 7.2 (Agarwal et al., 2015) in order to find any further miRNAs potentially regulating the mRNA transcripts selected for validation (selected targets shown in the section below). From the several retrieved miRNAs, three miRNAs were also found to be regulated in human small RNA sequencing results and were also selected for validation in the animal tissue.

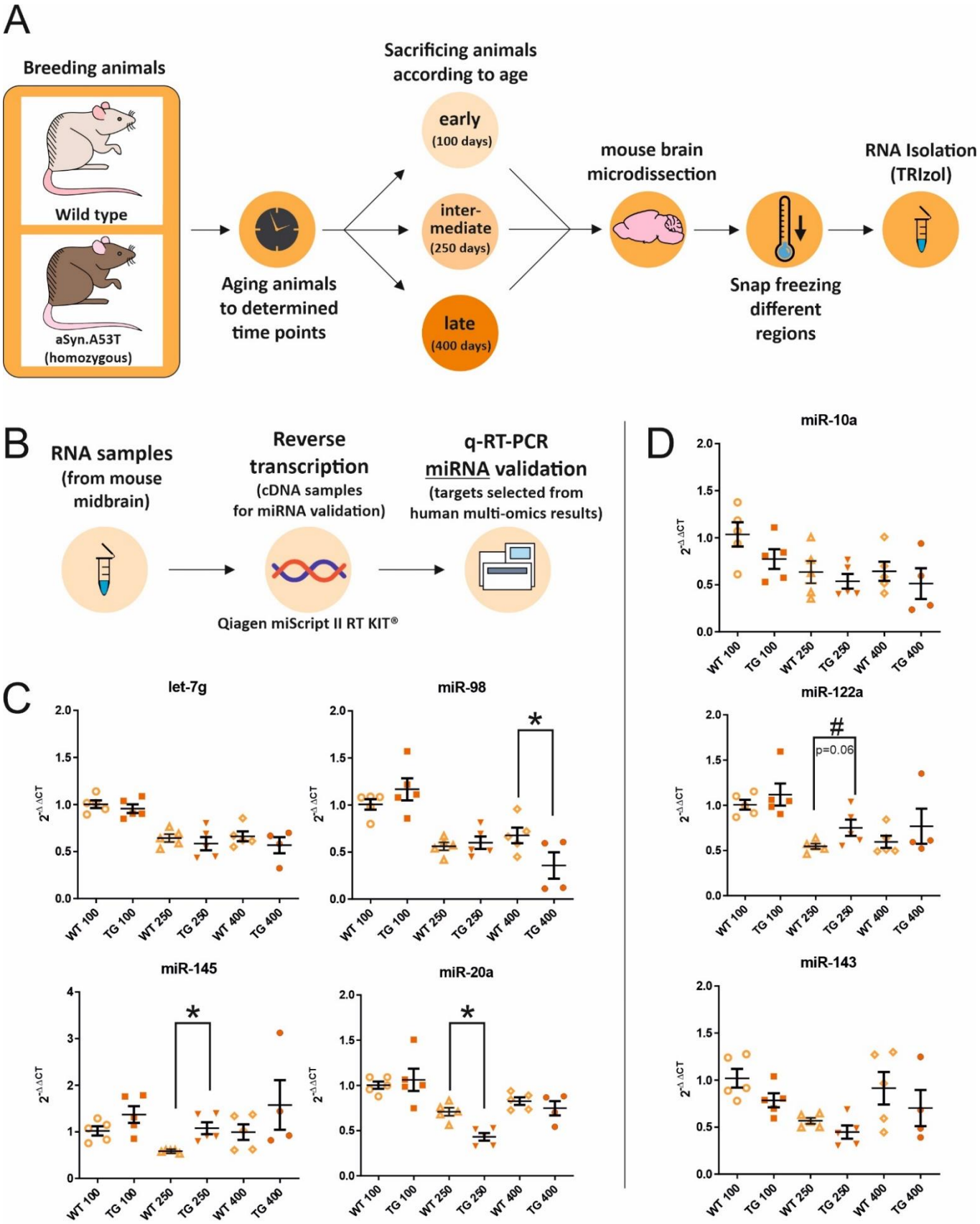

Figure 19. Mouse model - experimental setup and validation of selected miRNA targets. (A) Experimental setup for the mouse validation study. αSyn.A53T transgenic mice were bred from A53T heterozygous pair. Wild type and homozygous animals selected for further experiments.

Animals were sacrificed according to age (early-stage = 100 days; intermediate stage = 250 days; late-stage = 400 days; total number of groups = 6). Late-stage animals were sacrificed either at end point or when symptoms of paralysis / pronounced weight loss started to appear. After sacrifice, mouse brains were microdissected into different brain regions and snap-frozen for further use. RNA was isolated from midbrain samples from animals (n = 5 animals per group). Groups were tested for significance between mutated and wild-type genotypes within the different age groups. **(B)** Experimental setup for miRNA q-RT-PCR validation of targets selected from the human midbrain small RNA sequencing results. **(C ; D)** Relative expression levels of selected miRNAs in midbrains of transgenic animals. Panel C shows relative expression levels of selected miRNAs found deregulated in PD patients. Panel D shows relative expression levels of newly selected (see Figure 4 / section 3.14.1 for the selection of targets). Error bars show standard error of the mean. Data analyzed by mixed-effects ANOVA followed by Bonferroni post-hoc test. * $p < 0.05$, ** $p < 0.01$, *** $p < 0.001$

The validation results indicate no differences between the genotypes at the early-stage groups, an evidence for a possible age-related alterations in miRNA expression. The relative expression levels of all miRNAs show a trend to reduced expression in both wild type and homozygous genotypes in the intermediate stage groups compared to their expression levels at the early-stage group. The relative expression of miRNAs at late-stage groups seems to be more variable, although significant changes were only found for one miRNA species there (miR-98).

For two candidates (mir-98 and miR-20a), alterations in late-stage and intermediate-stage groups, respectively, were concordant to the results presented in the human midbrain tissue validation. The expression levels for both miRNAs were significantly down-regulated in homozygous groups in comparison to the respective controls at the given time points. Another miRNA (miR-145) presented significantly up-regulated levels in homozygous animals in comparison to wild-type groups at the intermediate stage - an opposite finding to the results from the human tissue validation (Figure 19C). miR-122a presented a trend for up-regulation in mutated animals (Figure 19D). Outlier values for relative expression results were excluded from the analyses.

3.14.2 Validation of PD deregulated mRNAs in αSyn.A53T midbrains

Similar to the miRNA candidate selection described in the previous chapter, mRNA species successfully validated in human tissue by q-RT-PCR were now selected for validation the αSyn.A53T mouse model (Figure 20B). Furthermore, in order to have a deeper look into the possible correlation of pathological features presented by the αSyn.A53T mice in relation to PD pathology in humans, further transcripts were selected for validation by q-RT-PCR. First, genes that were previously described to be involved in PD pathogenesis and pathophysiology in humans were retrieved from a comprehensive review of PD and the cellular processes involved the pathogenesis of the disease (Kalia and Lang, 2015). Next, a screening of the results of the largest genomic-wide association study in PD (which involved the analysis of 7.8 million *single nucleotide polymorphism [SNPs]* in dozens of thousands of PD cases and more than one million control cases) was performed (Nalls et al., 2018). For both strategies, the cut-off criterion was that candidates had to be significantly regulated in the RNA sequencing results from the human midbrain study. With the aforementioned setting, 9 further transcripts were selected for validation by q-RT-PCR in the αSyn.A53T mouse tissue (Figure 20C).

Similar to the miRNA validation in the previous section, the statistical evaluation of the results focused on the differences between the different genotypes in each stage. The results showed that in general, most of the evaluated genes present changes between genotype groups either at an earlier stage (already at 100 days of age) or at an intermediate time points (250 days of age). Significant differences in the relative expression levels of SOCS4 (intermediate stage) fitted the findings from the transcriptomics validation in the human tissue, while the significant findings for MIER2 (both in early and in intermediate stages) were opposed to the ones found in humans. Interestingly, for the further selected targets, all the relative expression changes were observed as an up-regulation in the homozygous animals: DYRK1a (both in early and in intermediate stages), GALC (early stage), HSPA1 (intermediate stage), PINK1 (both in early and in intermediate stages), POLG1 (early stage), RIMS1 (intermediate stage) and SQSTM1 (early stage). No differences were found in the late stage groups, suggesting again that relative expression might be influenced by cellular changes linked to aging in the control animals.

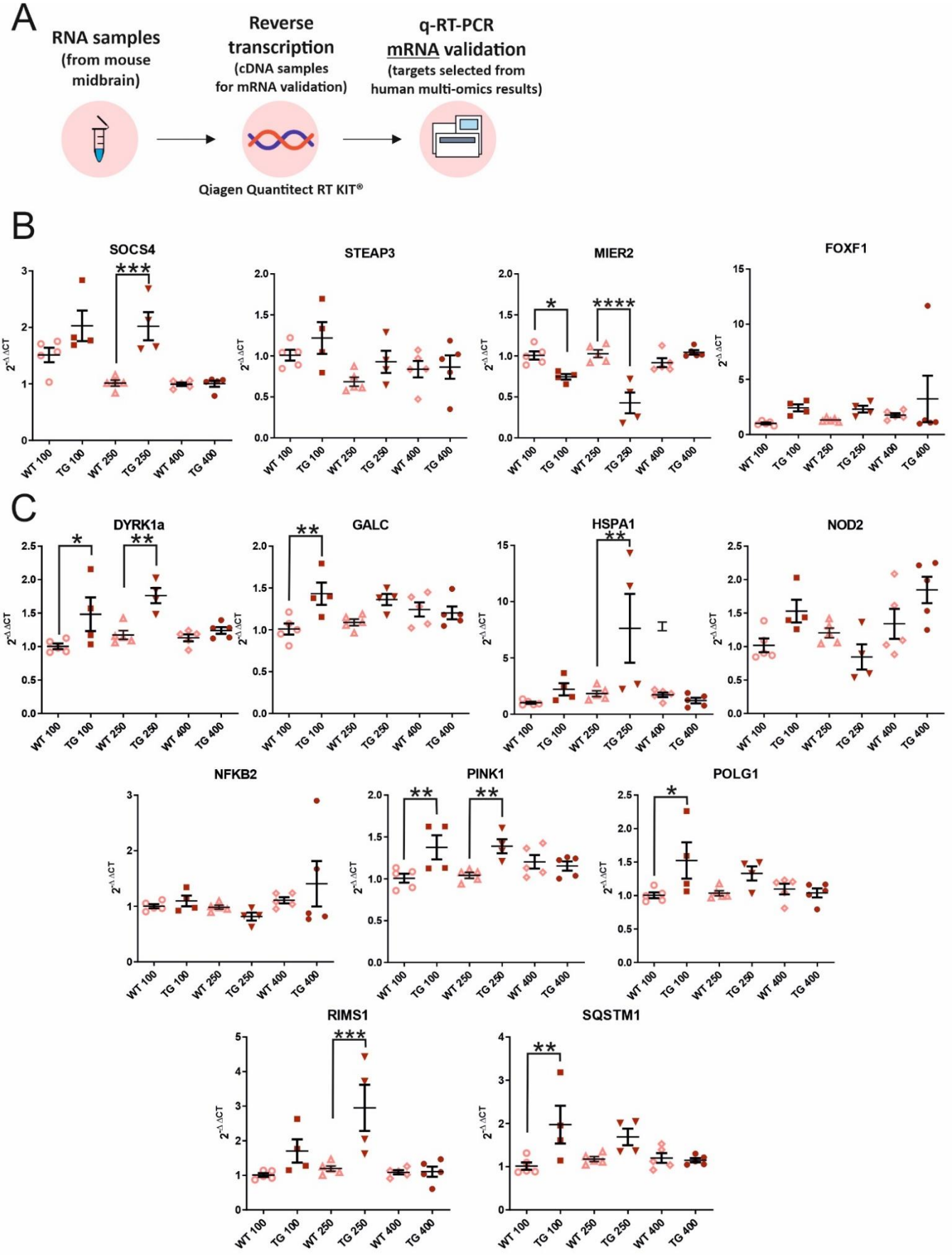

Figure 20. Experimental setup and validation of selected mRNA targets in midbrains of control and transgenic animals. (A) Experimental setup for mRNA q-RT-PCR validation of targets selected

from the human midbrain small RNA sequencing results. **(B)** Relative expression levels of selected mRNAs (previously validated in human midbrain tissue) in midbrains of transgenic animals. **(C)** Relative expression levels of further selected targets for q-RT-PCR validation with the αSyn.A53T mouse midbrain tissue. Error bars show standard error of the mean. Data analyzed by mixed-effects ANOVA followed by Bonferroni post-hoc test. * $p < 0.05$, ** $p < 0.01$, *** $p < 0.001$

4 Discussion

To this date, the exact molecular mechanisms underlying the pathogenesis and progression of PD are not completely understood. In addition, the diagnosis of PD mainly relies on clinical criteria related to the motor dysfunction presented by the patients. Since the symptoms only start to appear at advanced stages of the nigrostriatal degeneration characteristic in PD, there is a strong limitation for the promotion of therapeutic strategies that might be able to change the course of the disease. Allied to that, the limited regenerative capabilities of cells in the central nervous system complicate the development of restorative treatment options.

Profiling the expression of molecular elements such as miRNAs, transcripts and proteins in brains affected by PD might reveal a series of pathological events taking place both at cellular and systemic levels in the course of the disease. Ultimately, these approaches might provide valuable insights into PD progression and facilitate the development of novel disease-modifying therapies. The present doctoral thesis aimed to analyze midbrain tissue samples from a cohort of PD patients and controls in a multi-*omics* set of experiments, looking into the genetic background of the selected subjects, as well as characterizing the expression patterns of miRNAs, transcripts and proteins on those samples. By approaching the multi-*omics* techniques both individually and in an integrative way, we aimed to identify patterns of deregulation potentially containing novel pathomechanisms related to PD, with special focus to miRNA-based regulatory processes underlying the disease. Finally, an animal model of PD was evaluated in respect to the changes observed in the human tissue, in order to assess the similarity of the pathological mechanisms occurring in both systems.

4.1 No major genetic alterations are found in the PD patient cohort

In order to evaluate the genetic background of the present PD-patient cohort and explore possible alterations influencing the course of the disease, targeted gene evaluation was performed with both gene panel sequencing and MLPA techniques for pre-selected known PD-associated genes. With the latter technique, the presence of deletions, duplications and triplications for given genes is screened by PCR-based reactions. MLPA

results revealed no alterations for the present cohort, indicating the absence of copy number abnormalities for the genes examined.

Gene panel sequencing experiments identified a VUS (variation of uncertain significance) for the POLG gene in one out of the nineteen PD patients (variant NM_001126131.1:c.2542G>A in patient PD666). A couple of studies linked the presence of POLG variants to PD predisposition in Finnish and Chinese populations, based on alterations in mitochondrial DNA copy number in the variant carriers (Gui et al., 2015b; Luoma et al., 2007). Nevertheless, no mechanistic evidence for this specific VUS in the pathophysiology of PD is found in the literature. All in all, the MLPA and gene panel sequencing experiments showed that no significant genetic alterations are present in the analyzed patients for the classical PD-related genes. These results indicate that the present PD cohort seems to be homogeneously composed of idiopathic cases. However, it is important to highlight that the techniques employed here are targeted and, therefore, restricted in terms of screening for alterations in the whole genome. Thus, the presence of causative mutations in genes not contained in the pre-selected panel cannot be excluded. Although studying genetic cases might reveal a number of important mechanisms in the context of PD pathology, the main focus of this study was to investigate the molecular events taking place in idiopathic PD midbrains, which account for the vast majority of cases. Therefore, for the subsequent analyses presented here, we did not focus on any particular pathomechanisms related to the known autosomal forms of PD.

4.2 Small RNA sequencing results reveals differentially expressed miRNAs in PD including candidates with potential discriminative power

Small RNA sequencing experiments were employed in order to evaluate the small RNA content and profile miRNA expression patterns in the present midbrain samples. The sequencing results revealed that the vast majority of mapped small RNA reads accounted to miRNAs species in both PD and control patients. Relative to the whole small RNA content in the samples, miRNAs represented 90.39 % and 92.61 % of all mapped reads, respectively, in agreement to the small RNA composition found in human CNS tissue in reference studies in the field (Landgraf et al., 2007; Shao et al., 2010). Interestingly, among the top 15 miRNA

with highest average expression in these samples, at least 4 miRNAs have been reported to be brain-specific (miR-181a-5p, miR-127-3p, miR-99b-5p, miR-9-5p) (Hinske et al., 2014; Lukiw, 2012), confirming the quality of the sequencing readouts acquired from the midbrain tissue of the analyzed individuals.

A number of significantly deregulated miRNAs were identified by DE analyses with the small RNA sequencing data. When comparing the sequencing results from PD samples with the ones from the controls, 27 miRNAs were found deregulated – 20 of which are up-regulated in the PD condition. This miRNA up-regulation in almost two-thirds of the DE species in PD samples is a phenomenon widely reported for neurodegenerative diseases like PD and AD (Gui et al., 2015a; Loring et al., 2001; Lukiw, 2007; Lukiw et al., 2012; Sethi and Lukiw, 2009; Starhof et al., 2019), and was also observed in a parallel study performing small RNA sequencing with CSF-exosomes of PD and control patients (Roser & Caldi Gomes et al, in preparation). This general miRNA upregulation might be related to a number of factors, for instance, the presence of a marked neuroinflammation and a high number of immune cells being recruited to the brain tissue of these patients (De Virgilio et al., 2016; Hunot and Hirsch, 2003; Kempuraj et al., 2016), as well as to the disruption of blood-brain barrier that takes place in PD and AD brains (Desai et al., 2007; Gray and Woulfe, 2015; Kortekaas et al., 2005; Rite et al., 2007), which could also be a potential source for exogenous miRNAs (e.g., from blood cells) being transported to the brain tissue and captured by sequencing techniques. Remarkably, the opposite is reported for amyotrophic lateral sclerosis (ALS), where the miRNA machinery and biogenesis is impaired in the affected motor neurons, resulting in a global downregulation of miRNAs (Eitan and Hornstein, 2016; Emde et al., 2015).

Overall, a high inter-individual variability is observed for small RNA expression patterns even within conditions (portrayed in the heatmap from Figure 7), indicating that the disease state does not correspond entirely to the expression levels of the identified small RNAs. These findings evidence a molecular variability seen throughout the datasets presented in this work and might indicate the presence of individual subtypes of the disease. In order to explore the aforementioned inter-individual differences even further, a Bayesian hierarchical clustering was performed with the miRNA expression data of a subgroup of PD patients considering clinical parameters that included age, gender, disease

duration, PMI for tissue extraction and neuropathological diagnosis. In accordance with the overall picture given by the miRNA expression heatmap, the PD samples present a high heterogeneity in terms of miRNA expression. The hierarchical clustering was able to identify three sub-clusters of samples, two of them presenting more obvious similarities for miRNA expression levels within patients. Nevertheless, there seems to be no clear correlation for any of the clusters with the clinical features. Very similar findings were observed in PD CSF in a concomitant study conducted in this laboratory (Roser & Caldi Gomes et al., in preparation). These results indicate a potential pathological diversity at the molecular level that is reflected by miRNA expression. Interestingly, this diversity appears to result in a clinical Parkinsonism phenotype that does not permit to deduce the molecular background.

Next, aiming to identify potential discriminative miRNAs between disease states, the small RNA sequencing results were employed in the development of an iterative feature analysis based on machine learning approaches with the miRNA expression data. A variable ranking was built for the selection of candidates that are more efficient in classifying disease states. Interestingly, four of the candidates identified as potential discriminative signatures were also found deregulated in DE analyses (namely, miR-29a-3p, miR-223-3p, miR-29c-3p, let-7g-5p), suggesting an important role of these miRNAs both in the context of PD pathophysiology and also as potential diagnostic biomarkers for PD. In addition, these candidates have been frequently found in altered levels in biomarker studies using body fluids of PD / controls patients (as reviewed in Roser et al., 2018), adding another level of evidence to the importance of these candidates in the context of PD. The mechanistic relevance of these and several other DE miRNAs found here was explored in the context of PD pathology in subsequent experiments of this work. Ideally, replication studies both in midbrain samples and in circulating body fluids from independent patient cohorts would be required for the verification of the biomarker potential of the aforementioned candidates.

In addition to the bioinformatical analyses, a thorough literature screening was performed using the DE miRNAs found in the present study in the context of neuronal-related processes, neurodegeneration and other related processes. A list of all the searched key-terms and related miRNAs is depicted in Figure 9. Remarkably, 12 out of the 27

deregulated miRNAs identified here were already reported to play an important role in dopaminergic neuronal function and/or PD pathology (Batistela et al., 2017; Caggiu et al., 2018; Chi et al., 2018; Ghanbari et al., 2016; Lin et al., 2019; Singh and Sen, 2017; Wang et al., 2017; Xie et al., 2017). A number of these miRNAs have also been identified as putative circulating biomarkers in dozens of PD and AD studies up to now (extensively reviewed by three recent publications (Batistela et al., 2017; Mushtaq et al., 2016; Roser et al., 2018b)). Several of the deregulated miRNAs are linked to key-terms that include *aging, neurodegeneration and brain injury* (Dluzen et al., 2017; Gaudet et al., 2016; Goedeke and Fernández-Hernando, 2014; Kangas et al., 2017; Kim et al., 2016; Li et al., 2013a; Mo et al., 2016; Xie et al., 2017) and *neurogenesis, neuronal development and differentiation* (Basak et al., 2016; Oh et al., 2018; Pieczora et al., 2017; Pons-Espinal et al., 2017; Qu et al., 2019). Another search category with a considerable number of hits for the DE miRNAs is *inflammatory/immune response* (Cardoso et al., 2012; Ge et al., 2016; Haneklaus et al., 2013; Lambert et al., 2018; Sawant et al., 2015; Thome et al., 2016; Wu et al., 2018). More than a third of the miRNAs found up-regulated in the PD condition has been previously linked to processes related to immune response and inflammation, possibly indicating a feedback regulatory mechanism responding to the neuroinflammation observed in PD. The aforementioned processes are of extreme importance in PD pathology and progression and are discussed in more detail in section 4.4. It is important to highlight that *postmortem* midbrain samples are employed in this work, exclusively. Thus, the changes in miRNA expression (and also for the further molecular elements analyzed here) must reflect a very advanced stage of the PD pathology. Therefore, the relevance of the identified candidates for the pathogenesis of the disease has to be interpreted with caution.

4.3 Pathway enrichment analysis reveals important biological roles for the targets of differentially expressed miRNAs in the context of PD

Aiming to explore the functional role of the deregulated miRNAs both in neuronal function and homeostasis, as well as in neuropathological states, pathway enrichment analyses were conducted with experimentally validated targets of the deregulated miRNAs identified in the DE analyses. Using validated targets exclusively obviously restricts the

number of potential miRNA-mRNA pairs offered by computational target prediction (usually based on prediction by nucleotide complementarity), but offers the highest level of evidence for enriched biological processes and excludes the bias of non-canonical miRNA pairing or imperfect seed match that would not lead to any relevant biological consequence to the cell or organism (Agarwal et al., 2015; Friedman et al., 2008; Garcia et al., 2011). The enrichment analyses were conducted for targets of up- and down-regulated miRNAs individually.

For up-regulated targets, the significantly enriched biological processes were characterized as neuron-related (32%), nucleus/chromosome related (30%) and cytoskeleton/cell growth-related (20%) (as the most representative GO categories). These findings indicate an important involvement of the up-regulated candidates in neuronal processes and also suggest that several of these miRNAs are likely originated in neurons, fitting well with the RNA samples of midbrain source analyzed here. Moreover, midbrain tissue biopsies contain a variety of neuronal and glial cell types (La Manno et al., 2016), which are likely accounting to the different categories annotated for the regulated miRNAs (depicted in figure 10). The top 5 most significant biological processes are related to regulation of cell proliferation, differentiation, cell cycle and neurogenesis, well in line with the results retrieved by the literature screening (Basak et al., 2016; Oh et al., 2018; Pieczora et al., 2017; Pons-Espinal et al., 2017; Qu et al., 2019). Remarkably, cell proliferation- and cell cycle-related proteins are known to play an important role also in the survival and maintenance of mature neurons (Herrup and Yang, 2007; Omais et al., 2018). Aberrant cell cycle was also reported to be intimately linked to apoptosis of post-mitotic neurons and neurodegeneration overall (Feddersen et al., 1992; Heintz, 1993). Interestingly, the regulation of targets related to cell proliferation and cell death seems to happen in both directions, being enriched for both up- and down-regulated miRNAs. That might indicate that the enrichment on the aforementioned categories might be related both to a response to the neurodegenerative processes occurring in the PD-affected brains, as well as reflect an impairment of mechanisms related to cell maintenance and survival leading to the neurodegeneration in PD. More to that, *regulation of cell death* and *apoptotic process* also figure among the enriched GO terms for the validated targets of up-regulated miRNAs,

providing further evidence for the involvement of these candidates in (or as a response to) the cell death occurring in PD midbrains (Kim et al., 2016; Li et al., 2013a; Xie et al., 2017).

On the other hand, for the target of PD down-regulated miRNAs, the majority of the enriched GO terms belong to nucleus/chromosome-related processes (26%), cytoskeleton/cell growth-related processes (24%) and vesicular-related processes (19%). Interestingly, no enriched processes seem to be directly related to neuronal processes for the validates targets of PD down-regulated miRNAs. It's important to account, though, that the number of down-regulated miRNAs in the PD condition is almost 3 times smaller than the up-regulated category, which consequently decreases the number of analyzed targets substantially. Some of the enriched biological processes seem to be related to mitochondrial mechanisms (7%), which also have fundamental implications in PD pathophysiology (Bose and Beal, 2016; Liu et al., 2017; Rocha et al., 2018). When analyzed individually, the biological processes enriched for the targets of down-regulated miRNAs are mostly related to the regulation of gene expression, transcription / RNA metabolism and regulation of biosynthetic processes, in line to what was observed for the results from the up-regulated miRNAs. Interestingly, GO terms related to *apoptotic process* and *cellular response to stress* figure among the enriched categories for the targets of down-regulated miRNAs, indicating that a possible insufficient miRNA regulation of stress- and apoptotic-related genes might be taking place for some of the identified candidates.

In general, for the functional annotation of miRNA targets, it is important to consider that RNA material from a diversity of cells populating the analyzed midbrains was used for the sequencing. Thus, the enriched biological processes annotated for miRNA-targets are reflecting cellular changes not only of neurons but also of glial and immune cells present at the analyzed tissue. This is especially important since a massive activation of the immune response was observed when analyzing the transcriptomics results for these samples (as discussed in section 4.4). As many of the most significant pathways enriched for targets of the deregulated miRNAs were related to cell proliferation and cell cycle and positive regulation of cellular biosynthetic processes, it is likely that several of the enriched pathways are related not only to the apoptosis of dopaminergic cells but also to an immune cell proliferation taking place in the PD-affected brains, for example(Hirsch and Hunot, 2009; Hunot and Hirsch, 2003; Kempuraj et al., 2016; McGeer et al., 1988a; Nazmi et al.,

2019; Rea et al., 2018; Viviani, 2004). To a certain extent, the aforementioned findings indicate a disturbance in the homeostatic state of the cell populations present in the analyzed midbrains and might reflect possible cellular responses to dopaminergic insults and the neurodegenerative events taking place at the PD-affected midbrains. The exact events happening at the transcriptomic and proteomic levels and detailed miRNA-mRNA interaction pairs were further explored in subsequent steps of this work.

4.4 Transcriptomic profiling documents dopaminergic depletion and indicates an important inflammatory reaction in PD midbrains

Aiming to explore the gene expression patterns in the analyzed samples, transcriptomic profiling through RNA sequencing and subsequent DE analyses were performed. In comparison to the DE results from miRNA expression depicted above, a much higher number of genes are found significantly deregulated in the transcriptomics analysis. Following pre-defined cut-offs, a total of 1452 transcripts were found altered when comparing PD samples to controls. Similar to the miRNA data, the majority of the deregulated candidates were found up-regulated in the PD condition, accounting to 67.1% of the significant results (975 transcripts). Furthermore, also similar to the findings of miRNA DE analyses, a rather high inter-individual variability in gene expression is observed. Nevertheless, in spite of some individuals presenting a general gene expression that differs from the other subjects within their disease state group, the majority of the PD patients seem to present an inversed pattern of expression for the genes found DE in comparison to the control subjects (as shown in heatmap from Figure 12). Moreover, the control group presents more homogeneous patterns of gene expression within subjects, while the PD once again presented a much higher expression heterogeneity, as observed in the hierarchical clustering analyses done with the miRNA data. That might be due to the fact that the postmortem midbrain samples used as controls here are obtained from patients that died from a variety of diseases but presented no neurological disorder besides age-related changes. Remarkably, the opposite has been found in CSF studies in PD conducted in this lab, where controls presented a higher variability in miRNA expression (Roser & Caldi Gomes, in preparation). Nevertheless, the CSF study contained almost one hundred control

samples (in comparison to 15 analyzed here). Taken together, these findings support the concept that idiopathic PD is not a uniform disorder regarding its molecular pathogenesis and that there may exist multiple pathogenic subgroups among the affected subjects (Dexter and Jenner, 2013b; Johnson et al., 2019).

In order to verify the functional role of the deregulated transcripts and explore the pathophysiological events taking place in the midbrains of the analyzed patients, pathway enrichment analyses were performed with the DE results for transcriptomics experiments, considering up-and down-regulated transcripts separately. The results for transcripts found down-regulated in PD revealed enrichment for dopamine-related biological processes, indicating that dopamine biosynthesis and dopaminergic transmission are indeed depleted in the patient samples, as expected for midbrain PD pathology (Dauer and Przedborski, 2003a; Langston et al., 1983). The annotated genes for the enriched categories included key players for dopamine metabolism and function, for instance, tyrosine hydroxylase (TH), Dopa decarboxylase (DDC), dopamine transporters (SLC6A3 and SLC18A1) and dopamine receptor D2 (DRD2). Further, dopamine-related GO processes retrieved included *locomotory behavior, learning, social behavior* and *dopamine biosynthetic process* per se, all annotated for down-regulated genes in the PD condition. Moreover, KEGG pathways analyses retrieved *Parkinson's disease* as the third most significant pathway for down-regulated transcripts in PD samples. The term *dopaminergic synapse* is also enriched for those transcripts. Interestingly, the most significant KEGG pathway for PD down-regulated genes was the *metabolic pathway.* Although the enriched term is rather unspecific, metabolic dysfunctions, in general, have been often linked to PD pathology previously (Fai Poon et al., 2005; Hoepken et al., 2007; Huang et al., 2007; Perry et al., 1982; Polito et al., 2012). Dopaminergic neurons are also known to be especially sensitive to metabolic alterations, oxidative stress and mitochondrial dysfunction, for example (Anandhan et al., 2017; Dexter and Jenner, 2013b; Greenamyre et al., 1999; Hauser and Hastings, 2013; Lin and Beal, 2006; Winklhofer and Haass, 2010). Another interesting enriched pathway for down-regulated transcripts in PD is annotated for genes playing a role in *ribosomal processes*. Coincidentally, it figures as the second most significant KEGG pathway for PD down-regulated transcripts, matching the strong enrichment for biological processes related to *cell proliferation, cell cycle* and *regulation of biosynthetic processes* reported for

up-regulated miRNAs in PD (and consequent down-regulation of their targets). Similarly, processes related to the translational machinery figure at the top of the list of significantly enriched GO terms for PD down-regulated transcripts. Those findings support the connection between the miRNA and gene expression datasets and encourage the integrative efforts for the multi-*omics* approaches presented in this work. Overall, the dopamine-related enrichment results presented here indicate that molecular events related to dopaminergic pathology were indeed captured in the present experiments and is also an indicator for the quality of sample preparation and sequencing and for the plausibility of the results obtained.

Remarkably, for genes up-regulated in the PD samples, the pathway enrichment results are predominantly related to a marked inflammatory response and immune system activation taking place in the patient midbrains. Eight out of the top 10 most significant GO terms enriched for those genes are directly or indirectly related to the immune / inflammatory response. Actually, the GO terms entitled *inflammatory response* and *innate immune response* figure at the very top of the list. Similarly, the vast majority of the KEGG pathway enrichment results are either related to immune system activation or to a variety of infectious diseases – probably due to the fact that the pathways for that kind of diseases also present a massive enrichment for genes related to immune cell activation and inflammation, as observed in the PD midbrains analyzed here.

In more detail, highly significant enriched GO terms included, for example, *interferon-gamma (IFNγ) mediated signaling, positive regulation of interferon type I production* and *positive regulation of NF-kappa B (NFKB) activity/signaling,* processes intrinsically related to both adaptative and innate immune response (Dev et al., 2010; Kopitar-Jerala, 2015; Le Page et al., 2000). These processes have also been extensively linked to aging and neurodegeneration previously (Kaltschmidt et al., 1993; Kempuraj et al., 2016; Nazmi et al., 2019; Rea et al., 2018; Taylor et al., 2018; Viviani, 2004). In fact, NFKB signaling has been considered as the culprit of the so-called “inflammaging”, since this pathway seems to regulate immune and inflammatory responses at the cellular level both in aging and in age-related disorders (Balistreri et al., 2013; Salminen et al., 2008). An important study described an intense inflammatory reaction and dopaminergic cell damage in rats upon intranigral injections of the immunostimulant lipopolysaccharide (LPS)

(Castaño et al., 2002). Interestingly, *lipopolysaccharide-mediated signaling pathway* also figures among the enriched GO terms for PD up-regulated genes.

There is also ample evidence for the participation of inflammatory cytokines in the pathophysiology and progression of PD. Neuroinflammatory and increased immune activity are known to contribute to the cascades of mechanisms that result to the neurodegeneration in PD (Hirsch and Hunot, 2009; Hunot and Hirsch, 2003; McGeer et al., 1988a). Moreover, several postmortem studies have found a substantial increase of proinflammatory cytokines in parkinsonian brains (Imamura et al., 2003; Mogi et al., 1996a, 1996b, 1996c; Nagatsu and Sawada, 2005; Sawada et al., 2006). Interestingly, the infiltration/activation of immune cells and marked neuroinflammation have been considered as aggravators of the disease, taking place at late stages of the neurodegenerative pathology in PD (Johnson et al., 2019; Maetzler et al., 2007; Menza et al., 2010). Oppositely, very early glial changes in PD brains seem to be related to αSyn deposition and a resultant astrocytic dysfunction (rather than microglia activation/leucocyte infiltration) (Gu et al., 2010; Halliday and Stevens, 2011; Johnson et al., 2019; Lee et al., 2010). These findings indicate that the marked changes in neuroinflammatory markers identified by us and the above-referred postmortem studies are most likely related to end-stage changes in PD-affected brains.

Furthermore, a handful of studies have specifically implicated the cytokines NFKB and IFNγ – especially important in the context of our transcriptomic findings - in PD pathophysiology. Mogi and colleagues found elevated levels of both NFKB and IFNγ in the postmortem brain tissue (substantia nigra, caudate nucleus and putamen) of PD-affected brains (Mogi et al., 2007). Furthermore, increased levels of IFNγ were reported to induce both a progressive degeneration of neurons in the nigrostriatal system and calcification of the basal ganglia (Chakrabarty et al., 2011). Another study pointed to the involvement of IFNγ in microglial-mediated dopaminergic neurodegeneration taking place in PD brains (Mount et al., 2007). Microglial activation seems to be closely related to the nigral degeneration in PD. They seem to produce deleterious effects to dopaminergic neurons by the release of multiple cytotoxic mediators, leading to a chronic and progressive neuroinflammatory state that directly influences the dopaminergic neurodegeneration (Joers et al., 2017). Large numbers of activated microglia have been found in nigral areas

of extensive dopaminergic degeneration in PD midbrains (Langston et al., 1983, 1999; McGeer et al., 1988a). Additionally, reactive microglia were shown to be highly detrimental to dopaminergic neurons in *in vitro/in vivo* models of PD (Chen et al., 1998; Le et al., 1995, 2001). Others showed that peripheral immune cells might also take part in the neuroinflammation occurring in PD. Cytotoxic CD4+ and CD8+ T lymphocytes were found in increased amounts in the substantia nigra of PD patients and, less extensively, in the substantia nigra of AD-affected brains (McGeer et al., 1988a). A subsequent study also showed that lymphocyte infiltration powered the dopaminergic degeneration in a mouse model of PD (Brochard et al., 2008). Similarly, postmortem studies identified increased amounts of T cells throughout AD-affected brains (Togo et al., 2002). Interestingly, immunostaining approaches revealed that cytotoxic lymphocytes cells are located close to blood vessels and also in the vicinity of neuromelanin-positive dopaminergic neurons in postmortem PD midbrains, suggesting that these immune cells are able to penetrate the brain from the bloodstream through the brain parenchyma, and that they might effectively interact with the degenerating dopaminergic neurons in those regions (Brochard et al., 2008). The insults promoted by microglial and other immune cells in PD could be mediated by oxidative damage resultant from the cytotoxic activity of these cells, to which dopaminergic neurons are very sensitive (Hirsch and Hunot, 2009). However, other mechanisms, e.g. neuro-glial gliapse formation and subsequent phagocytosis, could also be involved (Barcia et al., 2012).

For the few enriched pathways not linked to immune/inflammatory reactions, some terms are also relevant and worth mentioning for the up-regulated transcripts found in PD. The GO term entitled *positive regulation of GTPase activity* is also enriched for these transcripts and has been object of intense study by our group. The Rho family of GTPases, for example, are involved in several crucial neuronal processes including actin dynamics, axon growth, stabilization and guidance and synaptic plasticity. Some of these players and related interactors (e.g., RhoA; CDC42; RAC1; ROCK) are known to be important regulators of neuronal death, axon de- and regeneration, for example (Bustelo et al., 2007; Koch et al., 2018; Ridley, 2016). Preclinical studies have also shown that inhibiting the activity of these kinases could prevent degeneration and promote regeneration in *in vitro* and *in vivo* models of PD (Koch et al., 2014, 2018; Tatenhorst et al., 2014; Tönges et al., 2011, 2012).

Additionally, KEGG pathways for *apoptosis* and *MAPK signaling pathways* are both enriched for the PD up-regulated transcripts. These pathways are very likely reflecting the neurodegenerative processes and alterations in mechanisms related to cell survival taking place in the midbrains of the patients (Dauer and Przedborski, 2003a; Dexter and Jenner, 2013b). Furthermore, *positive regulation of transcription* (and related) GO terms are also enriched. The MAPK signaling cascade is not only linked to cell survival and stress responses, but also to the regulation of gene expression, for example (Cargnello and Roux, 2011). These findings once again match the *positive regulation of gene expression, RNA biosynthetic processes* and *cell response to stress* found enriched for the deregulated miRNAs, suggesting once again an interplay between the miRNA and the gene expression data.

All in all, the functional annotation with the transcripts found up-regulated in the PD condition showed that the inflammatory and immune responses are major processes in the physiopathology in the affected patients. In fact, there is a present consensus that neuroinflammation is an important factor in the context of PD (Hirsch and Hunot, 2009; Johnson et al., 2019; Kalia and Lang, 2015). Neuroinflammation has also been considered also a predictive feature for the development of cognitive decline and non-motor symptoms in PD, another indication for its role in intensifying the dopaminergic damage, directly influencing the progression of the disease (Maetzler et al., 2007; Menza et al., 2010). As we have analyzed postmortem midbrain samples from patients presenting PD pathology at advanced stages, it is not possible to determine whether the neuroinflammation-related mechanisms contributed to the initiation of the disease. Nonetheless, our transcriptomics findings provided additional evidence that neuroinflammatory changes are indeed playing a major role in the pathophysiology of PD, at least in advanced stages. As a matter of fact, end stages of the disease are the most complicated to target therapeutically, and dramatically burden the quality of life of PD patients (Lim et al., 2009). Therefore, exploring whether the attenuation of the neuroinflammation in advanced stages of PD could lead to any improvements to disease progression would be essential, and might lead to promising novel therapeutic strategies for this devastating disorder.

4.5 Proteomic profiling reveals enrichment in PD-related pathways matching the transcriptomic results

In order to explore the differences in protein expression in the analyzed midbrain samples, mass spectrometry experiments were performed, followed by DE and functional enrichment analyses. In comparison to the small RNA and transcriptomics datasets, only proteins uniquely identified within all analyzed samples are considered for the quantitation, making the coverage and the size of the proteomics dataset substantially smaller. After peptide mapping and protein quantitation, a total of 2,257 proteins were uniquely identified, and DE analyses revealed 127 significantly regulated proteins when comparing the PD condition to the respective controls. In line with what was observed in the previous datasets, the majority of the DE proteins (69%) were found up-regulated in the PD samples (87 proteins), while only 31% of the significantly regulated proteins (40 out of 127) were down-regulated in PD. Also similar to the small RNA and transcriptomics, the protein expression data presented high inter-individual differences within subjects. The protein expression data shows a high inter-individual variability even within diseased/control cohorts (Figure 13). Similar findings were observed for all approaches employed here and again suggests multiple molecular subtypes in PD patients.

Expectedly, the DE results for the protein expression data revealed a down-regulation in TH - the most robust marker for dopamine metabolism and dopamine depletion in PD (Molinoff and Axelrod, 1971; Perez et al., 2002) - in line with the TH down-regulation found for the transcriptomics experiments. Remarkably, functional annotation revealed the pathway *immune effector process* as significantly enriched for the DE proteins in PD, matching the massive immune/inflammatory activation reported for the transcriptomics results. Several cytokines, immune mediators and receptors seem to be deregulated in PD, indicating that the alterations seen in the previous *omics* results presented here are also captured at the proteomic level. For instance, the category *immune effector process* was annotated for a variety of important genes that included CD47, C1QC, CHI3L1, LAMP2, RAB18 (full list portrayed in table 12). A strong enrichment is shown for the process entitled *negative regulation of protein folding* - the most significant of all enriched categories. Defects in protein folding and metabolism have been extensively linked to neurodegeneration and also PD (both in patients and in models for the disease)

(Dauer and Przedborski, 2003a; Ebrahimi-Fakhari et al., 2013; Ross and Pickart, 2004; Ryu et al., 2002; Selkoe, 2004). It is important to mention that the mechanisms for protein folding involve a multitude of players, but this particular category enriched in our proteomics DE results (GO term ID: 1903333) is composed of only 5 genes (BAG5, PDCD5, PDCL, SNRNP70, ST13) – 2 of which are present in our dataset (SNRNP70, ST13). ST13 and SNRNP70 are both found up-regulated in PD. ST13 (encoding for the Hsc-70 interacting protein) is a co-chaperone that activates the heat-shock protein 70 (HSP70), a chaperone known to reduce αSyn aggregation and toxicity (Klucken et al., 2004; Nollen et al., 2001). Alterations in levels of ST13 have been already reported in PD blood, with decreased levels of this protein being found in PD patients in comparison to controls and to AD patients (Scherzer et al., 2007). Although ST13 levels in our proteomics study are opposed to the ones reported for PD blood, a compensatory mechanism in response to increased αSyn aggregation may be involved in the up-regulation of ST13 in PD midbrains. SNRNP70 (Small Nuclear Ribonucleoprotein U1 Subunit 70), a protein originally involved in spliceosome formation (Will and Lührmann, 2001), is reported to selectively associate with Tau neurofibrillary tangles and aggregate in the brains of AD patients (Bai et al., 2013). SNRNP70 was also found in increased levels in the brains of AD patients through proteomics approaches (Diner et al., 2014; Hales et al., 2016). Tau pathology has been increasingly implicated in synucleinopathies, Lewy body formation and PD pathology (Ishizawa et al., 2003; Wills et al., 2010; Zhang et al., 2018), reinforcing the relevance of the findings presented here.

Another important enriched category for the DE proteins in PD is entitled *Oxidation-reduction process*. As discussed in section 4.4, oxidative damage is especially important in the context of dopaminergic degeneration in PD and may be responsible for the increased selective vulnerability of dopaminergic neurons (Anandhan et al., 2017; Dexter and Jenner, 2013b; Hauser and Hastings, 2013; Lin and Beal, 2006). The presence of deregulated proteins annotated to these processes matches the previous datasets presented here and indicate that previously described pathological mechanisms are indeed captured by our multi-*omics* analysis. Up-regulated proteins in this category included MAOB, NADH-ubiquinone oxidoreductase core subunits B3 and S2, CBR1, PRDX 1 and 6 – all of them also annotated to another enriched category, *Drug metabolic process*, and several of them also

common to the pathway entitled *organophosphate metabolic process*. Table 12 encloses the list of all enriched pathways and annotated proteins. Interestingly, MAOB inhibitors have been reported to have neuroprotective effects for dopaminergic neurons. Furthermore, MAOB polymorphisms were associated with increased risk for PD development (Dezsi and Vecsei, 2017). Pre-clinical results motivated a number of clinical trials with MAOB inhibitors for PD. These candidates presented inconsistent results at the trials and have not been considered as clinically relevant for PD (Clarke et al., 2011; Olanow et al., 2009). Nevertheless, MAOB inhibitors are still considered as relevant in terms of PD pathomechanisms and have been object of a handful of recent studies (Bar-Am et al., 2015; Guo et al., 2016; Huleatt et al., 2015; Robakis and Fahn, 2015; Tong et al., 2017). Studies have also linked the activity of mitochondrial NADH-ubiquinone oxidoreductase to MTPT and MPP+ dopaminergic neurotoxicity, for example (Conn et al., 2001; Mizuno et al., 1986). The enriched pathways *secretion by cell* and *vesicle-mediated transport* contain several overlapping proteins, and despite being very broad pathways with thousands of involved proteins, the might be very relevant for PD pathology. Recent studies have suggested that both αSyn and Tau are propagated through neurons trans-synaptically, being secreted and uptaken by neurons via extracellular vesicles fueling the αSyn pathology spreading hypothesis and relating it to PD progression (Cheng et al., 2018; Gustafsson et al., 2018; Okuzumi et al., 2018; Vasili et al., 2019). Furthermore, several studies have also indicated an important synaptic dysfunction as one of the pathogenic mechanisms in PD, particularly in the early stages of the disease (Abeliovich and Gitler, 2016; Bagetta et al., 2010; Burke and O'Malley, 2014; Schirinzi et al., 2016).

Overall, the functional enrichment results for the multi-*omics* experiments presented above showed several processes of importance in the context of PD, validating known pathways and providing evidence for the involvement of previously less-regarded pathomechanisms involved in PD (e.g. inflammatory responses). Efforts into integrating the results across the *omics* studies guided the subsequent experiments of this project and are presented below.

4.6 Multi-*omics* integration identifies common pathways in matched datasets

4.6.1 Integration of small RNA and transcriptomics

In order to explore pathways of deregulation within the multi-*omics* studies presented here, a step-wise integration of the datasets was performed using the DE results for each of the techniques (miRNAomics, transcriptomics and proteomics). First, the integration of the small RNA and transcriptomics data was performed. After a computational target prediction for the DE miRNAs, both a bioinformatical tool (RRHO)(Plaisier et al., 2010) and a manual cross-correlation were performed in parallel for the identification of overlapping candidates. The discordant overlap between the two lists was retrieved in order to extract the valid miRNA-mRNA interacting pairs. The list of overlapping candidates contained potential pairs that would support hypotheses of miRNA regulation of gene expression in the samples (up-regulated miRNAs were considered for the retrieval of the respective down-regulated targets mRNA, and vice-versa). The RRHO algorithm was less stringent in the overlap retrieval since it used the full sequencing results including very lowly expressed transcripts and miRNAs that were manually disregarded for downstream analyses. Therefore, the number of transcripts and miRNAs identified there was much higher than in the manual cross-correlation (that considered cut-offs for fold change in expression and a minimum number of reads). Nevertheless, when comparing the results from both approaches, a big overlap is observed, with 22 out of the 23 DE transcripts found with the manual approach being also present in the RRHO output results. Therefore, the manual method was considered as a refinement of the automated bioinformatical approach. A final list of 22 transcripts and 9 miRNAs was thus considered for further steps (Figure 15B). Finally, in order to select the most relevant interacting pairs, the candidates were filtered according to the highest probability of conserved targeting (Friedman et al., 2008). With that, twelve out of the 22 retrieved transcripts and all of the 9 miRNAs potentially regulating them were selected for validation of the sequencing results. The selected mRNAs included *DHX57, RNF170, TMEM178B, BRWD1, ENTPD5, C7orf73, SOCS4, STEAP3, MIER2, FOXF1, RIMS1 and PPTC7.* For the miRNAs, the selected candidates were the following: *let-7i-5p; miR-26a-5p; miR-2018-5p; miR-424-5p; miR-29c-3p; let-7g-5p; miR-20a-5p; miR-145-5p and miR-98-5p*.

The relevance of several of the selected miRNAs in processes as neurodegeneration, neuroinflammation and PD pathology was discussed in sections 4.2 and 4.3. For the selected DE transcripts, several of them have been studied in the context of neurodegenerative diseases. For example, SOCS4 (Suppressor of cytokine signaling 4), found in increased levels in PD in the transcriptomics results, is known to be involved in both JAK-STAT and PTEN-mTOR signaling pathways, influencing processes that include cell growth, apoptosis, survival, neuroinflammation and neurodegeneration (Nicolas et al., 2013; Park et al., 2004, 2008, 2009; Sekine et al., 2018). In addition, an important study showed that deleting a protein of the same family of SOCS4 (SOCS3) promoted regeneration in optic nerve neurons in vivo (Smith et al., 2009). All members of the SOCS family share a central *Src homology 2* (SH2) domain, as well as an extended SH2 domain and a C-terminal SOCS box (Palmer and Restifo, 2009). Interestingly, the triplet composed by SOCS3/SOCS4/SOCS5 is reported to have a marked pair-wise homology (Duncan et al., 2017), indicating the importance of these findings for in the context of neurode- and regeneration. Another important candidate is RNF170 (Ring finger protein 170), known to be involved in protein ubiquitination/degradation (Claessen et al., 2012; Nakamura, 2011). RNF170 seems to be especially important for the metabolism of inositol-1,4,5-triphosphate (IP3), and might thereby play a role in regulating autophagy-related mechanisms, a mechanism that plays an important role in PD pathology due to its involvement in protein and aggregate degradation (Anglade et al., 1997; Lu et al., 2011; Sarkar and Rubinsztein, 2006; Williams et al., 2008; Winslow and Rubinsztein, 2011). Moreover, a study showed that a point mutation in the RNF170 gene is responsible for autosomal cases of sensory ataxia by impairing IP3-mediated Ca^{2+} signaling (Wright et al., 2015). The protein STEAP3 (Six-Transmembrane Epithelial Antigen Of Prostate 3), a metalloreductase, also figures as an interesting candidate among the selected transcripts. It has been implicated in processes that include apoptosis and survival, and also in the regulation of inflammatory responses (Grunewald et al., 2012; Passer et al., 2003; Zhang et al., 2012). It has also shown robust pro-amyloidogenic properties in vitro, suggesting that it might influence protein aggregation also in PD (Roberts et al., 2017). Interestingly, STEAP3 is involved in iron homeostasis (Lambe et al., 2009) and can also regulate copper metabolism (Ohgami et al., 2006). Both elements are known to play an important role in PD and have also been object of study in previous projects of our lab (Javier Jiménez-Jiménez et al., 1992; Joppe et al.,

2019; Maass et al., 2018; Montes et al., 2014). The final list of selected candidates (portrayed in Figure 15) was considered for the q-RT-PCR validation of the sequencing studies. The relevance of all validated candidates is further discussed in the subsequent sections.

4.6.2 Integration of and transcriptomics and proteomics

Similar to what was done with the small RNA and transcriptomics datasets, the overlapping DE results for transcriptomics and proteomics experiments were also explored in an integrative fashion. In this case, we looked for the concordant overlap between the coding mRNAs and their respective protein product (i.e. up- and down-regulated transcript-protein pairs). Factors related to protein metabolism and kinetics (e.g., synthesis and degradation rates of proteins) were out of the scope of this study and were therefore not considered for the integrative analyses presented here, although they are likely to significantly contribute to the overall picture.

Proteomics and RNA sequencing results are fundamentally very different, starting by the nature of the signals and the coverage of those techniques. That makes the comparison of quantitative values (in this case, counts and intensities) by bioinformatical pipelines rather challenging. Therefore, we decided to apply a manual cross-correlation method for the integration, similarly to what was done for the manual integration of the miRNA and transcriptomics data. The much smaller range of DE proteins (127) was also favorable for the employment of such an approach. As presented in section 3.11.2, the total number of uniquely identified proteins was more than 20 times smaller than the number of mapped transcripts. Therefore, several of the DE transcripts found in the RNA sequencing results did not have their respective protein product identified in the proteomics results. The opposite also happened, to a lesser extent. Overall, disregarding the validity of the interaction pairs (i.e. the directionality of the fold changes in expression) the integrative approaches applied here revealed that 30 candidates were found significantly regulated in both transcriptomics and proteomics experiments (around 24% of all the proteomics DE results). When considering the valid pairs with concordant fold change in expression in both datasets, a final list of 13 candidates was retrieved from the

integration of the transcriptomics and proteomics datasets. Seven of them presented up-regulation in the PD samples (*ATP6V1E1, C9ORF47, CD47, ACOT7, RPL35, SEC23A and RPN1)* while six candidates were found down-regulated in PD, both in transcriptomics and proteomics (TH, DBT, CD200, RAB18, NIPSNAP3A UBE2L3). It is important to mention that the final list of candidates selected from the integration of transcriptomics and proteomics is currently being validated by Western Blotting and the results will not figure in the scope of this thesis. As discussed in sections 4.4 and 4.5, the presence of the dopamine marker TH among the down-regulated candidates in both datasets, as well as the present of coincidentally enriched pathways throughout the *omics* datasets (e.g. inflammatory response, metabolism- and apoptosis-related processes) provide additional reliability to the functional annotation presented for each approach.

4.7. Validation of sequencing results in human midbrain tissue by q-RT-PCR

4.7.1. miRNA data validation

After integration and the final miRNA candidate selection (section 3.11.1), nine miRNAs were validated in the human midbrain tissue (upon fresh RNA isolation and reverse transcription for cDNA preparation). For the miRNAs found down-regulated in PD by sequencing experiments, all selected candidates (let-7g-5p, miR-20a-5p, miR-145-5p, miR-98-5p) were successfully validated by q-RT-PCR, presenting the same expression directionality as observed in the sequencing. For the miRNAs found up-regulated in PD by small RNA sequencing, 2 out of 5 (let-7i and miR-29c) presented significant differences in the validation studies with a regulation in the opposite direction compared to what was observed in the sequencing. Similar findings with an opposing regulation of one and the same target from discovery to validation studies have been frequently reported in biomarker studies using PD body fluids (Roser et al., 2018b; Halbgebauer et al., 2016). A number of factors might influence the outcome of validation studies. For example, alternative splicing often leads to discordant results between sequencing and q-RT-PCR experiments (Nazarov et al., 2017). The sensitivity of the two methods might also be an issue. A study reported a sensitivity threshold for the validation of sequencing results by q-RT-PCR. Validation of significantly DE miRNAs identified by Solexa sequencing was not

possible for species presenting very low sequencing reads (<100 reads per species) (Cristino et al., 2011). In addition, the design of different commercially available primers and the number of amplified exons might also interfere with the validation of candidates identified by the sequencing. The opposing results presented here could be further explored by repeating the experiments with additional primers for the selected candidates, for example. Overall, the results showed that four out of the nine selected miRNA candidates were successfully validated by q-RT-PCR and concordant to the small RNA sequencing data.

An overview of the biological relevance of all DE miRNAs is presented in section 4.4. For the validated miRNAs (let-7g-5p, miR-20a-5p, miR-145-5p, miR-98-5p), several of them have been implicated in neuronal- and neurodegeneration-related processes. A comprehensive study showed that let-7g-5p is among the top 40 highly expressed miRNA found in human brains (Shao et al., 2010). Deregulation of let-7g-5p has been also linked to neurodegenerative diseases. For instance, this miRNA has been included in a plasma biomarker panel of signature miRNAs able to distinguish AD patients from controls with high accuracy (Kumar et al., 2013). It has been also found significantly down-regulated in peripheral blood of Amyotrophic Lateral Sclerosis (ALS) patients (Liguori et al., 2018). Let-7g-5p has also been shown be deregulated in PD models of αSyn overexpression (Asikainen et al., 2010), and the complementary strand of this miRNA, let-7g-3p, has been found differentially expressed in PD CSF (Gui et al., 2015a). Similarly, miR-20a-5p has been found in altered levels in both AD CSF and PD cortical brain regions (Chatterjee and Roy, 2017; Riancho et al., 2017). This miRNA is known to regulate neuronal differentiation (Cui et al., 2016). Another of the validated miRNAs, miR-98-5p, has been extensively linked to AD. It has been shown to regulate amyloid β-peptide (Aβ) protein production (Li et al., 2016) and has been found in decreased levels in AD serum (Tan et al., 2014). Finally, miR-145-5p has been implicated in a variety of neuronal-related processes. For example, it is known to play a role in neuronal differentiation as well as to induce glial inflammatory insults (Jauhari et al., 2018; Li et al., 2013b). Remarkably, miR-145-5p is known to regulate, for example, microglia activation and astrocyte injury in models of cerebral stroke (Qi et al., 2017; Xie et al., 2017; Zheng et al., 2017), matching the intense inflammatory and immune response activation observed in our PD samples. Our findings provide more robust evidence for the

validated miRNA candidates as important regulators in neurodegenerative processes taking place in PD.

4.7.2. Transcriptomics data validation

Similarly, the mRNA candidates selected by the integration of miRNA and transcriptomics datasets (section 3.11.1) were validated by q-RT-PCR in the midbrain samples of PD and controls studied here. Seven of the selected candidates were found in up-regulated levels in PD by the RNA sequencing results. Out of these, four mRNAs were successfully validated and presented the same pattern of regulation in the validation experiments. These were SOCS4, STEAP3, MIER2 and FOXF1. The relevance of the first two for PD pathology has been extensively discussed in section 4.6.1. MIER2 (Mesoderm induction early response protein 2) is a chromatin-binding transcript and is involved in histone deacetylation (Derwish et al., 2017), a process extensively linked to the development of neurodegenerative disorders as AD and PD (Abel and Zukin, 2008; Chuang et al., 2009; Fischer, 2014; Harrison and Dexter, 2013; Sharma and Taliyan, 2015; Stilling and Fischer, 2011). FOXF1 (Forkhead box protein F1) is an important transcription factor regulating embryonic development and is reported to play a role in dopaminergic differentiation through interaction with sonic hedgehog (SHH) (Peterson and Turnbull, 2012; Wu et al., 2012).

On the other hand, for the transcripts found down-regulated in PD by RNA sequencing experiments, none of the selected candidates presented significant differences in relative expression levels in the q-RT-PCR validation results. Nevertheless, all transcripts presented, on average, lower expression levels in PD samples when compared to controls. The same effect was observed several times both for the mRNA and the miRNA validation experiments. One plausible possibility is that the limited cohort size might influence the statistical power of the experiments presented here, being a technical limitation for the validation of the sequencing results. As discussed above (section 4.7.1), it is also worth mentioning that the different methods employed for discovery and subsequent validation of transcripts and miRNAs present obvious differences in sensitivity, what could account for the divergent findings presented here. Several factors are reported to influence validation outcomes, including alternative splicing, sensitivity limitations for the validation

of candidates presenting a low number of sequencing reads, primer design and differences in exonal region amplification might influence the outcome of validation studies (Cristino et al., 2011; Nazarov et al., 2017). Thus, similar to the miRNA validation, the transcriptomics validation results could also be further explored by repeating q-RT-PCR experiments with additional primers for the selected transcripts.

In conclusion, a substantial number of the selected miRNA and mRNA candidates found DE in RNA sequencing experiments were successfully validated by q-RT-PCR. A number of the candidates also presented similar tendency for the expression levels in the validation studies in comparison to the sequencing results, but the results were not statistically significant - likely because of the aforementioned technical limitations of the methods employed here. Nevertheless, the patterns of the relative expression levels determined by q-RT-PCR were similar to the ones found in RNA sequencing experiments for the majority of the selected species. Interestingly, there was a good match for the validated miRNA-mRNA interacting pairs: down-regulated miRNAs in PD were successfully validated, and PD up-regulated transcripts – known targets of the validated miRNAs – were also validated by q-RT-PCR. The valid interaction pairs validated here were the following: let-7g-5p/SOCS4; let-7g-5p/STEAP3; miR-20a-5p/MIER2; miR-20a-5p/FOXF1. Those findings indicate that these candidates are likely to play an important mechanistic role in the pathology presented by the affected patients. Further validation studies (e.g. immunoblotting) will be conducted with these and the additional candidates identified in integrative approaches.

4.8. Validation of PD-deregulated miRNAs and transcripts in αSyn.A53T midbrains

To complement our studies of human tissue, we compared the miRNA and mRNA expression results obtained in human midbrains with corresponding results from a transgenic mouse model of PD. For that, male mice overexpressing human αSyn containing the A53T mutation under the prnp promoter were employed. This mouse model reproduces a genetic (autosomal-dominant) form of PD, but it also resembles features of the idiopathic form of the disease, such as αSyn aggregation: Studies showed that the mutant forms seem to be more prone to aggregate in comparison the wild-type forms

(Conway et al., 1998; Dauer and Przedborski, 2003a; Krüger et al., 1998). Thus, the αSyn.A53T mouse model is considered a useful tool to study synucleinopathies as PD. The transgenic mice develop a progressive and severe motor phenotype starting around 8 months of age. The appearance of αSyn aggregate inclusions matches the onset of the motor impairments (Giasson et al., 2002). Here, we evaluated the expression levels of the human validated miRNAs and transcripts in different stages of the pathology presented by the transgenic mice. In summary, the aim of the animal experiments presented here was to verify whether the alterations observed in the human midbrain tissue correlate with the patterns found in the same cerebral region in the mouse model. Details about cohort design and experimental setups are described in sections 2.2.2.1 and 3.14.

The miRNA validation in αSyn.A53T mice midbrains revealed that no significant alterations are observed in miRNA levels in early time points, indicating that deregulation of miRNA expression is likely linked to the development of the progressive motor phenotype presented in later stages. At an intermediate time point, the levels of two miRNAs are found significantly deregulated in the transgenic condition in comparison to control animals. miR-20a-5p is found down-regulated in transgenic animals – in line with the human findings - while miR-145-5p is up-regulated in those individuals, inversely to the expression presented in PD-affected human midbrains. At late stages of the αSyn pathology in the mice, the results seem to be more variable within the subjects of individual cohorts, potentially denoting a misbalance in the miRNA machinery in older animals. Another miRNA, miR-98-5p, presented significant changes in relative expression, being down-regulated in the transgenic animal, also in line with the human results.

For the mRNA validation, not only the human validated transcripts were considered for q-RT-PCR experiments, but an extended candidate selection was conducted (section 3.14.2). In order to explore possible correlations in further pathological features presented by the transgenic mice in relation to the PD pathology in humans, a set of PD-related genes was also selected for validation experiments. The cut-off criterion for further-selected genes was that candidates must be significantly regulated in the human transcriptomics results. Classical genes previously described to be involved in PD pathogenesis and progression were retrieved from a comprehensive review (Kalia and Lang, 2015). In addition, we considered the largest genomic-wide association study in PD (which included

the analysis of 7.8 million SNPs in dozens of thousands of PD cases / over a million control cases) (Nalls et al., 2018). In the end, a total of 9 transcripts were additionally selected for the validation by q-RT-PCR.

The mRNA validation results showed that most of the analyzed transcripts presented changes in relative expression at early and intermediate ages, suggesting that, at the transcriptomic level, pathological mechanisms related to the motor phenotype might start taking place very early in the course of the lifespan of these animals. No differences were observed for any of the genes at late time points, indicating that not only the pathology but also aging *per se* might cause changes in the expression level of the evaluated genes in control animals. Only one gene, MIER2 (extensively discussed above), presented significant differences discordant to the human results, being down-regulated in the transgenic animals at intermediate ages. For all the other genes presenting significant altered relative expression levels, the results were concordant with the human findings for the validated targets. Genes as SOCS4, HSPA1, PINK1, GALC, POLG1, RIMS1, DYRK1a and SQSTM1 presented elevation in relative expression levels in the transgenic animals either at 100 days of age or at 250 days of age (or for both in the case of PINK1 and DYRK1a. As discussed in previous sections, SOCS4 is involved in processes that include cell growth, apoptosis and survival, neuroinflammation and neurodegeneration, thus, showing to be relevant for the pathology and progression of PD (Nicolas et al., 2013; Park et al., 2004, 2008, 2009; Sekine et al., 2018). HSPA1 is a member of the heat shock proteins and plays an important role in protein folding and degradation and is also linked to neuronal apoptosis (Leak, 2014; Mayer and Bukau, 2005). Another gene related to protein degradation is SQSTM1, important for the formation of autophagosomes and ubiquitin-related protein degradation (Bjørkøy et al., 2005; Clausen et al., 2010; Isakson et al., 2013; Taillebourg et al., 2012). Defects in protein degradation are known to be important in the context of αSyn aggregation, LB formation and for PD pathology in general, indicating that these players might be relevant for the pathology related to the αSyn.A53T mutation.

Furthermore, PINK1 is a classical PD gene and encodes a protein kinase important for mitochondrial function and energy metabolism, for example. PINK1 mutations are known to cause early-onset PD cases (Dagda et al., 2014; Lazarou et al., 2013; Narendra et al., 2010; Truban et al., 2017). Interestingly, PINK1 is one of the genes presenting up-

regulation in the transgenic mice midbrains both at early and intermediate stages, indicating that mitochondrial dysfunction might be one of the pathomechanisms caused by the synucleinopathy presented by the animals. DYRK1a also presented elevated relative expression levels both at early and intermediate stages in transgenic animals. DYRK1a is known to interact with αSyn and enhance the intracellular formation of inclusions (Kim et al., 2006; Wegiel et al., 2011). It is also known to influence the survival of dopaminergic neurons upon development (Barallobre et al., 2014) and DYRK1a polymorphisms have been associated with the development of sporadic PD (Cen et al., 2016). Thus, our findings suggest that DYRK1a might play an important role in the development of the synucleinopathy in transgenic mice.

Some studies linked defects in POLG1 to PD predisposition and progression (Gui et al., 2015a; Luoma et al., 2007). Moreover, a VUS in the POLG gene was even identified for one of the PD patients analyzed here. The results presented here provide an additional indication that POLG1 might indeed play a role in the neurodegenerative processes in PD. Another transcript found deregulated in αSyn.A53T midbrains was RIMS1, a member of the Ras superfamily and regulator of GTPase activity. GTPase activity is very relevant for axonal degeneration and PD progression (Koch et al., 2014, 2018; Tatenhorst et al., 2014; Tönges et al., 2011, 2012). RIMS1 is also important for regulation of neurotransmitter release (Coppola et al., 2001; Ohtsuka et al., 2002; Takao-Rikitsu et al., 2004), and the deregulation in the affected midbrains might be related to the dopaminergic dysfunction present in the PD-like pathology. Finally, GALC was also found in elevated levels in the transgenic animals at the early time point. GALC is an enzyme responsible for the lysosomal catabolism of myelin-containing lipids. Interestingly, alterations in myelination have already been reported in PD (Dean et al., 2016; Gattellaro et al., 2009).

In conclusion, the findings presented here for the miRNA/mRNA validation in the midbrain of αSyn.A53T mice indicate that a substantial number of pathological processes are overlapping between the PD animal model and the pathology in humans. To a certain extent, our longitudinal study with the αSyn.A53T animals yielded insights to the pathology presented by the transgenic animals upon aging and indicated a satisfactory validity of the model in regard to the miRNA/mRNA expression patterns observed in PD-affected midbrains. It is important to point out that in spite of several significant findings, the

conducted validation study presented limited cohort numbers and strong outlier values have been excluded from the analysis, decreasing the statistical power of the analyses. Several of the analyzed transcripts/miRNAs presented a high intra-cohort relative expression variability, which could possibly be ameliorated with the inclusion of more animals. Additional animals were sacrificed by the time of the experiment execution, and the repetition of the presented experiments in bigger cohorts would provide stronger evidence to the aforementioned findings.

5. Concluding remarks

The experiments conducted in the course of this doctoral thesis demonstrated that the use of high-throughput *omics* techniques allows the generation of comprehensive datasets for the exploration of molecular pathomechanisms of complex diseases, such as neurodegenerative disorders. Exploring the molecular events taking place in PD-affected brains is fundamental for better understanding the pathogenesis and progression of the disease and for the development of novel therapeutic avenues for PD. Nevertheless, results from post-mortem analyses always have to be put into context of an advanced disease stage.

Here, several levels of deregulation were identified across multi-*omics* datasets in human midbrains affected by PD. Important players and molecular networks that seem to be relevant for advanced stages of PD pathology were revealed: we showed that a marked inflammation and immune response activation takes place in the analyzed midbrains, in addition to defects in protein degradation and metabolic dysfunctions. Our data thus strongly suggest that neuroinflammation may be a veritable therapeutic target, at least in advanced stages of the disease.

Furthermore, we have been especially interested in the miRNA regulation of gene expression in PD. We identified and validated four miRNAs (let-7g-5p, miR-20a-5p, miR-145-5p, miR-98-5p) in postmortem PD midbrains that have been previously linked to neurodegenerative / neuroinflammatory processes, providing additional evidence for the importance of these targets in the context of PD pathology. Furthermore, our multi-*omics* analyses allowed not only the profiling of miRNA expression patterns but also to verify the expression of miRNA direct targets and their protein products, providing insightful evidence for the participation of miRNAs in the neurodegenerative processes linked to the disease. Remarkably, miRNA-mRNA interacting pairs were identified and validated in the present samples (let-7g-5p/SOCS4; let-7g-5p/STEAP3; miR-20a-5p/MIER2; miR-20a-5p/FOXF1). These pairs are likely to play an important mechanistic role in the pathology presented by the affected patients and will be further explored.

All in all, our approaches also evidence that efforts into optimizing the integration of large scale high-throughput datasets are absolutely required for the meaningful treatment and exploration of the data.

Another important aspect shown here is that PD patients present a high inter-individual variability for the expression of all types of molecular elements analyzed in our study, suggesting that patients with similar clinical phenotypes may have different molecular phenotypes. Moreover, our results also provided additional evidence for known pathomechanisms in PD (such as the aforementioned inflammatory changes, oxidative stress and metabolic dysfunctions). miRNAs possibly mediating these alterations were identified in our study and should be further validated in larger human cohorts as well as in animal models as therapeutic targets. Therefore, our findings might contribute to the exploration of novel disease-modifying avenues, which may increase the chances of attenuating disease progression.

Finally, we have also assessed the validity of the prnp. αSyn.A53T mouse model of PD in terms of the overlap in miRNA and mRNA expression with human pathology. A number of correlating results were identified in our longitudinal animal study, providing insight into the time course of pathological changes in the animal brains upon aging that are similar to the ones occurring in human PD patients.

All in all, the findings presented in this thesis yielded new insight in the pathomechanisms involved in PD, may contribute to the development of novel experimental PD models based on miRNA regulation and could establish promising new therapeutic targets for future studies.

6. Summary

Parkinson's Disease (PD) is the second most prevalent and fastest-growing neurological disorder. The number of affected individuals is expected to double in the next 20 years. The exact molecular mechanisms underlying PD pathology are not completely understood. In addition, its diagnosis mainly relies on clinical criteria related to the characteristic motor dysfunction in PD. Since the symptoms only start to appear at advanced stages of the nigrostriatal degeneration characteristic in PD, there is a strong limitation for the promotion of therapeutic strategies that might be able to change the course of the disease. Allied to that, the limited regenerative capabilities of cells in the CNS complicate the development of restorative treatments. Therefore, understanding the key pathogenetic mechanisms of PD is fundamental for the the development of disease-modifying therapies. Profiling the expression of molecular element such as miRNAs, transcripts and proteins in brains affected by PD might reveal a series of pathological events taking place both at cellular and systemic levels in the course of the disease.

The present doctoral thesis aimed to analyze midbrain tissue samples from a cohort of PD patients and controls in a multi-*omics* set of experiments, looking into the genetic background of the selected subjects, as well as characterizing the expression patterns of miRNAs, transcripts and proteins on those samples. Here, several levels of deregulation were identified across multi-*omics* datasets in human midbrains affected by PD. Important players and molecular networks that seem to be relevant for advanced stages of PD pathology were revealed: we showed that a marked inflammation and immune response activation takes place in the analyzed midbrains, in addition to defects in protein degradation and metabolic dysfunctions. Our data thus strongly suggest that neuroinflammation may be a veritable therapeutic target, at least in advanced stages of the disease. In addition, we identified not only deregulated transcripts and proteins linked with pathological processes, but also miRNAs that might be involved in the pathophysiology of the disease. Finally, we have also assessed the validity of the prnp. αSyn.A53T mouse model of PD in terms of the overlap in miRNA and mRNA expression with human pathology. A number of correlating results were identified in our longitudinal animal study, providing insight into the time course of pathological changes in the animal brains upon aging that are similar to the ones occurring in human PD patients.

7. References

Abel, T., and Zukin, R. (2008). Epigenetic targets of HDAC inhibition in neurodegenerative and psychiatric disorders. Current Opinion in Pharmacology *8*, 57–64.

Abeliovich, A., and Gitler, A.D. (2016). Defects in trafficking bridge Parkinson's disease pathology and genetics. Nature *539*, 207–216.

Agarwal, V., Bell, G.W., Nam, J.-W., and Bartel, D.P. (2015). Predicting effective microRNA target sites in mammalian mRNAs. ELife *4*, e05005.

Agid, Y. (1987). Biochemistry of neurotransmitters in Parkinson's disease. Movement Disorders 166–230.

Agid, Y. (1991). Parkinson's disease: pathophysiology. The Lancet *337*, 1321–1324.

Alafuzoff, I., Ince, P.G., Arzberger, T., Al-Sarraj, S., Bell, J., Bodi, I., Bogdanovic, N., Bugiani, O., Ferrer, I., Gelpi, E., et al. (2009). Staging/typing of Lewy body related α-synuclein pathology: a study of the BrainNet Europe Consortium. Acta Neuropathol *117*, 635–652.

Allen, M. (2015). Compelled by the Diagram: Thinking through C. H. Waddington's Epigenetic Landscape. Contemporaneity: Historical Presence in Visual Culture *4*, 119.

Anandhan, A., Jacome, M.S., Lei, S., Hernandez-Franco, P., Pappa, A., Panayiotidis, M.I., Powers, R., and Franco, R. (2017). Metabolic Dysfunction in Parkinson's Disease: Bioenergetics, Redox Homeostasis and Central Carbon Metabolism. Brain Research Bulletin *133*, 12–30.

Anders, S., and Huber, W. (2010). Differential expression analysis for sequence count data. Genome Biol *11*, R106.

Anders, S., Pyl, P.T., and Huber, W. (2015). HTSeq--a Python framework to work with high-throughput sequencing data. Bioinformatics *31*, 166–169.

Andrews, S., Krueger, F., Segonds-Pichon, A., Biggins, L., Krueger, C., and Wingett, S. (2010). FastQC. A quality control tool for high throughput sequence data. (Babraham, UK).

Anglade, P., Vyas, S., Javoy-Agid, F., Herrero, M.T., Michel, P.P., Marquez, J., Mouatt-Prigent, A., Ruberg, M., Hirsch, E.C., and Agid, Y. (1997). Apoptosis and autophagy in nigral neurons of patients with Parkinson's disease. Histol. Histopathol. *12*, 25–31.

Asikainen, S., Rudgalvyte, M., Heikkinen, L., Louhiranta, K., Lakso, M., Wong, G., and Nass, R. (2010). Global microRNA Expression Profiling of Caenorhabditis elegans Parkinson's Disease Models. J Mol Neurosci *41*, 210–218.

Atanassov, I., and Urlaub, H. (2013). Increased proteome coverage by combining PAGE and peptide isoelectric focusing: comparative study of gel-based separation approaches. Proteomics *13*, 2947–2955.

References

Babicki, S., Arndt, D., Marcu, A., Liang, Y., Grant, J.R., Maciejewski, A., and Wishart, D.S. (2016). Heatmapper: web-enabled heat mapping for all. Nucleic Acids Res *44*, W147–W153.

Baek, D., Villén, J., Shin, C., Camargo, F.D., Gygi, S.P., and Bartel, D.P. (2008). The impact of microRNAs on protein output. Nature *455*, 64–71.

Bagetta, V., Ghiglieri, V., Sgobio, C., Calabresi, P., and Picconi, B. (2010). Synaptic dysfunction in Parkinson's disease: Figure 1. Biochm. Soc. Trans. *38*, 493–497.

Bai, B., Hales, C.M., Chen, P.-C., Gozal, Y., Dammer, E.B., Fritz, J.J., Wang, X., Xia, Q., Duong, D.M., Street, C., et al. (2013). U1 small nuclear ribonucleoprotein complex and RNA splicing alterations in Alzheimer's disease. Proceedings of the National Academy of Sciences *110*, 16562–16567.

Balistreri, C.R., Candore, G., Accardi, G., Colonna-Romano, G., and Lio, D. (2013). NF-κB pathway activators as potential ageing biomarkers: targets for new therapeutic strategies. Immun Ageing *10*, 24.

Barallobre, M.J., Perier, C., Bové, J., Laguna, A., Delabar, J.M., Vila, M., and Arbonés, M.L. (2014). DYRK1A promotes dopaminergic neuron survival in the developing brain and in a mouse model of Parkinson's disease. Cell Death Dis *5*, e1289–e1289.

Bar-Am, O., Amit, T., Kupershmidt, L., Aluf, Y., Mechlovich, D., Kabha, H., Danovitch, L., Zurawski, V.R., Youdim, M.B.H., and Weinreb, O. (2015). Neuroprotective and neurorestorative activities of a novel iron chelator-brain selective monoamine oxidase-A/monoamine oxidase-B inhibitor in animal models of Parkinson's disease and aging. Neurobiology of Aging *36*, 1529–1542.

Barcia, C., Fernández Barreiro, A., Poza, M., and Herrero, M.-T. (2003). Parkinson's disease and inflammatory changes. Neurotox Res *5*, 411–418.

Barcia, C., Ros, C.M., Annese, V., Carrillo-de Sauvage, M.A., Ros-Bernal, F., Gómez, A., Yuste, J.E., Campuzano, C.M., de Pablos, V., Fernandez-Villalba, E., et al. (2012). ROCK/Cdc42-mediated microglial motility and gliapse formation lead to phagocytosis of degenerating dopaminergic neurons in vivo. Sci Rep *2*, 809.

Bartel, D.P. (2004). MicroRNAs. Cell *116*, 281–297.

Basak, I., Patil, K.S., Alves, G., Larsen, J.P., and Møller, S.G. (2016). microRNAs as neuroregulators, biomarkers and therapeutic agents in neurodegenerative diseases. Cell. Mol. Life Sci. *73*, 811–827.

Batistela, M.S., Josviak, N.D., Sulzbach, C.D., and de Souza, R.L.R. (2017). An overview of circulating cell-free microRNAs as putative biomarkers in Alzheimer's and Parkinson's Diseases. International Journal of Neuroscience *127*, 547–558.

Bendor, J.T., Logan, T.P., and Edwards, R.H. (2013). The Function of α-Synuclein. Neuron *79*, 1044–1066.

Berezikov, E., Cuppen, E., and Plasterk, R.H.A. (2006). Approaches to microRNA discovery. Nat Genet *38*, S2–S7.

Bird, A. (2007). Perceptions of epigenetics. Nature *447*, 396–398.

References

Bjørkøy, G., Lamark, T., Brech, A., Outzen, H., Perander, M., Øvervatn, A., Stenmark, H., and Johansen, T. (2005). p62/SQSTM1 forms protein aggregates degraded by autophagy and has a protective effect on huntingtin-induced cell death. J Cell Biol *171*, 603–614.

Bose, A., and Beal, M.F. (2016). Mitochondrial dysfunction in Parkinson's disease. J. Neurochem. *139*, 216–231.

Braak, H., Del Tredici, K., Rüb, U., De Vos, R. a I., Jansen Steur, E.N.H., and Braak, E. (2003). Staging of brain pathology related to sporadic Parkinson's disease. Neurobiology of Aging *24*, 197–211.

Bredesen, D.E., Rao, R.V., and Mehlen, P. (2006). Cell death in the nervous system. Nature *443*, 796–802.

Brochard, V., Combadière, B., Prigent, A., Laouar, Y., Perrin, A., Beray-Berthat, V., Bonduelle, O., Alvarez-Fischer, D., Callebert, J., Launay, J.-M., et al. (2008). Infiltration of CD4+ lymphocytes into the brain contributes to neurodegeneration in a mouse model of Parkinson disease. J. Clin. Invest. JCI36470.

Burke, R.E., and O'Malley, K. (2014). Axon Degeneration in Parkinson ' s Disease. 72–83.

Bustelo, X.R., Sauzeau, V., and Berenjeno, I.M. (2007). GTP-binding proteins of the Rho/Rac family: regulation, effectors and functions in vivo. Bioessays *29*, 356–370.

Caggiu, E., Paulus, K., Mameli, G., Arru, G., Sechi, G.P., and Sechi, L.A. (2018). Differential expression of miRNA 155 and miRNA 146a in Parkinson's disease patients. ENeurologicalSci *13*, 1–4.

Calabresi, P., Picconi, B., Tozzi, A., Ghiglieri, V., and Di Filippo, M. (2014). Direct and indirect pathways of basal ganglia: a critical reappraisal. Nat Neurosci *17*, 1022–1030.

Cardoso, A.L., Guedes, J.R., Pereira de Almeida, L., and Pedroso de Lima, M.C. (2012). miR-155 modulates microglia-mediated immune response by down-regulating SOCS-1 and promoting cytokine and nitric oxide production: miR-155 role during microglia activation. Immunology *135*, 73–88.

Cargnello, M., and Roux, P.P. (2011). Activation and Function of the MAPKs and Their Substrates, the MAPK-Activated Protein Kinases. Microbiology and Molecular Biology Reviews *75*, 50–83.

Castaño, A., Herrera, A.J., Cano, J., and Machado, A. (2002). Lipopolysaccharide Intranigral Injection Induces Inflammatory Reaction and Damage in Nigrostriatal Dopaminergic System. Journal of Neurochemistry *70*, 1584–1592.

Cen, L., Xiao, Y., Wei, L., Mo, M., Chen, X., Li, S., Yang, X., Huang, Q., Qu, S., Pei, Z., et al. (2016). Association of DYRK1A polymorphisms with sporadic Parkinson's disease in Chinese Han population. Neuroscience Letters *632*, 39–43.

Chakrabarty, P., Ceballos-Diaz, C., Lin, W.-L., Beccard, A., Jansen-West, K., McFarland, N.R., Janus, C., Dickson, D., Das, P., and Golde, T.E. (2011). Interferon-γ induces progressive nigrostriatal degeneration and basal ganglia calcification. Nat Neurosci *14*, 694–696.

Chatterjee, P., and Roy, D. (2017). Comparative analysis of RNA-Seq data from brain and blood samples of Parkinson's disease. Biochemical and Biophysical Research Communications *484*, 557–564.

Chen, W., and Qin, C. (2015). General hallmarks of microRNAs in brain evolution and development. RNA Biology *12*, 701–708.

Chen, S., Le, W.D., Xie, W.J., Alexianu, M.E., Engelhardt, J.I., Siklós, L., and Appel, S.H. (1998). Experimental Destruction of Substantia Nigra Initiated by Parkinson Disease Immunoglobulins. Arch Neurol *55*, 1075.

Chendrimada, T.P., Gregory, R.I., Kumaraswamy, E., Norman, J., Cooch, N., Nishikura, K., and Shiekhattar, R. (2005). TRBP recruits the Dicer complex to Ago2 for microRNA processing and gene silencing. Nature *436*, 740–744.

Cheng, J., Lu, Q., Song, L., and Ho, M.S. (2018). **α** -Synuclein Trafficking in Parkinson's Disease: Insights From Fly and Mouse Models. ASN Neuro *10*, 175909141881258.

Chi, J., Xie, Q., Jia, J., Liu, X., Sun, J., Deng, Y., and Yi, L. (2018). Integrated Analysis and Identification of Novel Biomarkers in Parkinson's Disease. Front. Aging Neurosci. *10*, 178.

Chou, C.-H., Shrestha, S., Yang, C.-D., Chang, N.-W., Lin, Y.-L., Liao, K.-W., Huang, W.-C., Sun, T.-H., Tu, S.-J., Lee, W.-H., et al. (2018). miRTarBase update 2018: a resource for experimentally validated microRNA-target interactions. Nucleic Acids Research *46*, D296–D302.

Chuang, D.-M., Leng, Y., Marinova, Z., Kim, H.-J., and Chiu, C.-T. (2009). Multiple roles of HDAC inhibition in neurodegenerative conditions. Trends in Neurosciences *32*, 591–601.

Claessen, J.H.L., Kundrat, L., and Ploegh, H.L. (2012). Protein quality control in the ER: balancing the ubiquitin checkbook. Trends in Cell Biology *22*, 22–32.

Clarke, C.E., Patel, S., Ives, N., Rick, C., Wheatley, K., and Gray, R. (2011). Should treatment for Parkinson's disease start immediately on diagnosis or delayed until functional disability develops? Mov. Disord. *26*, 1187–1193.

Clausen, T.H., Lamark, T., Isakson, P., Finley, K.D., Larsen, K.B., Brech, A., Øvervatn, A., Stenmark, H., Bjørkøy, G., Simonsen, A., et al. (2010). p62/SQSTM1 and ALFY interact to facilitate the formation of p62 bodies/ALIS and their degradation by autophagy. Autophagy *6*, 330–344.

Conn, K.J., Ullman, M.D., Eisenhauer, P.B., Fine, R.E., and Wells, J.M. (2001). Decreased expression of the NADH:ubiquinone oxidoreductase (complex I) subunit 4 in 1-methyl-4-phenylpyridinium - treated human neuroblastoma SH-SY5Y cells. Neuroscience Letters *306*, 145–148.

Connolly, B.S., and Lang, A.E. (2014). Pharmacological Treatment of Parkinson Disease: A Review. JAMA *311*, 1670.

Conway, K.A., Harper, J.D., and Lansbury, P.T. (1998). Accelerated in vitro fibril formation by a mutant α-synuclein linked to early-onset Parkinson disease. Nat Med *4*, 1318–1320.

Cookson, M.R., Xiromerisiou, G., and Singleton, A. (2005). How genetics research in Parkinson's disease is enhancing understanding of the common idiopathic forms of the disease: Current Opinion in Neurology *18*, 706–711.

Coppola, T., Magnin-Lüthi, S., Perret-Menoud, V., Gattesco, S., Schiavo, G., and Regazzi, R. (2001). Direct Interaction of the Rab3 Effector RIM with Ca $^{2+}$ Channels, SNAP-25, and Synaptotagmin. J. Biol. Chem. *276*, 32756–32762.

Cristino, A.S., Tanaka, E.D., Rubio, M., Piulachs, M.-D., and Belles, X. (2011). Deep Sequencing of Organ- and Stage-Specific microRNAs in the Evolutionarily Basal Insect Blattella germanica (L.) (Dictyoptera, Blattellidae). PLoS ONE *6*, e19350.

Cui, Y., Han, J., Xiao, Z., Chen, T., Wang, B., Chen, B., Liu, S., Han, S., Fang, Y., Wei, J., et al. (2016). The miR-20-Rest-Wnt signaling axis regulates neural progenitor cell differentiation. Sci Rep *6*, 23300.

Dagda, R.K., Pien, I., Wang, R., Zhu, J., Wang, K.Z.Q., Callio, J., Banerjee, T.D., Dagda, R.Y., and Chu, C.T. (2014). Beyond the mitochondrion: cytosolic PINK1 remodels dendrites through Protein Kinase A. J. Neurochem. *128*, 864–877.

Dauer, W., and Przedborski, S. (2003a). Parkinson's Disease: mechanisms and models. Neuron *39*, 889–909.

Dauer, W., and Przedborski, S. (2003b). Parkinson's Disease: mechanisms and models. Neuron *39*, 889–909.

De Guire, V., Robitaille, R., Tétreault, N., Guérin, R., Ménard, C., Bambace, N., and Sapieha, P. (2013). Circulating miRNAs as sensitive and specific biomarkers for the diagnosis and monitoring of human diseases: Promises and challenges. Clinical Biochemistry *46*, 846–860.

De Lau, L., and Breteler, M. (2013). Epidemiology of parkinson's disease. Neurology Asia *18*, 231–238.

De Virgilio, A., Greco, A., Fabbrini, G., Inghilleri, M., Rizzo, M.I., Gallo, A., Conte, M., Rosato, C., Ciniglio Appiani, M., and de Vincentiis, M. (2016). Parkinson's disease: Autoimmunity and neuroinflammation. Autoimmunity Reviews *15*, 1005–1011.

Dean, D.C., Sojkova, J., Hurley, S., Kecskemeti, S., Okonkwo, O., Bendlin, B.B., Theisen, F., Johnson, S.C., Alexander, A.L., and Gallagher, C.L. (2016). Alterations of Myelin Content in Parkinson's Disease: A Cross-Sectional Neuroimaging Study. PLoS ONE *11*, e0163774.

Denk, J., Boelmans, K., Siegismund, C., Lassner, D., Arlt, S., and Jahn, H. (2015). MicroRNA Profiling of CSF Reveals Potential Biomarkers to Detect Alzheimer's Disease. PLoS ONE *10*, e0126423.

Derwish, R., Paterno, G.D., and Gillespie, L.L. (2017). Differential HDAC1 and 2 Recruitment by Members of the MIER Family. PLoS ONE *12*, e0169338.

Desai, B.S., Monahan, A.J., Carvey, P.M., and Hendey, B. (2007). Blood–Brain Barrier Pathology in Alzheimer's and Parkinson's Disease: Implications for Drug Therapy. Cell Transplant *16*, 285–299.

Dev, A., Iyer, S., Razani, B., and Cheng, G. (2010). NF-κB and Innate Immunity. In NF-KB in Health and Disease, M. Karin, ed. (Berlin, Heidelberg: Springer Berlin Heidelberg), pp. 115–143.

Dexter, D.T., and Jenner, P. (2013a). Parkinson disease: from pathology to molecular disease mechanisms. Free Radical Biology and Medicine *62*, 132–144.

Dexter, D.T., and Jenner, P. (2013b). Parkinson disease: from pathology to molecular disease mechanisms. Free Radical Biology & Medicine *62*, 132–144.

Dezsi, L., and Vecsei, L. (2017). Monoamine Oxidase B Inhibitors in Parkinson's Disease. CNSNDDT *16*.

Diner, I., Hales, C.M., Bishof, I., Rabenold, L., Duong, D.M., Yi, H., Laur, O., Gearing, M., Troncoso, J., Thambisetty, M., et al. (2014). Aggregation Properties of the Small Nuclear Ribonucleoprotein U1-70K in Alzheimer Disease. J. Biol. Chem. *289*, 35296–35313.

Dluzen, D.F., Noren Hooten, N., and Evans, M.K. (2017). Extracellular RNA in aging: Extracellular RNA in aging. WIREs RNA *8*, e1385.

Dobin, A., Davis, C.A., Schlesinger, F., Drenkow, J., Zaleski, C., Jha, S., Batut, P., Chaisson, M., and Gingeras, T.R. (2013). STAR: ultrafast universal RNA-seq aligner. Bioinformatics *29*, 15–21.

Dorsey, E.R., and Bloem, B.R. (2018). The Parkinson Pandemic—A Call to Action. JAMA Neurol *75*, 9.

Doxakis, E. (2010). Post-transcriptional Regulation of α-Synuclein Expression by mir-7 and mir-153. J. Biol. Chem. *285*, 12726–12734.

Duncan, S.A., Baganizi, D.R., Sahu, R., Singh, S.R., and Dennis, V.A. (2017). SOCS Proteins as Regulators of Inflammatory Responses Induced by Bacterial Infections: A Review. Front. Microbiol. *8*, 2431.

Eacker, S.M., Dawson, T.M., and Dawson, V.L. (2009). Understanding microRNAs in neurodegeneration. Nat Rev Neurosci *10*, 837–841.

Ebrahimi-Fakhari, D., Saidi, L.-J., and Wahlster, L. (2013). Molecular chaperones and protein folding as therapeutic targets in Parkinson's disease and other synucleinopathies. Acta Neuropathol Commun *1*, 79.

Eitan, C., and Hornstein, E. (2016). Vulnerability of microRNA biogenesis in FTD–ALS. Brain Research *1647*, 105–111.

Elkan-Miller, T., Ulitsky, I., Hertzano, R., Rudnicki, A., Dror, A.A., Lenz, D.R., Elkon, R., Irmler, M., Beckers, J., Shamir, R., et al. (2011). Integration of transcriptomics, proteomics, and microRNA analyses reveals novel microrna regulation of targets in the mammalian inner ear. PLoS ONE *6*, 1–12.

Emde, A., Eitan, C., Liou, L., Libby, R.T., Rivkin, N., Magen, I., Reichenstein, I., Oppenheim, H., Eilam, R., Silvestroni, A., et al. (2015). Dysregulated miRNA biogenesis downstream of cellular stress and ALS-causing mutations: a new mechanism for ALS. EMBO J *34*, 2633–2651.

Fabian, M.R., Sonenberg, N., and Filipowicz, W. (2010). Regulation of mRNA Translation and Stability by microRNAs. Annu. Rev. Biochem. *79*, 351–379.

Fahn, S., and Cohen, G. (1992). The oxidant stress hypothesis in Parkinson's disease: Evidence supporting it. Ann Neurol. *32*, 804–812.

Fai Poon, H., Frasier, M., Shreve, N., Calabrese, V., Wolozin, B., and Butterfield, D.A. (2005). Mitochondrial associated metabolic proteins are selectively oxidized in A30P α-synuclein transgenic mice—a model of familial Parkinson's disease. Neurobiology of Disease *18*, 492–498.

Farh, K.K.-H. (2005). The Widespread Impact of Mammalian MicroRNAs on mRNA Repression and Evolution. Science *310*, 1817–1821.

Feddersen, R.M., Ehlenfeldt, R., Yunis, W.S., Clark, H.B., and Orr, H.T. (1992). Disrupted cerebellar cortical development and progressive degeneration of Purkinje cells in SV40 T antigen transgenic mice. Neuron *9*, 955–966.

Feigin, V.L., Abajobir, A.A., Abate, K.H., Abd-Allah, F., Abdulle, A.M., Abera, S.F., Abyu, G.Y., Ahmed, M.B., Aichour, A.N., Aichour, I., et al. (2017). Global, regional, and national burden of neurological disorders during 1990–2015: a systematic analysis for the Global Burden of Disease Study 2015. The Lancet Neurology *16*, 877–897.

Fischer, A. (2014). Epigenetic memory: The Lamarckian brain. EMBO Journal *33*, 945–967.

Fiszer, U., Mix, E., Fredrikson, S., Kostulas, V., and Link, H. (2009). Parkinson's disease and immunological abnormalities: increase of HLA-DR expression on monocytes in cerebrospinal fluid and of CD45RO+ T cells in peripheral blood. Acta Neurologica Scandinavica *90*, 160–166.

Forno, L.S. (1996). Neuropathology of Parkinson's Disease: Journal of Neuropathology and Experimental Neurology *55*, 259–272.

Friedman, J.M., and Jones, P.A. (2009). MicroRNAs: critical mediators of differentiation, development and disease. Swiss Med Wkly *139*, 466–472.

Friedman, R.C., Farh, K.K.-H., Burge, C.B., and Bartel, D.P. (2008). Most mammalian mRNAs are conserved targets of microRNAs. Genome Research *19*, 92–105.

Galasso, M., Sana, M.E., and Volinia, S. (2010). Non-coding RNAs: a key to future personalized molecular therapy? Genome Med *2*, 12.

Gao, H.-M., Kotzbauer, P.T., Uryu, K., Leight, S., Trojanowski, J.Q., and Lee, V.M.-Y. (2008). Neuroinflammation and Oxidation/Nitration of -Synuclein Linked to Dopaminergic Neurodegeneration. Journal of Neuroscience *28*, 7687–7698.

Garcia, D.M., Baek, D., Shin, C., Bell, G.W., Grimson, A., and Bartel, D.P. (2011). Weak seed-pairing stability and high target-site abundance decrease the proficiency of lsy-6 and other microRNAs. Nat Struct Mol Biol *18*, 1139–1146.

Gattellaro, G., Minati, L., Grisoli, M., Mariani, C., Carella, F., Osio, M., Ciceri, E., Albanese, A., and Bruzzone, M.G. (2009). White Matter Involvement in Idiopathic Parkinson Disease: A Diffusion Tensor Imaging Study. AJNR Am J Neuroradiol *30*, 1222–1226.

Gaudet, A.D., Mandrekar-Colucci, S., Hall, J.C.E., Sweet, D.R., Schmitt, P.J., Xu, X., Guan, Z., Mo, X., Guerau-de-Arellano, M., and Popovich, P.G. (2016). miR-155 Deletion in Mice Overcomes Neuron-Intrinsic and Neuron-Extrinsic Barriers to Spinal Cord Repair. Journal of Neuroscience *36*, 8516–8532.

Ge, X., Huang, S., Gao, H., Han, Z., Chen, F., Zhang, S., Wang, Z., Kang, C., Jiang, R., Yue, S., et al. (2016). miR-21-5p alleviates leakage of injured brain microvascular endothelial barrier in vitro through suppressing inflammation and apoptosis. Brain Research *1650*, 31–40.

Ghanbari, M., Darweesh, S.K.L., de Looper, H.W.J., van Luijn, M.M., Hofman, A., Ikram, M.A., Franco, O.H., Erkeland, S.J., and Dehghan, A. (2016). Genetic Variants in MicroRNAs and Their Binding Sites Are Associated with the Risk of Parkinson Disease. Human Mutation *37*, 292–300.

Giasson, B.I., Duda, J.E., Quinn, S.M., Zhang, B., Trojanowski, J.Q., and Lee, V.M.-Y. (2002). Neuronal α-Synucleinopathy with Severe Movement Disorder in Mice Expressing A53T Human α-Synuclein. Neuron *34*, 521–533.

Gillardon, F., Mack, M., Rist, W., Schnack, C., Lenter, M., Hildebrandt, T., and Hengerer, B. (2008). MicroRNA and proteome expression profiling in early-symptomatic α-synuclein(A30P)-transgenic mice. Proteomics - Clinical Applications *2*, 697–705.

Gillet, L.C., Navarro, P., Tate, S., Röst, H., Selevsek, N., Reiter, L., Bonner, R., and Aebersold, R. (2012). Targeted Data Extraction of the MS/MS Spectra Generated by Data-independent Acquisition: A New Concept for Consistent and Accurate Proteome Analysis. Mol Cell Proteomics *11*, O111.016717.

Glass, C.K., Saijo, K., Winner, B., Marchetto, M.C., and Gage, F.H. (2010). Mechanisms Underlying Inflammation in Neurodegeneration. Cell *140*, 918–934.

Goedeke, L., and Fernández-Hernando, C. (2014). microRNAs: A connection between cholesterol metabolism and neurodegeneration. Neurobiology of Disease *72*, 48–53.

Gray, M.T., and Woulfe, J.M. (2015). Striatal Blood–Brain Barrier Permeability in Parkinson'S Disease. J Cereb Blood Flow Metab *35*, 747–750.

Greenamyre, J.T., MacKenzie, G., Peng, T.-I., and Stephans, S.E. (1999). Mitochondrial dysfunction in Parkinson's disease. Biochem. Soc. Symp. *66*, 85–97.

Gregory, R.I., Chendrimada, T.P., Cooch, N., and Shiekhattar, R. (2005). Human RISC Couples MicroRNA Biogenesis and Posttranscriptional Gene Silencing. Cell *123*, 631–640.

Grunewald, T.G.P., Bach, H., Cossarizza, A., and Matsumoto, I. (2012). The STEAP protein family: Versatile oxidoreductases and targets for cancer immunotherapy with overlapping and distinct cellular functions. Biology of the Cell *104*, 641–657.

Gu, X.-L., Long, C.-X., Sun, L., Xie, C., Lin, X., and Cai, H. (2010). Astrocytic expression of Parkinson's disease-related A53T α-synuclein causes neurodegeneration in mice. Mol Brain *3*, 12.

Gui, Y., Liu, H., Zhang, L., Lv, W., and Hu, X. (2015a). Altered microRNA profiles in cerebrospinal fluid exosome in Parkinson disease and Alzheimer disease. Oncotarget *6*, 37043–37053.

Gui, Y.-X., Xu, Z.-P., Lv, W., Zhao, J.-J., and Hu, X.-Y. (2015b). Evidence for polymerase gamma, POLG1 variation in reduced mitochondrial DNA copy number in Parkinson's disease. Parkinsonism & Related Disorders *21*, 282–286.

Guo, B., Zheng, C., Cai, W., Cheng, J., Wang, H., Li, H., Sun, Y., Cui, W., Wang, Y., Han, Y., et al. (2016). Multifunction of Chrysin in Parkinson's Model: Anti-Neuronal Apoptosis, Neuroprotection via Activation of MEF2D, and Inhibition of Monoamine Oxidase-B. J. Agric. Food Chem. *64*, 5324–5333.

Gustafsson, G., Lööv, C., Persson, E., Lázaro, D.F., Takeda, S., Bergström, J., Erlandsson, A., Sehlin, D., Balaj, L., György, B., et al. (2018). Secretion and Uptake of α-Synuclein Via Extracellular Vesicles in Cultured Cells. Cell Mol Neurobiol *38*, 1539–1550.

Haase, A.D., Jaskiewicz, L., Zhang, H., Lainé, S., Sack, R., Gatignol, A., and Filipowicz, W. (2005). TRBP, a regulator of cellular PKR and HIV-1 virus expression, interacts with Dicer and functions in RNA silencing. EMBO Rep *6*, 961–967.

Halbgebauer, S., Öckl, P., Wirth, K., Steinacker, P., and Otto, M. (2016). Protein biomarkers in Parkinson's disease: Focus on cerebrospinal fluid markers and synaptic proteins: Protein Biomarkers in Parkinson's Disease. Mov Disord. *31*, 848–860.

Hales, C.M., Dammer, E.B., Deng, Q., Duong, D.M., Gearing, M., Troncoso, J.C., Thambisetty, M., Lah, J.J., Shulman, J.M., Levey, A.I., et al. (2016). Changes in the detergent-insoluble brain proteome linked to amyloid and tau in Alzheimer's Disease progression. Proteomics *16*, 3042–3053.

Halliday, G.M., and Stevens, C.H. (2011). Glia: Initiators and progressors of pathology in Parkinson's disease. Mov. Disord. *26*, 6–17.

Hammond, S.M. (2015). An overview of microRNAs. Advanced Drug Delivery Reviews *87*, 3–14.

Han, J. (2004). The Drosha-DGCR8 complex in primary microRNA processing. Genes & Development *18*, 3016–3027.

Haneklaus, M., Gerlic, M., O'Neill, L.A.J., and Masters, S.L. (2013). miR-223: infection, inflammation and cancer. J Intern Med *274*, 215–226.

Harrison, I.F., and Dexter, D.T. (2013). Epigenetic targeting of histone deacetylase: Therapeutic potential in Parkinson's disease? Pharmacology & Therapeutics *140*, 34–52.

Hauser, D.N., and Hastings, T.G. (2013). Mitochondrial dysfunction and oxidative stress in Parkinson's disease and monogenic parkinsonism. Neurobiology of Disease *51*, 35–42.

He, L., and Hannon, G.J. (2004). MicroRNAs: small RNAs with a big role in gene regulation. Nat Rev Genet *5*, 522–531.

Hebert, S.S., and De Strooper, B. (2007). MOLECULAR BIOLOGY: miRNAs in Neurodegeneration. Science *317*, 1179–1180.

Heintz, N. (1993). Cell death and the cell cycle: a relationship between transformation and neurodegeneration? Trends Biochem. Sci. *18*, 157–159.

Heller, K.A., and Ghahramani, Z. (2005). Bayesian hierarchical clustering. In Proceedings of the 22nd International Conference on Machine Learning - ICML '05, (New York, New York, USA: ACM Press), pp. 297–304.

Herrup, K., and Yang, Y. (2007). Cell cycle regulation in the postmitotic neuron: oxymoron or new biology? Nat Rev Neurosci *8*, 368–378.

Hinske, L.C., França, G.S., Torres, H.A.M., Ohara, D.T., Lopes-Ramos, C.M., Heyn, J., Reis, L.F.L., Ohno-Machado, L., Kreth, S., and Galante, P.A.F. (2014). miRIAD—integrating microRNA inter- and intragenic data. Database *2014*.

Hirsch, E.C., and Hunot, S. (2009). Neuroinflammation in Parkinson's disease: a target for neuroprotection? The Lancet Neurology *8*, 382–397.

Hoepken, H.-H., Gispert, S., Morales, B., Wingerter, O., Del Turco, D., Mülsch, A., Nussbaum, R.L., Müller, K., Dröse, S., Brandt, U., et al. (2007). Mitochondrial dysfunction, peroxidation damage and changes in glutathione metabolism in PARK6. Neurobiology of Disease *25*, 401–411.

Holliday, R. (2006). Epigenetics, A Historical Overview. Epigenetics 1:2 *1*, 352–355.

Hornykiewicz, O. (1966). Dopamine (3-hydroxytyramine) and brain function. Pharmacol. Rev. *18*, 925–964.

Huang, C., Mattis, P., Tang, C., Perrine, K., Carbon, M., and Eidelberg, D. (2007). Metabolic brain networks associated with cognitive function in Parkinson's disease. NeuroImage *34*, 714–723.

Huang, D.W., Sherman, B.T., and Lempicki, R.A. (2009a). Bioinformatics enrichment tools: paths toward the comprehensive functional analysis of large gene lists. Nucleic Acids Research *37*, 1–13.

Huang, D.W., Sherman, B.T., and Lempicki, R.A. (2009b). Systematic and integrative analysis of large gene lists using DAVID bioinformatics resources. Nat Protoc *4*, 44–57.

Huleatt, P.B., Khoo, M.L., Chua, Y.Y., Tan, T.W., Liew, R.S., Balogh, B., Deme, R., Gölöncsér, F., Magyar, K., Sheela, D.P., et al. (2015). Novel Arylalkenylpropargylamines as Neuroprotective, Potent, and Selective Monoamine Oxidase B Inhibitors for the Treatment of Parkinson's Disease. J. Med. Chem. *58*, 1400–1419.

Hunot, S., and Hirsch, E.C. (2003). Neuroinflammatory processes in Parkinson's disease. Ann. Neurol. *53 Suppl 3*, S49-58; discussion S58-60.

Imamura, K., Hishikawa, N., Sawada, M., Nagatsu, T., Yoshida, M., and Hashizume, Y. (2003). Distribution of major histocompatibility complex class II-positive microglia and cytokine profile of Parkinson's disease brains. Acta Neuropathologica *106*, 518–526.

Isakson, P., Lystad, A.H., Breen, K., Koster, G., Stenmark, H., and Simonsen, A. (2013). TRAF6 mediates ubiquitination of KIF23/MKLP1 and is required for midbody ring degradation by selective autophagy. Autophagy *9*, 1955–1964.

Ishizawa, T., Mattila, P., Davies, P., Wang, D., and Dickson, D.W. (2003). Colocalization of Tau and Alpha-Synuclein Epitopes in Lewy Bodies. J Neuropathol Exp Neurol *62*, 389–397.

Jain, G. (2018). GJSrMap: The smallRNA mapping pipeline (GitHub).

Jauhari, A., Singh, T., and Yadav, S. (2018). Expression of miR-145 and Its Target Proteins Are Regulated by miR-29b in Differentiated Neurons. Mol Neurobiol *55*, 8978–8990.

Javier Jiménez-Jiménez, F., Fernández-Calle, P., Martínez-Vanaclocha, M., Herrero, E., Antonio Molina, J., Vázquez, A., and Codoceo, R. (1992). Serum levels of zinc and copper in patients with Parkinson's disease. Journal of the Neurological Sciences *112*, 30–33.

Jegga, A.G., Schneider, L., Ouyang, X., and Zhang, J. (2011). Systems biology of the autophagy-lysosomal pathway. Autophagy *7*, 477–489.

Jenner, P. (2003). Oxidative stress in Parkinson's disease. Ann Neurol. *53*, S26–S38.

Jenner, P., and Olanow, C.W. (1996). Oxidative stress and the pathogenesis of Parkinson's disease. Neurology *47*, S161-170.

Jenner, P., Dexter, D.T., Sian, J., Schapira, A.H.V., Marsden, C.D., and The Royal Kings And Queens Parkinson's Disease Research Group (1992). Oxidative stress as a cause of nigral cell death in Parkinson's disease and incidental lewy body disease. Ann Neurol. *32*, S82–S87.

Joers, V., Tansey, M.G., Mulas, G., and Carta, A.R. (2017). Microglial phenotypes in Parkinson's disease and animal models of the disease. Progress in Neurobiology *155*, 57–75.

Johnson, M.E., Stecher, B., Labrie, V., Brundin, L., and Brundin, P. (2019). Triggers, Facilitators, and Aggravators: Redefining Parkinson's Disease Pathogenesis. Trends in Neurosciences *42*, 4–13.

Joppe, K., Roser, A.-E., Maass, F., and Lingor, P. (2019). The Contribution of Iron to Protein Aggregation Disorders in the Central Nervous System. Front. Neurosci. *13*, 15.

Junn, E., Lee, K.-W., Jeong, B.S., Chan, T.W., Im, J.-Y., and Mouradian, M.M. (2009). Repression of -synuclein expression and toxicity by microRNA-7. Proceedings of the National Academy of Sciences *106*, 13052–13057.

Kalia, L.V., and Lang, A.E. (2015). Parkinson's disease. The Lancet *386*, 896–912.

Kaltschmidt, B., Baeuerle, P.A., and Kaltschmidt, C. (1993). Potential involvement of the transcription factor NF-κB in neurological disorders. Molecular Aspects of Medicine *14*, 171–190.

Kangas, R., Törmäkangas, T., Fey, V., Pursiheimo, J., Miinalainen, I., Alen, M., Kaprio, J., Sipilä, S., Säämänen, A.-M., Kovanen, V., et al. (2017). Aging and serum exomiR content in women-effects of estrogenic hormone replacement therapy. Sci Rep *7*, 42702.

Kapsimali, M., Kloosterman, W.P., de Bruijn, E., Rosa, F., Plasterk, R.H., and Wilson, S.W. (2007). MicroRNAs show a wide diversity of expression profiles in the developing and mature central nervous system. Genome Biol *8*, R173.

Kempuraj, D., Thangavel, R., Natteru, P.A., Selvakumar, G.P., Saeed, D., Zahoor, H., Zaheer, S., Iyer, S.S., and Zaheer, A. (2016). Neuroinflammation Induces Neurodegeneration. J Neurol Neurosurg Spine *1*.

Kim, E.J., Sung, J.Y., Lee, H.J., Rhim, H., Hasegawa, M., Iwatsubo, T., Min, D.S., Kim, J., Paik, S.R., and Chung, K.C. (2006). Dyrk1A Phosphorylates α-Synuclein and Enhances Intracellular Inclusion Formation. J. Biol. Chem. *281*, 33250–33257.

Kim, J., Inoue, K., Ishii, J., Vanti, W.B., Voronov, S.V., Murchison, E., Hannon, G., and Abeliovich, A. (2007). A MicroRNA Feedback Circuit in Midbrain Dopamine Neurons. Science *317*, 1220–1224.

Kim, V.N., Han, J., and Siomi, M.C. (2009). Biogenesis of small RNAs in animals. Nat Rev Mol Cell Biol *10*, 126–139.

Kim, W., Noh, H., Lee, Y., Jeon, J., Shanmugavadivu, A., McPhie, D.L., Kim, K.-S., Cohen, B.M., Seo, H., and Sonntag, K.C. (2016). MiR-126 Regulates Growth Factor Activities and Vulnerability to Toxic Insult in Neurons. Mol Neurobiol *53*, 95–108.

Klucken, J., Shin, Y., Masliah, E., Hyman, B.T., and McLean, P.J. (2004). Hsp70 Reduces α-Synuclein Aggregation and Toxicity. J. Biol. Chem. *279*, 25497–25502.

Koch, J.C., Tönges, L., Barski, E., Michel, U., Bähr, M., and Lingor, P. (2014). ROCK2 is a major regulator of axonal degeneration, neuronal death and axonal regeneration in the CNS. Cell Death & Disease *5*, e1225.

Koch, J.C., Tatenhorst, L., Roser, A.-E., Saal, K.-A., Tönges, L., and Lingor, P. (2018). ROCK inhibition in models of neurodegeneration and its potential for clinical translation. Pharmacology & Therapeutics *189*, 1–21.

Kopitar-Jerala, N. (2015). Innate Immune Response in Brain, NF-Kappa B Signaling and Cystatins. Front. Mol. Neurosci. *8*.

Kortekaas, R., Leenders, K.L., van Oostrom, J.C.H., Vaalburg, W., Bart, J., Willemsen, A.T.M., and Hendrikse, N.H. (2005). Blood-brain barrier dysfunction in parkinsonian midbrain in vivo. Ann Neurol. *57*, 176–179.

Krüger, R., Kuhn, W., Müller, T., Woitalla, D., Graeber, M., Kösel, S., Przuntek, H., Epplen, J.T., Schols, L., and Riess, O. (1998). AlaSOPro mutation in the gene encoding α-synuclein in Parkinson's disease. Nat Genet *18*, 106–108.

Kulkarni, M., Ozgur, S., and Stoecklin, G. (2010). On track with P-bodies. Biochm. Soc. Trans. *38*, 242–251.

Kumar, P., Dezso, Z., MacKenzie, C., Oestreicher, J., Agoulnik, S., Byrne, M., Bernier, F., Yanagimachi, M., Aoshima, K., and Oda, Y. (2013). Circulating miRNA Biomarkers for Alzheimer's Disease. PLoS ONE *8*.

La Manno, G., Gyllborg, D., Codeluppi, S., Nishimura, K., Salto, C., Zeisel, A., Borm, L.E., Stott, S.R.W., Toledo, E.M., Villaescusa, J.C., et al. (2016). Molecular Diversity of Midbrain Development in Mouse, Human, and Stem Cells. Cell *167*, 566-580.e19.

Lambe, T., Simpson, R.J., Dawson, S., Bouriez-Jones, T., Crockford, T.L., Lepherd, M., Latunde-Dada, G.O., Robinson, H., Raja, K.B., Campagna, D.R., et al. (2009). Identification of a Steap3 endosomal targeting motif essential for normal iron metabolism. Blood *113*, 1805–1808.

Lambert, J.-P., Ivosev, G., Couzens, A.L., Larsen, B., Taipale, M., Lin, Z.-Y., Zhong, Q., Lindquist, S., Vidal, M., Aebersold, R., et al. (2013). Mapping differential interactomes by affinity purification coupled with data-independent mass spectrometry acquisition. Nat Methods *10*, 1239–1245.

Lambert, K.A., Roff, A.N., Panganiban, R.P., Douglas, S., and Ishmael, F.T. (2018). MicroRNA-146a is induced by inflammatory stimuli in airway epithelial cells and augments the anti-inflammatory effects of glucocorticoids. PLoS ONE *13*, e0205434.

Landgraf, P., Rusu, M., Sheridan, R., Sewer, A., Iovino, N., Aravin, A., Pfeffer, S., Rice, A., Kamphorst, A.O., Landthaler, M., et al. (2007). A Mammalian microRNA Expression Atlas Based on Small RNA Library Sequencing. Cell *129*, 1401–1414.

Langmead, B., Trapnell, C., Pop, M., and Salzberg, S.L. (2009). Ultrafast and memory-efficient alignment of short DNA sequences to the human genome. Genome Biol *10*, R25.

Langston, J., Ballard, P., Tetrud, J., and Irwin, I. (1983). Chronic Parkinsonism in humans due to a product of meperidine-analog synthesis. Science *219*, 979–980.

Langston, J.W., Forno, L.S., Tetrud, J., Reeves, A.G., Kaplan, J.A., and Karluk, D. (1999). Evidence of active nerve cell degeneration in the substantia nigra of humans years after 1-methyl-4-phenyl-1,2,3,6-tetrahydropyridine exposure. Ann. Neurol. *46*, 598–605.

Lazarou, M., Narendra, D.P., Jin, S.M., Tekle, E., Banerjee, S., and Youle, R.J. (2013). PINK1 drives Parkin self-association and HECT-like E3 activity upstream of mitochondrial binding. J Cell Biol *200*, 163–172.

Le, W., Rowe, D., Xie, W., Ortiz, I., He, Y., and Appel, S.H. (2001). Microglial Activation and Dopaminergic Cell Injury: An *In Vitro* Model Relevant to Parkinson's Disease. J. Neurosci. *21*, 8447–8455.

Le, W.D., Engelhardt, J., Xie, W.J., Schneider, L., Smith, R.G., and Appel, stanley H. (1995). Experimental autoimmune nigral damage in guinea pigs. Journal of Neuroimmunology *57*, 45–53.

Le Page, C., Génin, P., Baines, M.G., and Hiscott, J. (2000). Interferon activation and innate immunity. Rev Immunogenet *2*, 374–386.

Leak, R.K. (2014). Heat shock proteins in neurodegenerative disorders and aging. J. Cell Commun. Signal. *8*, 293–310.

Lee, H.-J., Suk, J.-E., Patrick, C., Bae, E.-J., Cho, J.-H., Rho, S., Hwang, D., Masliah, E., and Lee, S.-J. (2010). Direct Transfer of α-Synuclein from Neuron to Astroglia Causes Inflammatory Responses in Synucleinopathies. J. Biol. Chem. *285*, 9262–9272.

Lee, Y., Ahn, C., Han, J., Choi, H., Kim, J., Yim, J., Lee, J., Provost, P., Rådmark, O., Kim, S., et al. (2003). The nuclear RNase III Drosha initiates microRNA processing. Nature *425*, 415–419.

Lee, Y., Kim, M., Han, J., Yeom, K.-H., Lee, S., Baek, S.H., and Kim, V.N. (2004). MicroRNA genes are transcribed by RNA polymerase II. EMBO J *23*, 4051–4060.

Lees, A.J. (2007). Unresolved issues relating to the Shaking Palsy on the celebration of James Parkinson's 250th birthday. Mov Disord. *22*, S327–S334.

Li, Z., and Rana, T.M. (2014). Therapeutic targeting of microRNAs: current status and future challenges. Nat Rev Drug Discov *13*, 622–638.

Li, L., Chen, H.-Z., Chen, F.-F., Li, F., Wang, M., Wang, L., Li, Y.-Q., and Gao, D.-S. (2013a). Global MicroRNA Expression Profiling Reveals Differential Expression of Target Genes in 6-Hydroxydopamine-injured MN9D Cells. Neuromol Med *15*, 593–604.

Li, L., Chen, H., Chen, F., Li, F., Wang, M., Wang, L., Li, Y., and Gao, D. (2013b). Effects of glial cell line-derived neurotrophic factor on microRNA expression in a 6-hydroxydopamine-injured dopaminergic cell line. J Neural Transm *120*, 1511–1523.

Li, Q., Li, X., Wang, L., Zhang, Y., and Chen, L. (2016). miR-98-5p Acts as a Target for Alzheimer's Disease by Regulating Aβ Production Through Modulating SNX6 Expression. J Mol Neurosci *60*, 413–420.

Liao, Y., Wang, J., Jaehnig, E.J., Shi, Z., and Zhang, B. (2019). WebGestalt 2019: gene set analysis toolkit with revamped UIs and APIs. Nucleic Acids Research *47*, W199–W205.

Liddelow, S.A., Guttenplan, K.A., Clarke, L.E., Bennett, F.C., Bohlen, C.J., Schirmer, L., Bennett, M.L., Münch, A.E., Chung, W.-S., Peterson, T.C., et al. (2017). Neurotoxic reactive astrocytes are induced by activated microglia. Nature *541*, 481–487.

Liguori, M., Nuzziello, N., Introna, A., Consiglio, A., Licciulli, F., D'Errico, E., Scarafino, A., Distaso, E., and Simone, I.L. (2018). Dysregulation of MicroRNAs and Target Genes Networks in Peripheral Blood of Patients With Sporadic Amyotrophic Lateral Sclerosis. Front. Mol. Neurosci. *11*, 288.

Lim, L.P., Lau, N.C., Garrett-Engele, P., Grimson, A., Schelter, J.M., Castle, J., Bartel, D.P., Linsley, P.S., and Johnson, J.M. (2005). Microarray analysis shows that some microRNAs downregulate large numbers of target mRNAs. Nature *433*, 769–773.

Lim, S.-Y., Fox, S.H., and Lang, A.E. (2009). Overview of the extranigral aspects of Parkinson disease. Archives of Neurology *66*, 167–172.

Lin, M.T., and Beal, M.F. (2006). Mitochondrial dysfunction and oxidative stress in neurodegenerative diseases. Nature *443*, 787–795.

Lin, Q., Hou, S., Dai, Y., Jiang, N., and Lin, Y. (2019). LncRNA HOTAIR targets miR-126-5p to promote the progression of Parkinson's disease through RAB3IP. Biological Chemistry *400*, 1217–1228.

Liu, X., Wang, Y., Yu, X., Li, D., and Li, G. (2017). Mitochondria-mediated damage to dopaminergic neurons in Parkinson's disease (Review). Int J Mol Med.

Loring, J.F., Wen, X., Lee, J.M., Seilhamer, J., and Somogyi, R. (2001). A Gene Expression Profile of Alzheimer's Disease. DNA and Cell Biology *20*, 683–695.

Losensky, G., Jung, K., Urlaub, H., Pfeifer, F., Fröls, S., and Lenz, C. (2017). Shedding light on biofilm formation of *Halobacterium salinarum* R1 by SWATH-LC/MS/MS analysis of planktonic and sessile cells. Proteomics *17*, 1600111.

Love, M.I., Huber, W., and Anders, S. (2014). Moderated estimation of fold change and dispersion for RNA-seq data with DESeq2. Genome Biol *15*, 550.

Lu, J.P., Wang, Y., Sliter, D.A., Pearce, M.M.P., and Wojcikiewicz, R.J.H. (2011). RNF170 Protein, an Endoplasmic Reticulum Membrane Ubiquitin Ligase, Mediates Inositol 1,4,5-Trisphosphate Receptor Ubiquitination and Degradation. J. Biol. Chem. *286*, 24426–24433.

Lu, L., Neff, F., Alvarez-Fischer, D., Henze, C., Xie, Y., Oertel, W.H., Schlegel, J., and Hartmann, A. (2005). Gene expression profiling of Lewy body-bearing neurons in Parkinson's disease. Experimental Neurology *195*, 27–39.

Lukiw, W.J. (2007). Micro-RNA speciation in fetal, adult and Alzheimer??s disease hippocampus: NeuroReport *18*, 297–300.

Lukiw, W.J. (2012). Evolution and Complexity of Micro RNA in the Human Brain. Front. Gene. *3*.

Lukiw, W.J., Surjyadipta, B., Dua, P., and Alexandrov, P.N. (2012). Common micro RNAs (miRNAs) target complement factor H (CFH) regulation in Alzheimer's disease (AD) and in age-related macular degeneration (AMD). Int J Biochem Mol Biol *3*, 105–116.

Luoma, P.T., Eerola, J., Ahola, S., Hakonen, A.H., Hellstrom, O., Kivisto, K.T., Tienari, P.J., and Suomalainen, A. (2007). Mitochondrial DNA polymerase gamma variants in idiopathic sporadic Parkinson disease. Neurology *69*, 1152–1159.

Maass, F., Michalke, B., Leha, A., Boerger, M., Zerr, I., Koch, J.-C., Tönges, L., Bähr, M., and Lingor, P. (2018). Elemental fingerprint as a cerebrospinal fluid biomarker for the diagnosis of Parkinson's disease. J. Neurochem. *145*, 342–351.

Macchi, B., Paola, R., Marino-Merlo, F., Felice, M., Cuzzocrea, S., and Mastino, A. (2015). Inflammatory and Cell Death Pathways in Brain and Peripheral Blood in Parkinson's Disease. CNSNDDT *14*, 313–324.

Maetzler, W., Berg, D., Schalamberidze, N., Melms, A., Schott, K., Mueller, J.C., Liaw, L., Gasser, T., and Nitsch, C. (2007). Osteopontin is elevated in Parkinson's disease and its absence leads to reduced neurodegeneration in the MPTP model. Neurobiology of Disease *25*, 473–482.

Marsden, C.D. (1983). Neuromelanin and Parkinson's disease. J. Neural Transm. Suppl. *19*, 121–141.

Marsden, C.D. (1994). Problems with long-term levodopa therapy for Parkinson's disease. Clin Neuropharmacol *17 Suppl 2*, S32-44.

Martin, M. (2011). Cutadapt removes adapter sequences from high-throughput sequencing reads. EMBnet j. *17*, 10.

Mayer, M.P., and Bukau, B. (2005). Hsp70 chaperones: Cellular functions and molecular mechanism. CMLS, Cell. Mol. Life Sci. *62*, 670–684.

McGeer, P.L., Itagaki, S., Boyes, B.E., and McGeer, E.G. (1988a). Reactive microglia are positive for HLA-DR in the substantia nigra of Parkinson's and Alzheimer's disease brains. Neurology *38*, 1285–1285.

McGeer, P.L., Itagaki, S., Boyes, B.E., and McGeer, E.G. (1988b). Reactive microglia are positive for HLA-DR in the substantia nigra of Parkinson's and Alzheimer's disease brains. Neurology *38*, 1285–1285.

Menza, M., DeFronzo Dobkin, R., Marin, H., Mark, M.H., Gara, M., Bienfait, K., Dicke, A., and Kusnekov, A. (2010). The Role of Inflammatory Cytokines in Cognition and Other Non-Motor Symptoms of Parkinson's Disease. Psychosomatics *51*, 474–479.

Miñones-Moyano, E., Porta, S., Escaramís, G., Rabionet, R., Iraola, S., Kagerbauer, B., Espinosa-Parrilla, Y., Ferrer, I., Estivill, X., and Martí, E. (2011). MicroRNA profiling of Parkinson's disease brains identifies early downregulation of miR-34b/c which modulate mitochondrial function. Human Molecular Genetics *20*, 3067–3078.

Mizuno, Y., Sone, N., and Saitoh, T. (1986). Dopaminergic neurotoxins, MPTP and MPP+, inhibit activity of mitochondrial NADH-ubiquinone oxidoreductase. Proceedings of the Japan Academy. Ser. B: Physical and Biological Sciences *62*, 261–263.

Mo, M., Xiao, Y., Huang, S., Cen, L., Chen, X., Zhang, L., Luo, Q., Li, S., Yang, X., Lin, X., et al. (2016). MicroRNA expressing profiles in A53T mutant alpha-synuclein transgenic mice and parkinsonian. Oncotarget *8*, 15–28.

Mogi, M., Harada, M., Kondo, T., Mizuno, Y., Narabayashi, H., Riedere, P., and Nagatsu, T. (1996a). bcl-2 Protein is increased in the brain from parkinsonian patients. Neuroscience Letters *215*, 137–139.

Mogi, M., Harada, M., Narabayashi, H., Inagaki, H., Minami, M., and Nagatsu, T. (1996b). Interleukin (IL)-1β, IL-2, IL-4, IL-6 and transforming growth factor-α levels are elevated in ventricular cerebrospinal fluid in juvenile parkinsonism and Parkinson's disease. Neuroscience Letters *211*, 13–16.

Mogi, M., Harada, M., Kondo, T., Riederer, P., and Nagatsu, T. (1996c). Interleukin-2 but not basic fibroblast growth factor is elevated in parkinsonian brain. J. Neural Transmission *103*, 1077–1081.

Mogi, M., Kondo, T., Mizuno, Y., and Nagatsu, T. (2007). p53 protein, interferon-γ, and NF-κB levels are elevated in the parkinsonian brain. Neuroscience Letters *414*, 94–97.

Molinoff, P.B., and Axelrod, J. (1971). Biochemistry of Catecholamines. Annu. Rev. Biochem. *40*, 465–500.

Montes, S., Rivera-Mancia, S., Diaz-Ruiz, A., Tristan-Lopez, L., and Rios, C. (2014). Copper and Copper Proteins in Parkinson's Disease. Oxidative Medicine and Cellular Longevity *2014*, 1–15.

Moraes, L.N., Fernandez, G.J., Vechetti-Júnior, I.J., Freire, P.P., Souza, R.W.A., Villacis, R.A.R., Rogatto, S.R., Reis, P.P., Dal-Pai-Silva, M., and Carvalho, R.F. (2017). Integration of miRNA and mRNA expression profiles reveals microRNA-regulated networks during muscle wasting in cardiac cachexia. Scientific Reports *7*, 1–13.

Mount, M.P., Lira, A., Grimes, D., Smith, P.D., Faucher, S., Slack, R., Anisman, H., Hayley, S., and Park, D.S. (2007). Involvement of Interferon- in Microglial-Mediated Loss of Dopaminergic Neurons. Journal of Neuroscience *27*, 3328–3337.

Mouradian, M.M. (2012). MicroRNAs in Parkinson's disease. Neurobiology of Disease *46*, 279–284.

Mushtaq, G., Greig, N.H., Anwar, F., Zamzami, M.A., Choudhry, H., Shaik, M.M., Tamargo, I.A., and Kamal, M.A. (2016). miRNAs as Circulating Biomarkers for Alzheimer's Disease and Parkinson's Disease. Med Chem *12*, 217–225.

Nagatsu, T., and Sawada, M. (2005). Inflammatory Process in Parkinsons Disease: Role for Cytokines. CPD *11*, 999–1016.

Nakamura, N. (2011). The Role of the Transmembrane RING Finger Proteins in Cellular and Organelle Function. Membranes *1*, 354–393.

Nalls, M.A., Blauwendraat, C., Vallerga, C.L., Heilbron, K., Bandres-Ciga, S., Chang, D., Tan, M., Kia, D.A., Noyce, A.J., Xue, A., et al. (2018). Expanding Parkinson's disease genetics: novel risk loci, genomic context, causal insights and heritable risk (Genetics).

Narayan, A., Bommakanti, A., and Patel, A.A. (2015). High-throughput RNA profiling via up-front sample parallelization. Nat Methods *12*, 343–346.

Narendra, D.P., Jin, S.M., Tanaka, A., Suen, D.-F., Gautier, C.A., Shen, J., Cookson, M.R., and Youle, R.J. (2010). PINK1 Is Selectively Stabilized on Impaired Mitochondria to Activate Parkin. PLoS Biol *8*, e1000298.

Nazarov, P.V., Muller, A., Kaoma, T., Nicot, N., Maximo, C., Birembaut, P., Tran, N.L., Dittmar, G., and Vallar, L. (2017). RNA sequencing and transcriptome arrays analyses show opposing results for alternative splicing in patient derived samples. BMC Genomics *18*, 443.

Nazmi, A., Field, R.H., Griffin, E.W., Haugh, O., Hennessy, E., Cox, D., Reis, R., Tortorelli, L., Murray, C.L., Lopez-Rodriguez, A.B., et al. (2019). Chronic neurodegeneration induces type I interferon synthesis via STING, shaping microglial phenotype and accelerating disease progression. Glia *67*, 1254–1276.

Nicolas, C.S., Amici, M., Bortolotto, Z.A., Doherty, A., Csaba, Z., Fafouri, A., Dournaud, P., Gressens, P., Collingridge, G.L., and Peineau, S. (2013). The role of JAK-STAT signaling within the CNS. JAK-STAT *2*, e22925.

Nollen, E.A.A., Kabakov, A.E., Brunsting, J.F., Kanon, B., Höhfeld, J., and Kampinga, H.H. (2001). Modulation of *in Vivo* HSP70 Chaperone Activity by Hip and Bag-1. J. Biol. Chem. *276*, 4677–4682.

Nowak, J.S., and Michlewski, G. (2013). miRNAs in development and pathogenesis of the nervous system. Biochm. Soc. Trans. *41*, 815–820.

Nutt, J.G., Woodward, W.R., Beckner, R.M., Stone, C.K., Berggren, K., Carter, J.H., Gancher, S.T., Hammerstad, J.P., and Gordin, A. (1994). Effect of peripheral catechol-O-methyltransferase inhibition on the pharmacokinetics and pharmacodynamics of levodopa in parkinsonian patients. Neurology *44*, 913–913.

Obeso, J. a, Rodríguez-Oroz, M.C., Rodríguez, M., Lanciego, J.L., Artieda, J., Gonzalo, N., and Olanow, C.W. (2000). Pathophysiology of the basal ganglia in Parkinson's disease. Trends in Neurosciences *23*, S8–S19.

Oeppen, J., and Vaupel, J.W. (2002). Demography. Broken limits to life expectancy. Science *296*, 1029–1031.

Oh, Y., Park, J., Kim, J.-I., Chang, M.-Y., Lee, S.-H., Cho, Y.-H., and Hwang, J. (2018). Lin28B and miR-142-3p regulate neuronal differentiation by modulating Staufen1 expression. Cell Death Differ *25*, 432–443.

Ohgami, R.S., Campagna, D.R., McDonald, A., and Fleming, M.D. (2006). The Steap proteins are metalloreductases. Blood *108*, 1388–1394.

Ohtsuka, T., Takao-Rikitsu, E., Inoue, E., Inoue, M., Takeuchi, M., Matsubara, K., Deguchi-Tawarada, M., Satoh, K., Morimoto, K., Nakanishi, H., et al. (2002). Cast: a novel protein of the cytomatrix at the active zone of synapses that forms a ternary complex with RIM1 and munc13-1. J Cell Biol *158*, 577–590.

Okuzumi, A., Kurosawa, M., Hatano, T., Takanashi, M., Nojiri, S., Fukuhara, T., Yamanaka, T., Miyazaki, H., Yoshinaga, S., Furukawa, Y., et al. (2018). Rapid dissemination of alpha-synuclein seeds through neural circuits in an in-vivo prion-like seeding experiment. Acta Neuropathol Commun *6*, 96.

Olanow, C.W., Perl, D.P., DeMartino, G.N., and McNaught, K.S.P. (2004). Lewy-body formation is an aggresome-related process: a hypothesis. The Lancet Neurology *3*, 496–503.

Olanow, C.W., Rascol, O., Hauser, R., Feigin, P.D., Jankovic, J., Lang, A., Langston, W., Melamed, E., Poewe, W., Stocchi, F., et al. (2009). A Double-Blind, Delayed-Start Trial of Rasagiline in Parkinson's Disease. N Engl J Med *361*, 1268–1278.

Omais, S., Jaafar, C., and Ghanem, N. (2018). "Till Death Do Us Part": A Potential Irreversible Link Between Aberrant Cell Cycle Control and Neurodegeneration in the Adult Olfactory Bulb. Front. Neurosci. *12*, 144.

Ouchi, Y., Yoshikawa, E., Sekine, Y., Futatsubashi, M., Kanno, T., Ogusu, T., and Torizuka, T. (2005). Microglial activation and dopamine terminal loss in early Parkinson's disease. Ann Neurol. *57*, 168–175.

Palmer, D.C., and Restifo, N.P. (2009). Suppressors of cytokine signaling (SOCS) in T cell differentiation, maturation, and function. Trends in Immunology *30*, 592–602.

Papapetropoulos, S., Adi, N., Ellul, J., Argyriou, A.A., and Chroni, E. (2007). A Prospective Study of Familial versus Sporadic Parkinson's Disease. Neurodegener Dis *4*, 424–427.

Park, K., Luo, J., Hisheh, S., Harvey, A., and Cui, Q. (2004). Cellular Mechanisms Associated with Spontaneous and Ciliary Neurotrophic Factor-cAMP-Induced Survival and Axonal Regeneration of Adult Retinal Ganglion Cells. Journal of Neuroscience *24*, 10806–10815.

Park, K.K., Liu, K., Hu, Y., Smith, P.D., Wang, C., Cai, B., Xu, B., Connolly, L., Kramvis, I., Sahin, M., et al. (2008). Promoting Axon Regeneration in the Adult CNS by Modulation of the PTEN/mTOR Pathway. Science *322*, 963–966.

Park, K.K., Hu, Y., Muhling, J., Pollett, M.A., Dallimore, E.J., Turnley, A.M., Cui, Q., and Harvey, A.R. (2009). Cytokine-induced SOCS expression is inhibited by cAMP analogue: Impact on regeneration in injured retina. Molecular and Cellular Neuroscience *41*, 313–324.

Passer, B.J., Nancy-Portebois, V., Amzallag, N., Prieur, S., Cans, C., Roborel de Climens, A., Fiucci, G., Bouvard, V., Tuynder, M., Susini, L., et al. (2003). The p53-inducible TSAP6 gene product regulates apoptosis and the cell cycle and interacts with Nix and the Myt1 kinase. Proceedings of the National Academy of Sciences *100*, 2284–2289.

Perez, R.G., Waymire, J.C., Lin, E., Liu, J.J., Guo, F., and Zigmond, M.J. (2002). A Role for α-Synuclein in the Regulation of Dopamine Biosynthesis. J. Neurosci. *22*, 3090–3099.

Perry, T.L., Godin, D.V., and Hansen, S. (1982). Parkinson's disease: A disorder due to nigral glutathione deficiency? Neuroscience Letters *33*, 305–310.

Peterson, R., and Turnbull, J. (2012). Sonic Hedgehog is Cytoprotective against Oxidative Challenge in a Cellular Model of Amyotrophic Lateral Sclerosis. J Mol Neurosci *47*, 31–41.

Pieczora, L., Stracke, L., Vorgerd, M., Hahn, S., Theiss, C., and Theis, V. (2017). Unveiling of miRNA Expression Patterns in Purkinje Cells During Development. Cerebellum *16*, 376–387.

Plaisier, S.B., Taschereau, R., Wong, J.A., and Graeber, T.G. (2010). Rank–rank hypergeometric overlap: identification of statistically significant overlap between gene-expression signatures. Nucleic Acids Research *38*, e169–e169.

Polito, C., Berti, V., Ramat, S., Vanzi, E., De Cristofaro, M.T., Pellicanò, G., Mungai, F., Marini, P., Formiconi, A.R., Sorbi, S., et al. (2012). Interaction of caudate dopamine depletion and brain metabolic changes with cognitive dysfunction in early Parkinson's disease. Neurobiology of Aging *33*, 206.e29-206.e39.

Polymeropoulos, M.H. (1997). Mutation in the -Synuclein Gene Identified in Families with Parkinson's Disease. Science *276*, 2045–2047.

Pons-Espinal, M., de Luca, E., Marzi, M.J., Beckervordersandforth, R., Armirotti, A., Nicassio, F., Fabel, K., Kempermann, G., and De Pietri Tonelli, D. (2017). Synergic Functions of miRNAs Determine Neuronal Fate of Adult Neural Stem Cells. Stem Cell Reports *8*, 1046–1061.

Postuma, R.B., Berg, D., Stern, M., Poewe, W., Olanow, C.W., Oertel, W., Obeso, J., Marek, K., Litvan, I., Lang, A.E., et al. (2015). MDS clinical diagnostic criteria for Parkinson's disease: MDS-PD Clinical Diagnostic Criteria. Mov Disord. *30*, 1591–1601.

Qi, X., Shao, M., Sun, H., Shen, Y., Meng, D., and Huo, W. (2017). Long non-coding RNA SNHG14 promotes microglia activation by regulating miR-145-5p/PLA2G4A in cerebral infarction. Neuroscience *348*, 98–106.

Qu, M., Pan, J., Wang, L., Zhou, P., Song, Y., Wang, S., Jiang, L., Geng, J., Zhang, Z., Wang, Y., et al. (2019). MicroRNA-126 Regulates Angiogenesis and Neurogenesis in a Mouse Model of Focal Cerebral Ischemia. Molecular Therapy - Nucleic Acids *16*, 15–25.

Quinlan, S., Kenny, A., Medina, M., Engel, T., and Jimenez-Mateos, E.M. (2017). MicroRNAs in Neurodegenerative Diseases. In International Review of Cell and Molecular Biology, (Elsevier), pp. 309–343.

R Core Team (2017). R: A Language and Environment for Statistical Computing (Vienna, Austria: R Foundation for Statistical Computing).

Rao, P., Benito, E., and Fischer, A. (2013). MicroRNAs as biomarkers for CNS disease. Frontiers in Molecular Neuroscience *6*.

Rea, I.M., Gibson, D.S., McGilligan, V., McNerlan, S.E., Alexander, H.D., and Ross, O.A. (2018). Age and Age-Related Diseases: Role of Inflammation Triggers and Cytokines. Front. Immunol. *9*, 586.

Riancho, J., Vázquez-Higuera, J.L., Pozueta, A., Lage, C., Kazimierczak, M., Bravo, M., Calero, M., Gonalezález, A., Rodríguez, E., Lleó, A., et al. (2017). MicroRNA Profile in Patients with Alzheimer's Disease: Analysis of miR-9-5p and miR-598 in Raw and Exosome Enriched Cerebrospinal Fluid Samples. JAD *57*, 483–491.

Ridley, A.J. (2016). Anne Ridley: Networking with Rho GTPases. Trends in Cell Biology *26*, 465–466.

Riggs, A.D. (1996). Epigenetic mechanisms of gene regulation (Plainview, N.Y: Cold Spring Harbor Laboratory Press).

de Rijk, M.C., Launer, L.J., Berger, K., Breteler, M.M., Dartigues, J.F., Baldereschi, M., Fratiglioni, L., Lobo, A., Martinez-Lage, J., Trenkwalder, C., et al. (2000). Prevalence of Parkinson's disease in Europe: A collaborative study of population-based cohorts. Neurologic Diseases in the Elderly Research Group. Neurology *54*, S21-23.

Riley, J.C. (2001). Rising life expectancy: a global history (Cambridge ; New York: Cambridge University Press).

Risso, D., Ngai, J., Speed, T.P., and Dudoit, S. (2014). Normalization of RNA-seq data using factor analysis of control genes or samples. Nat Biotechnol *32*, 896–902.

Ritchie, M.E., Phipson, B., Wu, D., Hu, Y., Law, C.W., Shi, W., and Smyth, G.K. (2015). limma powers differential expression analyses for RNA-sequencing and microarray studies. Nucleic Acids Research *43*, e47–e47.

Rite, I., Machado, A., Cano, J., and Venero, J.L. (2007). Blood-brain barrier disruption induces in-vivo degeneration of nigral dopaminergic neurons. J Neurochem *101*, 1567–1582.

Robakis, D., and Fahn, S. (2015). Defining the Role of the Monoamine Oxidase-B Inhibitors for Parkinson's Disease. CNS Drugs *29*, 433–441.

Roberts, H.L., Schneider, B.L., and Brown, D.R. (2017). α-Synuclein increases β-amyloid secretion by promoting β-/γ-secretase processing of APP. PLoS ONE *12*, e0171925.

Rocha, E.M., De Miranda, B., and Sanders, L.H. (2018). Alpha-synuclein: Pathology, mitochondrial dysfunction and neuroinflammation in Parkinson's disease. Neurobiology of Disease *109*, 249–257.

Roser, A.-E., Caldi Gomes, L., Halder, R., Jain, G., Maass, F., Tönges, L., Tatenhorst, L., Bähr, M., Fischer, A., and Lingor, P. (2018a). miR-182-5p and miR-183-5p Act as GDNF Mimics in Dopaminergic Midbrain Neurons. Molecular Therapy - Nucleic Acids *11*, 9–22.

Roser, A.E., Caldi Gomes, L., Schünemann, J., Maass, F., and Lingor, P. (2018b). Circulating miRNAs as Diagnostic Biomarkers for Parkinson's Disease. Front. Neurosci. *12*, 625.

Ross, C.A., and Pickart, C.M. (2004). The ubiquitin–proteasome pathway in Parkinson's disease and other neurodegenerative diseases. Trends in Cell Biology *14*, 703–711.

Ross, C.A., and Poirier, M.A. (2004). Protein aggregation and neurodegenerative disease. Nat Med *10*, S10–S17.

Ryu, E.J., Harding, H.P., Angelastro, J.M., Vitolo, O.V., Ron, D., and Greene, L.A. (2002). Endoplasmic reticulum stress and the unfolded protein response in cellular models of Parkinson's disease. J. Neurosci. *22*, 10690–10698.

Salminen, A., Huuskonen, J., Ojala, J., Kauppinen, A., Kaarniranta, K., and Suuronen, T. (2008). Activation of innate immunity system during aging: NF-kB signaling is the molecular culprit of inflamm-aging. Ageing Research Reviews *7*, 83–105.

Sarkar, S., and Rubinsztein, D.C. (2006). Inositol and IP3 Levels Regulate Autophagy—Biology and Therapeutic Speculations. Autophagy *2*, 132–134.

Savage, R., Cook, E., Darkins, R., and Xu, Y. (2019). BHC: Bayesian Hierarchical Clustering.

Sawada, M., Imamura, K., and Nagatsu, T. (2006). Role of cytokines in inflammatory process in Parkinson's disease. J. Neural Transm. Suppl. 373–381.

Sawant, D., Yao, W., Wright, Z., Sawyers, C., Tepper, R., Gupta, S., Kaplan, M., and Dent, A. (2015). Serum MicroRNA-21 as a Biomarker for Allergic Inflammatory Disease in Children. MIRNA *4*, 36–40.

Schapira, A.H., and Jenner, P. (2011). Etiology and pathogenesis of Parkinson's disease. Mov. Disord. *26*, 1049–1055.

Scherzer, C.R., Eklund, A.C., Morse, L.J., Liao, Z., Locascio, J.J., Fefer, D., Schwarzschild, M.A., Schlossmacher, M.G., Hauser, M.A., Vance, J.M., et al. (2007). Molecular markers of early Parkinson's disease based on gene expression in blood. PNAS *104*, 955–960.

Schirinzi, T., Madeo, G., Martella, G., Maltese, M., Picconi, B., Calabresi, P., and Pisani, A. (2016). Early synaptic dysfunction in Parkinson's disease: Insights from animal models: Early Synaptic Dysfunction in PD. Mov Disord. *31*, 802–813.

Schmidt, W.J., and Kretschmer, B.D. (1997). Behavioural pharmacology of glutamate receptors in the basal ganglia. Neuroscience and Biobehavioral Reviews *21*, 381–392.

Schratt, G.M., Tuebing, F., Nigh, E.A., Kane, C.G., Sabatini, M.E., Kiebler, M., and Greenberg, M.E. (2006). A brain-specific microRNA regulates dendritic spine development. Nature *439*, 283–289.

Sekine, Y., Lin-Moore, A., Chenette, D.M., Wang, X., Jiang, Z., Cafferty, W.B., Hammarlund, M., and Strittmatter, S.M. (2018). Functional Genome-wide Screen Identifies Pathways Restricting Central Nervous System Axonal Regeneration. Cell Reports *23*, 415–428.

Selkoe, D.J. (2003). Folding proteins in fatal ways. Nature *426*, 900–904.

Selkoe, D.J. (2004). Cell biology of protein misfolding: The examples of Alzheimer's and Parkinson's diseases. Nat Cell Biol *6*, 1054–1061.

Sethi, P., and Lukiw, W.J. (2009). Micro-RNA abundance and stability in human brain: Specific alterations in Alzheimer's disease temporal lobe neocortex. Neuroscience Letters *459*, 100–104.

Shao, N.-Y., Hu, H., Yan, Z., Xu, Y., Hu, H., Menzel, C., Li, N., Chen, W., and Khaitovich, P. (2010). Comprehensive survey of human brain microRNA by deep sequencing. BMC Genomics *11*, 409.

Sharma, S., and Taliyan, R. (2015). Targeting Histone Deacetylases: A Novel Approach in Parkinson's Disease. Parkinson's Disease *2015*, 1–11.

Shioya, M., Obayashi, S., Tabunoki, H., Arima, K., Saito, Y., Ishida, T., and Satoh, J. (2010). Aberrant microRNA expression in the brains of neurodegenerative diseases: miR-29a decreased in Alzheimer disease brains targets neurone navigator 3: Aberrant miRNA expression in neurodegenerative disease brains. Neuropathology and Applied Neurobiology *36*, 320–330.

Singh, A., and Sen, D. (2017). MicroRNAs in Parkinson's disease. Experimental Brain Research *235*, 2359–2374.

Singleton, A.B. (2003). Synuclein Locus Triplication Causes Parkinson's Disease. Science *302*, 841–841.

Skovronsky, D.M., Lee, V.M.-Y., and Trojanowski, J.Q. (2006). NEURODEGENERATIVE DISEASES: New Concepts of Pathogenesis and Their Therapeutic Implications. Annu. Rev. Pathol. Mech. Dis. *1*, 151–170.

Smith, P.D., Sun, F., Park, K.K., Cai, B., Wang, C., Kuwako, K., Martinez-Carrasco, I., Connolly, L., and He, Z. (2009). SOCS3 Deletion Promotes Optic Nerve Regeneration In Vivo. Neuron *64*, 617–623.

Smyth, G.K., Michaud, J., and Scott, H.S. (2005). Use of within-array replicate spots for assessing differential expression in microarray experiments. Bioinformatics *21*, 2067–2075.

Spillantini, M.G., Schmidt, M.L., Lee, V.M.-Y., Trojanowski, J.Q., Jakes, R., and Goedert, M. (1997). α-Synuclein in Lewy bodies. Nature *388*, 839–840.

Starhof, C., Hejl, A.-M., Heegaard, N.H.H., Carlsen, A.L., Burton, M., Lilje, B., and Winge, K. (2019). The biomarker potential of cell-free microRNA from cerebrospinal fluid in Parkinsonian Syndromes: Cell-Free Csf-Micrornas in Parkinsonism. Mov Disord. *34*, 246–254.

Sticht, C., De La Torre, C., Parveen, A., and Gretz, N. (2018). miRWalk: An online resource for prediction of microRNA binding sites. PLoS ONE *13*, e0206239.

Stilling, R.M., and Fischer, A. (2011). The role of histone acetylation in age-associated memory impairment and Alzheimer's disease. Neurobiology of Learning and Memory *96*, 19–26.

Sun, E., and Shi, Y. (2015). MicroRNAs: Small molecules with big roles in neurodevelopment and diseases. Experimental Neurology *268*, 46–53.

Taillebourg, E., Gregoire, I., Viargues, P., Jacomin, A.-C., Thevenon, D., Faure, M., and Fauvarque, M.-O. (2012). The deubiquitinating enzyme USP36 controls selective autophagy activation by ubiquitinated proteins. Autophagy *8*, 767–779.

Takao-Rikitsu, E., Mochida, S., Inoue, E., Deguchi-Tawarada, M., Inoue, M., Ohtsuka, T., and Takai, Y. (2004). Physical and functional interaction of the active zone proteins, CAST, RIM1, and Bassoon, in neurotransmitter release. J Cell Biol *164*, 301–311.

Tan, L., Yu, J.-T., Tan, M.-S., Liu, Q.-Y., Wang, H.-F., Zhang, W., Jiang, T., and Tan, L. (2014). Genome-Wide Serum microRNA Expression Profiling Identifies Serum Biomarkers for Alzheimer's Disease. JAD *40*, 1017–1027.

Tatenhorst, L., Tönges, L., Saal, K.-A., Koch, J.C., Szegő, E.M., Bähr, M., and Lingor, P. (2014). Rho Kinase Inhibition by Fasudil in the Striatal 6-Hydroxydopamine Lesion Mouse Model of Parkinson Disease. Journal of Neuropathology and Experimental Neurology *73*, 770–779.

Taylor, J.M., Moore, Z., Minter, M.R., and Crack, P.J. (2018). Type-I interferon pathway in neuroinflammation and neurodegeneration: focus on Alzheimer's disease. J Neural Transm *125*, 797–807.

Thome, A.D., Harms, A.S., Volpicelli-Daley, L.A., and Standaert, D.G. (2016). microRNA-155 Regulates Alpha-Synuclein-Induced Inflammatory Responses in Models of Parkinson Disease. J. Neurosci. *36*, 2383–2390.

Tiwari, P.C., and Pal, R. (2017). The potential role of neuroinflammation and transcription factors in Parkinson disease. Dialogues Clin Neurosci *19*, 71–80.

Togo, T., Akiyama, H., Iseki, E., Kondo, H., Ikeda, K., Kato, M., Oda, T., Tsuchiya, K., and Kosaka, K. (2002). Occurrence of T cells in the brain of Alzheimer's disease and other neurological diseases. Journal of Neuroimmunology *124*, 83–92.

Tolosa, E., Wenning, G., and Poewe, W. (2006). The diagnosis of Parkinson's disease. The Lancet Neurology *5*, 75–86.

Tong, J., Rathitharan, G., Meyer, J.H., Furukawa, Y., Ang, L.-C., Boileau, I., Guttman, M., Hornykiewicz, O., and Kish, S.J. (2017). Brain monoamine oxidase B and A in human parkinsonian dopamine deficiency disorders. Brain *140*, 2460–2474.

Tönges, L., Koch, J.C., Bähr, M., and Lingor, P. (2011). ROCKing regeneration: Rho kinase inhibition as molecular target for neurorestoration. Front. Mol. Neurosci. *4*.

Tönges, L., Frank, T., Tatenhorst, L., Saal, K.A., Koch, J.C., Szego, E.M., Bahr, M., Weishaupt, J.H., and Lingor, P. (2012). Inhibition of rho kinase enhances survival of dopaminergic neurons and attenuates axonal loss in a mouse model of Parkinson's disease. Brain *135*, 3355–3370.

Trétiakoff, C. (1919). Contribution a l'etude de l'Anatomie pathologique du Locus Niger de Soemmering avec quelques deduction relatives a la pathogenie des troubles du tonus musculaire et de la maladie de Parkinson. Theses de Paris.

Tristão, F.S.M., Lazzarini, M., Martin, S., Amar, M., Stühmer, W., Kirchhoff, F., Gomes, L.A.C., Lanfumey, L., Prediger, R.D., Sepulveda, J.E., et al. (2016). CX3CR1 Disruption Differentially Influences Dopaminergic Neuron Degeneration in Parkinsonian Mice Depending on the Neurotoxin and Route of Administration. Neurotox Res *29*, 364–380.

Truban, D., Hou, X., Caulfield, T.R., Fiesel, F.C., and Springer, W. (2017). PINK1, Parkin, and Mitochondrial Quality Control: What can we Learn about Parkinson's Disease Pathobiology? JPD *7*, 13–29.

Tuljapurkar, S., Li, N., and Boe, C. (2000). A universal pattern of mortality decline in the G7 countries. Nature *405*, 789–792.

Ungerstedt, U., Ljungberg, T., and Steg, G. (1974). Behavioral, physiological, and neurochemical changes after 6-hydroxydopamine-induced degeneration of the nigro-striatal dopamine neurons. Adv Neurol *5*, 421–426.

Vasili, E., Dominguez-Meijide, A., and Outeiro, T.F. (2019). Spreading of α-Synuclein and Tau: A Systematic Comparison of the Mechanisms Involved. Front. Mol. Neurosci. *12*, 107.

Vibha, D., Sureshbabu, S., Shukla, G., Goyal, V., Srivastava, A.K., Singh, S., and Behari, M. (2010). Differences between familial and sporadic Parkinson's disease. Parkinsonism & Related Disorders *16*, 486–487.

Viviani, B. (2004). Cytokines role in neurodegenerative events. Toxicology Letters *149*, 85–89.

Waddington, C.H. (1942). CANALIZATION OF DEVELOPMENT AND THE INHERITANCE OF ACQUIRED CHARACTERS. Nature *150*, 563–565.

Waddington, C.H. (2012). The Epigenotype. Int. J. Epidemiol. *41*, 10–13.

Wang, Y., Yang, Z., and Le, W. (2017). Tiny But Mighty: Promising Roles of MicroRNAs in the Diagnosis and Treatment of Parkinson's Disease. Neuroscience Bulletin *33*, 543–551.

Wegiel, J., Gong, C.-X., and Hwang, Y.-W. (2011). The role of DYRK1A in neurodegenerative diseases: Role of DYRK1A in neurodegenerative diseases. FEBS Journal *278*, 236–245.

Wickham, H. (2009). Ggplot2: elegant graphics for data analysis (New York: Springer).

Will, C.L., and Lührmann, R. (2001). Spliceosomal UsnRNP biogenesis, structure and function. Current Opinion in Cell Biology *13*, 290–301.

Williams, A., Sarkar, S., Cuddon, P., Ttofi, E.K., Saiki, S., Siddiqi, F.H., Jahreiss, L., Fleming, A., Pask, D., Goldsmith, P., et al. (2008). Novel targets for Huntington's disease in an mTOR-independent autophagy pathway. Nat Chem Biol *4*, 295–305.

Wills, J., Jones, J., Haggerty, T., Duka, V., Joyce, J.N., and Sidhu, A. (2010). Elevated tauopathy and alpha-synuclein pathology in postmortem Parkinson's disease brains with and without dementia. Experimental Neurology *225*, 210–218.

Winklhofer, K.F., and Haass, C. (2010). Mitochondrial dysfunction in Parkinson's disease. Biochimica et Biophysica Acta (BBA) - Molecular Basis of Disease *1802*, 29–44.

Winslow, A.R., and Rubinsztein, D.C. (2011). The Parkinson disease protein α-synuclein inhibits autophagy. Autophagy *7*, 429–431.

Witjas, T., Kaphan, E., Azulay, J.P., Blin, O., and Ceccaldi, M. (2002). Nonmotor fluctuations in Parkinson ' s disease. Neurology *59*, 408–413.

Wright, F.A., Lu, J.P., Sliter, D.A., Dupré, N., Rouleau, G.A., and Wojcikiewicz, R.J.H. (2015). A Point Mutation in the Ubiquitin Ligase RNF170 That Causes Autosomal Dominant Sensory Ataxia Destabilizes the Protein and Impairs Inositol 1,4,5-Trisphosphate Receptor-mediated Ca^{2+} Signaling. J. Biol. Chem. *290*, 13948–13957.

Wu, J., He, Y., Luo, Y., Zhang, L., Lin, H., Liu, X., Liu, B., Liang, C., Zhou, Y., and Zhou, J. (2018). MiR-145-5p inhibits proliferation and inflammatory responses of RMC through regulating AKT/GSK pathway by targeting CXCL16. J Cell Physiol *233*, 3648–3659.

Wu, S.M., Tan, K.S., Chen, H., Beh, T.T., Yeo, H.C., Ng, S.K.-L., Wei, S., Lee, D.-Y., Choo, A.B.-H., and Chan, K.K.-K. (2012). Enhanced Production of Neuroprogenitors, Dopaminergic Neurons, and Identification of Target Genes by Overexpression of Sonic Hedgehog in Human Embryonic Stem Cells. Stem Cells and Development *21*, 729–741.

Xie, X., Peng, L., Zhu, J., Zhou, Y., Li, L., Chen, Y., Yu, S., and Zhao, Y. (2017). miR-145-5p/Nurr1/TNF-α Signaling-Induced Microglia Activation Regulates Neuron Injury of Acute Cerebral Ischemic/Reperfusion in Rats. Front. Mol. Neurosci. *10*, 383.

Yassouridis, A., Ludwig, T., Steiger, A., and Leisch, F. (2012). A New Way of Identifying Biomarkers in Biomedical Basic-Research Studies. PLoS ONE *7*, e35741.

Zhang, F., Tao, Y., Zhang, Z., Guo, X., An, P., Shen, Y., Wu, Q., Yu, Y., and Wang, F. (2012). Metalloreductase Steap3 coordinates the regulation of iron homeostasis and inflammatory responses. Haematologica *97*, 1826–1835.

Zhang, X., Gao, F., Wang, D., Li, C., Fu, Y., He, W., and Zhang, J. (2018). Tau Pathology in Parkinson's Disease. Front. Neurol. *9*, 809.

Zhang, Y., Bilbao, A., Bruderer, T., Luban, J., Strambio-De-Castillia, C., Lisacek, F., Hopfgartner, G., and Varesio, E. (2015). The Use of Variable Q1 Isolation Windows Improves Selectivity in LC–SWATH–MS Acquisition. J. Proteome Res. *14*, 4359–4371.

Zheng, L., Cheng, W., Wang, X., Yang, Z., Zhou, X., and Pan, C. (2017). Overexpression of MicroRNA-145 Ameliorates Astrocyte Injury by Targeting Aquaporin 4 in Cerebral Ischemic Stroke. BioMed Research International *2017*, 1–9.

Zovoilis, A., Agbemenyah, H.Y., Agis-Balboa, R.C., Stilling, R.M., Edbauer, D., Rao, P., Farinelli, L., Delalle, I., Schmitt, A., Falkai, P., et al. (2011). microRNA-34c is a novel target to treat dementias. The EMBO Journal *30*, 4299–4308.

8. Acknowledgements

First of all, I would like to thank Prof. Paul Lingor for the constant support, great supervision and guidance ever since I joined his laboratory for my Master's studies back in 2015. I can't express how grateful I am for Paul's trust, consideration and care for the past few years. It has been a pleasure being a part of the Lingor group, the experience(s) I collected working in his lab were fundamental to my professional and also personal development.

I would also like to thank the members of my Thesis committee, Prof. Dr. André Fischer and Prof. Dr. Silvio Rizzoli, for their availability and for the insightful discussions, as well as Prof. Mathias Bähr for having me working in his department and for the support in the past years. To the Neuroscience Program, the GGNB and the CNMPB, for providing all the necessary conditions and for making this thesis possible, my honest gratitude.

My sincere gratitude goes also to the members of Lingor Group in Göttingen. Having met amazing people like you made this journey very special for me. A special thank you to my direct supervisor and friend Dr. Anna-Elisa Roser - I am extremely grateful for your mentoring and your patience. Thank you for the mutual confidence and for the partnership we developed through these years. To my longest PhD-labmate, singing partner and dear friend, Karina Joppe: I can't thank you enough for sharing both happy and stressing moments of our PhD lifes. Our mutual support was warming and motivating in this phase! I am also immensely grateful to Vivian Dambeck and Elisabeth Barski, not only for the great technical support but for the companionship, mutual help and for the so many nice moments we shared. Vivian, thank you for being so kind and available every time asked for help with the endless microdissections. I wouldn't have made it without you! A special thanks also to Lars, Carmina, Jonas, Eleonora, Fabian and Jan, as well as the whole Waldweg and BIN members, for the nice talks and the great atmosphere in our labs.

I also have to thank the support of the Fischer group, especially Dr. Gaurav Jain, who has been always so kind and available, sparing no efforts into getting our bioinformatical analyses in shape. I can't really thank you enough for your contribution to this project!

Acknowledgements

To the many beloved friends I made in Göttingen (which I don't dare to name here, for space limitations), thank you for being my family so far away from home, for the unforgettable moments in this amazing city, and for being always there for me.

Finally, I would like to thank my family, from the bottom of my heart, for being my biggest support. To my wife, Tatiane, thank you for getting into this journey with me, for the continuous and mutual encouragement, for your strength and determination, for your patience and for all your efforts… thank you for being such an incredible and wonderful person! To my parents and siblings, being apart from daily life with you taught me many things (in a hard way), but has been strengthening our laces ever since. I am deeply thankful to you all for being incredibly supportive, for being my basis and the reason of every challenge I take.

9. List of abbreviations

AD: Alzheimer's Disease

AGO: argonaute proteins

ALS: Amyotrophic Lateral Sclerosis

ANOVA: Analysis of variance

BP: Biological process

CNS: Central nervous system

CSF: cerebrospinal fluid

DA: Dopamine

DAG: Directed Acyclic Graph

DAVID: Database for Annotation, Visualization and Integrated Discovery

DDC: Dopa decarboxylase

DE: differential expression / differentially expressed

DNA: deoxyribonucleic acid

FC: fold change

FDR: false discovery rate

GO: Gene ontology

HD: Huntington's Disease

IFNγ: interferon-gamma

KEGG: Kyoto Encyclopedia of Genes and Genomes

LB: Lewy Bodies

LBD-BS: Lewy body disease, brain stem predominant

LBDE: Lewy body disease, early-neocortical

LBD-N: Lewy body disease, neocortical

L-DOPA: L-3,4-dihydroxyphenylalanine

LNA: locked nucleic acid

LPS: lipopolysaccharide

MLPA: Multiplex Ligation-dependent Probe Amplification

PBS: Phosphate buffered saline

PD: Parkinson's Disease

PMI: Post-mortem intervals

q-RT-PCR: Quantitative real-time polymerase chain reaction

RISC: *RNA-induced silencing complex*

RNA: ribonucleic acid

RRHO: Rank-Rank Hypergeometric Overlap

RUV: Removal of unwanted variances

SEM: Standard error of the mean

SHH: sonic hedgehog

STN: Subthalamic nucleus

SWATH: sequential window acquisition of all theoretical fragment ion spectra

TH: tyrosine hydroxylas

UK: United Kingdom

UTR: untranslated regions

VUS: variation of uncertain significance

Herewith I declare, that I prepared the Doctoral Thesis "*Multi-omics analysis of human brain tissue and an animal model of Parkinson's disease*" on my own and with no other sources and aids than quoted.

Göttingen, September, 2019 **Lucas Caldi Gomes**